THE SYSTEM TRIETHYLAMINE + WATER

by

Jack Frederick Counsell

A dissertation submitted for the degree

of Doctor of Philosophy to the

University of Bristol.

Bristol August 1959

Memorandum

The work described in this thesis was carried out at the University of Bristol between October 1956 and July 1959, and has not been submitted for any other degree. The thesis contains two parts. The first part (chapters 1 - 3) is a review of recent experimental and theoretical work pertaining to systems near their critical points, with particular reference to binary liquid systems. This review has been compiled wholly by the author. The second part (chapters 4-8) describes experimental work on the system triethylamine + water. All the work described in this section is the original work of the author except where specific acknowledgement is made.

Triethylamine and water show a lower consolute temperature at 18.30°C, the consolute composition being 0.073 mole fraction of triethylamine. I have studied certain properties of this system in the single liquid phase region near the critical point and I have also measured the free energy of mixing at three temperatures below the critical temperature. My conclusions are given at the end of this thesis and I hope that they will contribute a little to the understanding of the occurrence of lower consolute points in binary liquid systems.

J. J. Bowsell

ACKNOWLEDGEMENTS

I wish to extend grateful thanks to Professor D.H. Everett for both suggesting the topics for research and for his help and guidance throughout.

I also wish to thank Mr. A.J.B. Cruickshank for discussions which have been most helpful in giving this dissertation its final form.

I am also indebted to the Department of Scientific and Industrial Research for the award of a Research Studentship (1956 - 1959).

G.J. Counsell

INDEX

CHAPTER ONE

Critical Solution Phenomena in Binary Liquid Systems

CHAPTER TWO

The Thermodynamics of Critical Behaviour

CHAPTER THREE

Solution Models in the Critical Region

CHAPTER FOUR

The Miscibility of Triethylamine and Water

CHAPTER FIVE

The Viscosity of the System Triethylamine + Water

CHAPTER SIX

The Electrical Conductivity of the System Triethylamine+Water

CHAPTER SEVEN

The Density of the System Triethylamine+Water

CHAPTER EIGHT

Free Energy of Mixing of the System Triethylamine+Water

LIST OF THE MOST IMPORTANT SYMBOLS

B Second virial coefficient

C Heat capacity

F Helmholtz free energy

G Gibbs free energy

H Enthalpy

I Intensity of light

N Number of molecules

R Gas constant

S Entropy

T Absolute Temperature

U Internal energy

V Volume

k Boltzmann's constant, and on other occasions to denote any constant value

n Number of moles

r Intermolecular distance

t Temperature in ^{o}C

x Mole fraction

γ Activity Coefficient

μ Chemical Potential

ϕ Volume fraction

The following operator signs are used

d	Complete differential
δ	Change in the value of a quantity
∂	Partial Differential
Δ	Excess of final over initial value
$\int$	Integral
Σ	Summation
Π	Product
ln	Natural logarithm
log	Logarithm to the base 10

CHAPTER ONE

CRITICAL SOLUTION PHENOMENA IN BINARY LIQUID SYSTEMS

1.1. Introduction

This thesis describes work carried out during the last three years on the system triethylamine + water in the region of its critical solution temperature. Above about 18°C these two components are only partially miscible, while at lower temperatures they are completely miscible; the lowest temperature at which two liquid phases can coexist is called the lower critical solution temperature. The various phenomena which characterise the critical region in binary liquid mixtures are closely related to the effect of temperature on the miscibility of liquids. Research into the mutual solubility of liquids probably began with the work of Abaschew [1]. He investigated the solubilities of many liquid pairs, but his experimental techniques did not lead to the discovery of miscibility curves as we know them today. The first systematic experiments on the effect of temperature on the miscibility of liquids were reported by Alexejew [2]. Reference 2 is a summary of many papers describing his work on this problem during the years 1876 - 1885. He expressed the miscibility of a liquid pair by plotting the concentrations of the equilibrium

phases against temperature on a suitable phase diagram; he also showed that for a liquid pair which had both upper and lower consolute temperatures the enthalpy of mixing changed sign at the temperature of minimum miscibility. This work, together with the experiments of Duclaux [3], Guthrie [4], Schreinemakers [5], Rothmund [6] and Kuenen [7,8], is discussed by Rothmund in 'Löslichkeit und Löslichkeitbeinflussung' [9].

Many liquid pairs are miscible in all proportions over the whole temperature range of the liquid state, while others appear to be completely immiscible. Between these two extremes there exist a large number of liquid pairs which, over certain temperature and composition ranges, form two coexisting liquid phases. These two conjugate liquid phases are also in equilibrium with a vapour phase, so that according to the phase rule such a system has one degree of freedom. If the temperature of this three phase system is defined, then the compositions of the phases and the vapour pressure are fixed. If the binary system is under a pressure which is greater than the three phase equilibrium pressure at that temperature, then no vapour phase will be present. Consequently for such a system it is necessary to define both the temperature and the pressure in order to specify the compositions of the two phases.

At constant temperature the compositions of the equilibrium phases depend upon pressure, and Le Chatelier's principle indicates that an increase in pressure will increase the mutual solubility of two liquids which mix with a contraction in volume. Kuenen [10] has derived thermodynamic equations describing these effects. He showed that the effects of both temperature and pressure upon the miscibility of two liquids are determined respectively by the signs of the enthalpy and volume of mixing.

The effect of temperature on the mutual solubility of two liquids is usually expressed graphically in the form of a miscibility curve on a phase diagram. For binary liquid systems miscibility curves can either be plotted at constant pressure, or at the equilibrium pressure for three phase coexistence which is temperature dependent. The phase diagram usually used for a binary liquid system shows the compositions of the equilibrium phases as a function of temperature. The boundary between the single liquid phase region and the two liquid phase region is called the miscibility curve. The compositions of the coexisting liquid phases are defined by the intersection of the horizontal (constant temperature) tie lines with the miscibility curve; and all points outside

this curve represent a stable one liquid phase system. Two distinct forms of miscibility curves are known to exist in binary liquid systems, and these are shown in figures 1.1.A. and 1.1.C. Figure 1.1.A. represents a system which shows an upper critical solution temperature. An upper critical solution temperature (U.C.T.) is defined as the temperature above which only one liquid phase can occur. It is thus the maximum point on the T,x miscibility curve. Systems which show this property are quite common as it is theoretically possible for any pair of partially miscible liquids to show a U.C.T. For any liquid pair the solubility will ultimately increase if the temperature is raised sufficiently, and a U.C.T. will occur if it is lower than the vapour-liquid critical temperature of the mixture. If this last condition is not fulfilled then the U.C.T. will not be reached and the miscibility curve will not close at the top (figure 1.1.B.). Figure 1.1.C. illustrates the case of a binary liquid mixture which has a lower critical solution temperature (L.C.T.) as well as a U.C.T. The L.C.T. is defined as the temperature below which only one liquid phase can occur and is the minimum of the miscibility curve. As in the previous example the top part of the curve may not

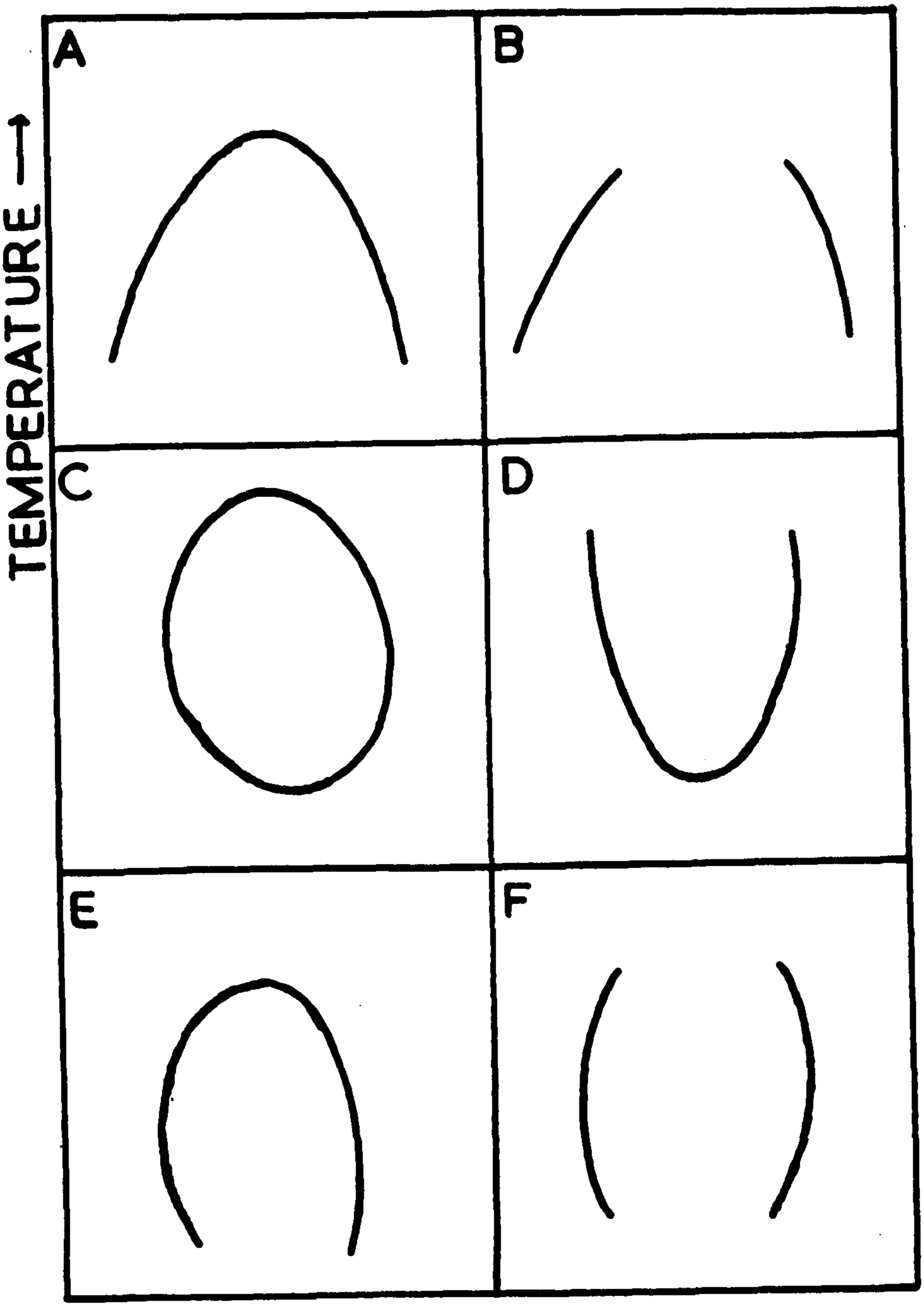

FIGURE 1·1 MISCIBILITY CURVES SHOWN BY BINARY LIQUID MIXTURE

exist due to the vaporisation of the components (figure 1.1.D.). The bottom part also may not exist, due to the components solidifying before the L.C.T. is reached (figure I.1.E.). Figure 1.1.F. is the miscibility curve when both these conditions occur.

The special properties of binary liquid mixtures which become important close to the critical solution point are termed critical properties. They occur because the critical solution point is a higher order transition; which means that certain properties, which can be related to differentials of the free energy of an order higher than unity, show large changes as the critical point is approached while the first differentials do not show these effects. These critical properties usually begin to appear within one or two degrees of the critical temperature, and rapidly become more significant as the critical temperature is approached; one of the most noticeable of them is critical opalescence which occurs in the one phase region near the critical point. In the following sections I shall discuss these properties and try to illustrate the various fe$_a$tures by examples drawn from recent research on the critical properties of binary liquid systems. Reference will be made not only to binary liquid systems but

also to properties near the gas-liquid critical point. There are three reasons for doing this. Firstly, many of the theories concerning critical behaviour have been developed for the gas-liquid critical point and are consequently best illustrated by reference to the behaviour of one component systems. The second is that much more work has been performed on the gas-liquid critical point, and thirdly certain effects can be observed more readily in this case than with binary liquid systems. The similarity between critical phenomena in one and two component systems is quite extensive, but for some properties a comparison between these two types may be of only limited validity.

1.2. Critical Fluctuations

In the one phase region near a critical point the variation of free energy with composition of a system is extremely small; and thus equilibria only establish themselves slowly and prove very sensitive to small disturbances. It is therefore difficult to obtain reproducible results as these small disturbances can produce large fluctuations in a system. The standard methods of statistical mechanics for computing these fluctuations lead to the result that the fluctuations tend to infinity at the critical point [11].

In reality the fluctuations are very large but remain finite. The smallness of molecular fluctuations is the prerequisite for the use of statistical mechanics and thermodynamics, so consequently both these methods reach the limit of their applicability at the critical point.

A discussion of the theory of fluctuations is given by Tisza in 'Phase transformations in Solids' [12], where he considers the classical concept of fluctuations and the amendments which are necessary in order to make the fluctuations finite at the critical point. The classical theory is based upon the relationship, $P \sim e^{-W/kT}$, where the probability (P) of any fluctuation is related to the minimum work needed to cause this fluctuation (W). Smoluchowski [13] proved that the energy needed to produce a fluctuation of volume ΔV in a one component system at constant temperature was $W = \frac{1}{2}a(\Delta V)^2$, where $a = -\left(\frac{\partial P}{\partial V}\right)_T = \frac{1}{V\beta}$, β being the isothermal compressibility. At the critical point fluctuations become infinite. This theory has been amended in order to deal with the critical point by assuming there are other terms in powers of ΔV in the expression for W. These terms are relatively small and are only significant in the critical region [14-19]. Tisza's [20] cellular method limits these fluctuations by dividing the phase

into regularly arranged cells whose contents may fluctuate between zero and the total mass of the phase. The application of this method leads to large but finite fluctuations. The equation obtained for critical light scattering in a fluid system is

$$\frac{I}{Io} \sim \frac{1}{\lambda^4} (1+\cos^2\theta) \left(\frac{1}{\beta} + c + d^2 \frac{\sin^2\theta/2}{\lambda^2} \right)^{-1} ,$$

where I/Io is the ratio of the intensities of scattered to incident light of wavelength λ observed at an angle θ; c and d are constants. For $c = 0$ the equation reduces to that of Ornstein and Zernike; for $d = 0$ to that of Rocard.

1.3. Critical Opalescence

One of the most striking results of critical fluctuations is the large amount of light scattering which is associated with the approach of a one phase system to the critical region. The appearance of critical opalescence is as general as it is striking for it occurs in the vicinity of critical points of all kinds. In a system showing upper or lower critical behaviour the opalescence, which is blue by scattered light and reddish-brown by transmitted light, is first observed in the one phase state of the system when its temperature is brought to within a few degrees of the critical temperature.

The closer the system approaches the critical point, both in concentration and temperature, the more intense is the opalescence. At a constant temperature the intensity of the opalescence is completely stable, and the temperature at which opalescence first gives way to cloudiness is generally taken to be the phase separation temperature.

No coherent scattering of light can take place in a truly continous and homogeneous medium, but if the refractive index varies irregularly from one volume element to the next then light scattering can take place [21,22]. In a one component system differences in the refractive indeces among the various volume elements can only occur if the two elements have different densities. In the case of a two component system volume elements may have different densities and different compositions. In a binary liquid system the opalescence is due primarily to differences in composition of the volume elements, the density differences being negligible[23]. Opalescence is only observed if these volume elements are small compared with the wavelength of light (λ). If the elements become larger than λ the solution will become cloudy and is considered to contain two phases.

The theory of the phenomenon of critical opalescence is

due primarily to Lord Rayleigh[24], who assumed that the scattering elements of volume ΔV were small compared with the wavelength (λ) of the primary unpolarised radiation; and obtained the following expression for the intensity (I) of light scattered at an angle θ to the primary beam of intensity (I_o) at a distance l from the scattering volume (V):

$$\frac{I}{I_o} = \frac{4\pi^2 V q^2 (\overline{\delta q^2}) \Delta V}{l^2 \lambda^4} \quad \frac{1+\cos^2\theta}{2} \quad ,$$

where $(\overline{\delta q^2})$ represents the mean square fluctuation of the refractive index (q) within the elements ΔV. The turbidity (τ) - the fraction of all the incident light scattered by unit length of the medium in all directions - is given by

$$\tau = \frac{32\pi^2 q^2 (\overline{\delta q^2}) \Delta V}{3\lambda^4} \quad ,$$

and this becomes, for a one component system[13,25],

$$\tau = \frac{8\pi^3}{3\lambda^4} (q^2 - 1)^2 \beta kT \quad ,$$

where β is the macroscopic compressibility. For a two component phase the refractive index also varies with the composition of the scattering elements, so we have[23]

$$\tau = \frac{32\pi^3}{3\lambda^4 N} \left\{ RT\beta \left(\rho \frac{dq}{d\rho}\right)^2 + \frac{v_1 \phi_2}{d\ln a_1 / d\phi_1} \left(\frac{q\,dq}{d\phi_2}\right)^2 \right\}$$

where ϕ_1 and ϕ_2 are the volume fractions of the two components,

and a_1 and v_1 are the activity and molar volume of the first component respectively: ρ is the density of the solution.

The first term in this equation involves the compressibility of a binary liquid system. This term is very small and may be neglected compared with the second term. The second term contains the slope of the activity isotherm ($d \ln a_1/d\phi_1$) and becomes very large as the critical point is approached. The slope of the activity isotherm in the critical region is of great interest, as it can help to decide between several theories which have been put forward to describe this region.

Mayer's theory of the critical point (Section 3.9) contains a region just above the critical temperature of a one component system where the activity isotherms are horizontal. Critical opalescence depends upon the slope of the activity isotherm and can be used to provide evidence to test Mayer's theory. Measurements of critical opalescence previous to the introduction of Mayer's theory [26,27,28] showed no sign of an anomalous region, but it is possible that this effect occurs over such a small temperature range that it was not noticed [23]. Maass stated [29] that even on Mayer's theory one would expect the critical opalescence to be a maximum

at the critical temperature, as at this temperature the activity isotherm would contain its longest horizontal section. All the more recent work on critical opalescence in a binary liquid mixture confirms the large increase in critical opalescence as the critical point is approached, but none show any evidence for Mayer's theory [23,29,30,31] The work of Zimm [23] on the perfluoromethylcyclohexane + carbon tetrachloride system was performed with the intention of obtaining these activity isotherms, and showed that they were of the classical type, having a slope greater than zero above the phase separation temperature and a discontinuity in the slope below this.

1.4. Activity Isotherms in the Region of the Critical Point

From a practical viewpoint, the study of the critical behaviour of systems involves three main experimental problems. These are the determination of activity isotherms, the determination of phase diagrams, and the analysis of properties in the critical region to investigate the existence of second or higher order transitions.

As was remarked in the previous section, research into the shape of activity isotherms was stimulated by the work of Mayer. His theory of a horizontal activity isotherm is also

associated with the possibility that the phase diagram may have a flat top. To test the theory Roberts and Mayer [32] determined the vapour pressure isotherms of the system triethylamine+water at various temperatures below the L.C.T. They determined the weight fraction of amine in the vapour and found that in a certain region it was, within the error of the experiment, independent of the liquid composition. They found this to be true at 18°, 16° and 13°C and decided the possible error by the fact that for a plot of the weight fraction of amine in the vapour against that in the liquid the 18°C isotherm gave a negative slope, while the positive slopes of the 16°C and 13°C isotherms were numerically less than this. Evidence to support Mayer's theory had been previously reported by McIntosh, Dacey and Maass [33], who measured the p - V isotherms of ethylene in the one phase region near the critical point. They found that a region existed from 9.90°C down to 9.50°C (the critical temperature as determined by the disappearance of the meniscus for the critical composition) in which, for a range of densities near the critical, $\left(\frac{\partial p}{\partial v}\right)_T = 0$. Their results may be criticised on the grounds that insufficient points were taken in this region.

Rowden and Rice[34] determined the vapour pressure as a function of composition for the system cyclohexane + aniline, and found that the slope appeared to increase linearly with temperature above the critical temperature. Zimm[23] observed the critical opalescence in the system perfluoromethylcyclohexane + carbon tetrachloride, and found that the slope of the activity isotherm was greater than zero in the one phase region above the critical point. Wentorf[35] determined the p-V isotherms of carbon dioxide and sulphur hexafluoride in their critical regions at $0.02^{\circ}C$ intervals. His results agree with those of MacCormack and Schneider[36] on sulphur hexafluoride and with Michels, Blaisse and Michels[37] on carbon dioxide. He found no definite evidence for horizontal isotherms, and said that if they did exist then the region could only be $0.04^{\circ}C$ high for sulphur hexafluoride and $0.02^{\circ}C$ high for carbon dioxide.

Rice[38] showed that the critical isotherm ($|p-p_c|$ vs. $|\rho-\rho_c|$) must be of one degree higher in $|\rho-\rho_c|$ than the coexistence curve ($|T-T_c|$ vs. $|\rho-\rho_c|$). This implies that the shape of the critical isotherm can be related to the shape of the phase diagram, the determination of which is discussed in the

next section. If the phase diagram shows a flat top then the critical isotherm is also flat. Guggenheim[39], in his paper on the principle of corresponding states, found by analysis of vapour-liquid equilibria that the coexistence curve could be represented by an equation of the form $|\rho - \rho_c| = a^{-\frac{1}{3}} |T-T_c|^{\frac{1}{3}}$ where a term containing $|T-T_c|$ has been omitted as being negligible compared with the one retained. This gives $|\rho-\rho_c|^3 = a^{-1}|T-T_c|$, and according to Rice the equation for the critical isotherm at the critical point should be, $a\left(\frac{\partial^2 p}{\partial T \partial \rho}\right)_c |\rho-\rho_c|^4 = |p-p_c|$. Widom and Rice[40] analysed data for xenon[41], carbon dioxide[37] and hydrogen[42], and found that in each case the critical isotherm is of the fourth degree, one degree higher than the coexistence curve. Therefore analysis of recent data on the shape of activity isotherms does not appear to produce any evidence in favour of Mayer's theory of the critical region.

Andon, Cox and Herington [43] suggested that certain binary mixtures came very close to separating into two phases over a certain range of mole fractions. They found that some solutions showed critical opalescence without phase separation, and a region in which the activity isotherm

had a small slope. Two liquid phases can be made to form if the deuterium content of the water (in the case of the system 3 methylpyridine+water[44]) is increased, or small amounts of a third component added[45]. Solutions under these conditions are very close to separating into two phases, and these workers[43] determined the 'closeness to phase separation' by a method which made use of the slope of the activity isotherm.

1.5 Phase Diagrams

Phase diagrams of one component systems have been of interest since Andrews[46] showed that over certain temperature ranges vapour and liquid can coexist, but that at other temperatures only the gas phase exists. Similar effects occur in binary liquid systems, where in certain temperature ranges the stable state of the system is two liquid phases, while in other temperature ranges only one liquid phase can exist. Guggenheim[39] found that most available data for one component systems fitted a cubic coexistence curve of the form $|\rho - \rho_c|^3 = a^{-1}|T-T_c|$; and it is also found that the miscibility curves of most binary liquid systems fit a similar equation of the form $|x-x_c|^3 = b|T-T_c|$.

Miscibility curves of binary liquid systems can be determined in two ways. In the first method a mixture of two

liquids is placed in a thermostat, and samples of the two phases are withdrawn when equilibrium has been attained. These can be analysed and the compositions of the phases determined. The drawbacks of this method are that the mixture is usually in contact with the atmosphere when samples are withdrawn, and also that it is necessary to perform an analysis of these samples. The compositions of the two layers can be determined while they are still in equilibrium by measuring their refractive indeces or some other property. In the second method weighed samples of both the components are placed in a tube and the tube is sealed off from the atmosphere. The tube is placed in a thermostat whose temperature is slowly altered until a point is reached when two phases form. The coexistence curves for vapour-liquid equilibria are similarly obtained either by measuring the densities of the two equilibrium phases when they are placed in a thermostat, or by lowering the temperature of a tube containing gas at a known density until two phases appear.

The main error involved in the determination of miscibility curves is due to the effect of impurity. It is not unusual for there to be a range of several degrees

for the reported values of the critical temperature, and miscibility curves reported by different authors may vary in shape. There are two types of impurity effect which can occur: the first is when the third component dissolves in one or both of the phases, and the second is when it is surface active; in both these cases the effect of a small amount of impurity can be very large [47]. A striking example of the varying results sometimes obtained is shown in the work of Flaschner [48], who found a closed solubility loop extending from 49°C to 153°C for the system 3 methylpyridine + water. Contrary to this Andon and Cox [45] found that these components were always completely miscible, although mixtures containing 60-75% of water showed opalescence at 60 - 90°C.

In recent years several workers have tried to determine whether miscibility curves contain a horizontal section in the region of the critical point [23,34,49,50,53]. Rice [47] suggested that most miscibility curves do contain a horizontal section, and that, in the cases where rounded tops appear to exist, the coexistence curve should be examined more carefully. In many cases the experimental points are not close enough together to enable a final decision to be made, and it is

often impossible to exclude a small horizontal section It is, of course, equally impossible to exclude a very flat maximum in a curve which appears to have a flat top. Only two binary liquid systems have been studied carefully enough in order to discover whether miscibility curves contain horizontal portions. These are the system perfluoromethylcyclohexane+carbon tetrachloride studied by Zimm [23] and Ram Gopal and Rice [53], and the system cyclohexane + aniline studied by Rowden and Rice [34] and Atack and Rice [49,50]. Zimm's measurements indicate that the miscibility curve of the system perfluoromethylcyclo-hexane + carbon tetrachloride does not have a flat top but is rounded and obeys a cubic relationship. Rice [51] suggested that Zimm did not include compositions close enough to the critical mole fraction, and that his materials were not sufficiently protected from atmospheric contamination. In the case of the system cyclohexane + aniline Rowden and Rice [34] found that for a range of mole fractions of aniline from 0.42 to 0.46 the transitions from a one phase system to a two phase system occured at the same temperature. Zimm [52] showed that within the stated limits of error, $\pm 0.003^{\circ}C$, the data could be fitted to a cubic curve which

also fitted mixtures of more extreme composition. Atack and Rice [48] said that the difference in the phase separation temperatures for the various solutions cited was probably less than 0.003°C. They found that for six solutions in the range 0.430 to 0.465 mole fraction of aniline, the phase separation temperatures all lay within 0.001°C. Similar results were obtained by Ram Gopal and Rice [53] when they measured the phase separation temperatures in the system perfluoromethylcyclohexane + carbon tetrachloride. They found a horizontal portion at the top ofthe miscibility curve extending from 0.5375 to 0.5625 volume fraction of carbon tetrachloride, and this was supported by the observation that the meniscus always appeared in the central part of the tube for this range of volume fractions.

It is more difficult to examine one component systems in order to see whether the coexistence curve has a flat top. Theoretically the two types of system appear to be similar, but from an experimental viewpoint they differ with respect to the effect of gravity. In the case of a liquid-liquid system Rice [51] calculated the effect of gravity on the sedimentation of particles, and found that

it was sufficient to establish a concentration gradient of only 10^{-6} to 10^{-5} mole fraction cm^{-1} day^{-1}. Hildebrand etal. (54) determined the effect of a large applied gravitational field, and found that the change in critical temperature due to the increase in pressure was much greater than that due to the sedimentation of cluster particles, having previously determined the effect of pressure alone in a separate experiment. In the case of the system n-perfluoroheptane + 2,2,4 trimethylpentane, where the densities of the two components (1.707 and 0.690 $g.ml^{-1}$ respectively at 25°C) differ considerably, the pressure effect caused a rise of 8.1°C in the critical temperature while the sedimentation effect caused a rise of only 1.9°C under a gravitational field of 10^8 $cm.sec^{-2}$. Under the same applied field the critical temperature of the system perfluoromethyl-cyclohexane + carbon tetrachloride was raised by 7.7°C, of which only 0.2°C can be attributed to sedimentation effects, and this quantity is approximately equal to the error of the experiment: the densities in this case are respectively 1.795 and 1.615 $g.ml^{-1}$ at 25°C. Consequently the effect of standard gravity on a binary liquid system is small, but in a one component system it is very important and arises because of the large compressibility of the gas in the

critical region.

Just above the critical temperature a gas has a large compressibility, and consequently gas in a tube is compressed by the weight of gas above it. A large density gradient is set up in the tube and consequently it is likely that at some particular height the density is equal to the critical density, even though the average density differs from the critical density. On cooling such a system to the critical temperature a meniscus appears at the point in the tube where the density equals the critical density. Since in most experiments the average density of filling is measured, there is an apparent range of densities for which the phase separation temperature is the same as the critical temperature. Consequently the coexistence curve determined in this way will have a flat top, which must be distinguished from a true flat top. It has been shown that this equilibrium with respect to gravity is established relatively quickly, taking only a few hours or, at the most, a day [55]. An excellent summary of the influence of gravity in the critical region is given by Baehr [56], who relates the shape of the coexistence curve and the density differences in a tube to the shape of the critical isotherm.

The appearance of a flat top as a result of the effect of gravity has been proven in many cases [55,57,58,59]. long tubes, in which there are large density ranges, show flat topped coexistence curves, and short tubes show round topped coexistence curves. Whiteway and Mason [59] suggest that the major portion of the flat top is in most cases due to gravity.

1.6 General Critical Properties

In the critical region many properties of a system show very large changes and even exhibit discontinuities at the critical point. Thus the phase changes which occur might be called transitions of either the second or higher order, depending upon the order of the derivative of the free energy which exhibits a discontinuity. Measurements of such properties have often given apparently anomalous results. This is the case, for instance, with Maass' measurements of the dielectric constant [60] and heat capacity [61] of a one component system. He interpreted his results by postulating a temperature dependent hysteresis, but later suggested that violent shaking would result in reversibility with respect to changes in temperature [29]. Semenchenko and Zorina [62] found that the hysteresis

which occurred in their viscosity measurements on the system triethylamine + water was greatest for solutions removed from the critical point but still in the critical region: it is probable that this hysteresis was due to the effect of impurities. Pall, Broughton and Maass [61] found that the heat capacity (Cv) of ethylene shows a large rise in the critical region, and this was supported by Michels and Strijland [63] in the case of carbon dioxide. Schneider [64,65] determined the velocity and absorption of sound in sulphur hexafluoride in the critical region. The velocity shows a sharp fall in this region while there is a peak of sound absorption. Schneider and Chynoweth [66] used the sound velocity data to calculate the heat capacity (Cv) of sulphur hexafluoride, ethylene and carbon dioxide. Their values of Cv for ethylene and carbon dioxide are smaller than the values obtained from calorimetric measurements [61,63] by about 50%; this was explained on the basis that the equation relating the quantities was only true for low frequency sound while the frequency used was about 600 K.c.

Similar large changes in the values of certain properties also occur in the critical regions of two component systems. Chynoweth and Schneider [67] measured the velocity of sound

in the systems aniline + n.hexane and triethylamine + water and found a marked change at the critical temperature; they also measured the attenuation, as did Alfrey and Schneider [68] and found a marked peak at the critical point. Sette [69] suggests that these absorption effects are due to two causes: the first is that when density fluctuations are present in the liquid the sound losses are due to viscosity increase, and secondly the sound losses are due to relaxation phenomena caused by perturbation of the equilibrium set up between clusters and the mother phase. The heat capacity of the system triethylamine + water has been measured by Jura, Fraga, Maki and Hildebrand [70] and Semenchenko and Skripov [71]: they found a maximum at the critical point. Semenchenko and Skripov determined the effects of adding a surface active impurity, Me_4NI, which raised the critical temperature and lowered the maximum heat capacity and the effect of adding inactive isoamyl alcohol which lowered both the critical temperature and the maximum heat capacity. Krichevski and Tsekhanskaya [72] measured the diffusion of terephthalic acid in the same system and found it to be very small, falling off to zero at the critical point. Semenchenko and Azimov [73]

found a large increase in the critical region for the dielectric constant of the nitrobenzene+hexane system.

1.7. Examples of Systems showing Incomplete Miscibility

This section will be discussed with reference to figure 1.1, which shows all the types of miscibility curves which can exist in binary liquid systems. Types A and B represent the majority of binary liquid systems, showing miscibility curves which can converge to give an upper consolute temperature. The miscibility continually decreases as the temperature falls and does not pass through a minimum. This last remark distinguishes types A and B from E and F, which can both tend to show mutual solubility minima. An example of type A is the system cyclohexane + aniline [34,48], and of type B the system benzene + water [74].

The earliest known example of a binary liquid system with a closed miscibility loop was the system nicotine + water found by Hudson [75]. Systems of type C appear to be restricted in the main to mixtures of amines, alcoholic ethers, or ketones with water, and to mixtures of amines or phenols with glycerol. Examples of this type are shown in the following table (where the mole fraction quoted is that of component 2).

Component 1	Component 2	L.C.Point T_l °C	L.C.Point x_l	U.C.Point T_u °C	U.C.Point x_u	Reference
water	nicotine	61	0.05	210	0.05	Hudson[75]
water	2:4 lutidine	23	0.054	189	0.093	Andon & Cox[45]
water	2:5 lutidine	13	0.058	207	0.095	"
water	2:6 lutidine	34	0.067	231	0.105	"
glycerol	guaiacol	40	-	83	-	McEwan[76]
glycerol	m-toluidine	7	-	120	-	Parvatiker & McEwan[77]

Types D,E and F are all modifications of the closed loop, and these are shown by pairs of liquids similar to those quoted above.

Type	Component 1	Component 2	T_l °C	T_u °C	Reference
D	water	triethylamine	18	-	Rothmund[6]
D	water	γ - collidine	6	-	"
E	water	methylethylketone	-	150	"
E	water	isobutyl alcohol	-	120	Dolgolenko[78]
F	water	diethyl ether	-	-	Klobbie[79]. Kuenen & Robson[7]

REFERENCES FOR CHAPTER ONE

1. D. Abaschew 'Recherches sur la dissolubilité mutuelle des liquides' - Bulletin de la société impériale des naturalistes de Moscau, 30, 271, (1857)
2. W. Alexejew, Wied.Ann., 28, 305, (1886)
3. J. Duclaux, Journ. de Phys., (1), 5, 13, (1876)
4. F. Guthrie, Phil.Mag. (5), 18, 29 and 499, (1884)
5. F. Schreinemakers, Z.Phys.Chem.,23, 417,(1897)
6. V. Rothmund, Z.Phys. Chem., 26, 433, (1898)
7. J. Kuenen and W. Robson, Phil.Mag.,(5), 48, 180,(1899)
8. J. Kuenen, Phil. Mag.,(6), 637, (1903).
9. V. Rothmund, 'Löslichkeit und Löslichkeitbeinflussung', J.A. Barth, Leipzig, (1907), p 66-78
10. J. Kuenen, 'Verdampfung und Verflüssigung von Gemischen', J.A. Barth, Leipzig, (1906), p 146-183
11. L. Tisza, J.Phys.Coll.Chem., 54, 1317, (1950)
12. L. Tisza, 'Phase Transformations in Solids', John Wiley and Sons, (1951), p.1.
13. M. Smoluchowski, Ann. Phys. (4), 25, 205, (1908)
14. L. Ornstein and F. Zernike, Proc. Acad.Sci. Amsterdam, 17, 793, (1914)
15. Idem, ibid, 18, 1529, (1916)
16. Idem, ibid, 19, 1321, (1917)

17. Idem, Physik.Z., 19, 134, (1918)

18. Idem, ibid, 27, 761, (1926)

19. Y. Rocard, J. Phys. (7), 4, 165, (1933)

20. O. Klein and L. Tisza, Phys.Rev., 76, 1861, (1949)

21. R. Fürth, 'Changements de Phases', Société de Chimie Physique, Paris, p 59,(1952)

22. R. Fürth and C.L. Williams, P.R.S., 224A, 104, (1954)

23. B.H. Zimm, J.Phys. Coll.Chem., 54, 1306, (1950)

24. Lord Rayleigh, Phil. Mag., 47, 375, (1899)

25. A. Einstein, Ann. Physik., 33, 1275, (1910)

26. A. Rousset, Ann. Phys. 5, 5, (1936)

27. R.S. Krishan, Proc. Ind.Acad. Sci., 2, 21, (1934)

28. Idem, ibid, 5, 577, (1937)

29. S.G. Mason and O. Maass., Can.J. Chem., 26B, 597, (1948)

30. Chow. Quantie, Proc.Roy.Soc., A224, 90 (1954)

31. A.L. Babb and H.G. Drickamer, Proc.Roy.Soc., 655, (1954)

32. L.D. Roberts and J.E. Mayer, J.Chem.Phys., 9, 852, (1941)

33. R.L. McIntosh, J.R. Dacey and O. Maass, Can.J.Res.,B17, 241, (1939)

34. R.W. Rowden and O.K. Rice, J. Chem. Phys., 19, 1423, (1951)

35. J.R. Wentorf, J.Chem. Phys., 24, 607, (1956)

36. K.E. MacCormack and W.G. Schneider, Can.J.Chem., 29, 699, (1951)

37. A. Michels, B Blaisse and C. Michels, Proc.Roy Soc., A 160, 358 (1937)

38. O.K. Rice, J.Chem.Phys., 23, 169 (1955)

39. E.A. Guggenheim, J.Chem.Phys., 13, 257 (1945)

40. B. Widom and O.K. Rice, J.Chem.Phys., 23, 1250 (1955)

41. H.W. Habgood and W.G. Schneider, Can.J.Chem., 32, 98 (1954)

42. H.L. Johnston, W.E. Keller and A.S. Friedman, J.Am.Chem.Soc., 76, 1482 (1954)

43. R.J.L. Andon, J.D. Cox and E.F.G. Herington, Trans.Farad., Soc., 53, 410 (1957)

44. J.D. Cox, J.Chem.Soc., 4606 (1952)

45. R.J.L. Andon and J.D. Cox, J.Chem.Soc., 4601 (1952)

46. T. Andrews, Phil.Trans.Roy.Soc., 159, 575 (1869)

47. O.K. Rice , Chem.Rev., 44, 69 (1949)

48. O. Flaschner, J Chem.Soc., 95, 668 (1909)

49. D. Atack and O.K. Rice, Dis.Farad.Soc., 15, 210 (1953)

50. D Atack and O.K. Rice, J.Chem.Phys., 22, 382 (1954)

51. O.K. Rice, J.Chem.Phys., 23, 164 (1955)

52. B.H. Zimm, J.Chem.Phys., 20, 538 (1952)

53. Ram Gopal and O.K. Rice, J.Chem.Phys., 23, 2428 (1955)

54. J.H. Hildebrand, B.J. Alder, J.W. Beams and H.M. Dixon, J.Phys. Chem., 58, 577 (1954)

55. M.A. Weinberger and W.G. Schneider, Can.J.Chem., 30, 422, (1952)

56. H.D. Baehr, Z. Electrochem., 58, 416, (1954)

57. M.A. Weinberger, W.G. Schneider and H.W. Habgood, Can.J.Chem., 30, 815, (1952)

58. W.G. Schneider and H.W. Habgood, J.Chem.Phys., 21, 2080, (1953)

59. S.G. Whiteway and S.G. Mason, Can.J.Chem., 31, 569, (1953)

60. J. Marsden and O. Maass, Can.J.Res., B13, 296, (1935)

61. D.B. Pall, J.W. Broughton and O. Maass, Can.J.Res., B16, 230, (1938)

62. V.K. Semenchenko and E.L. Zorina, Doklady Akad. Nauk. S.S.S.R., 84, 1191, (1952)

63. A. Michels and J. Strijland, Physica, 16, 813, (1950

64. W.G. Schneider, Can.J.Chem., 29, 243, (1951)

65. idem, J.Chem. Phys., 18, 1300 (1950)

66. W.G. Schneider and A. Chynoweth, J.Chem.Phys., 19, 1607, (1951)

67. A.G. Chynoweth and W.G. Schneider, J.Chem.Phys., 19, 1566, (1951)

68. G.F. Alfrey and W.G. Schneider, Dis.Farad.Soc., 15, 218, (1953)

69. D. Sette, J.Chem.Phys., 21, 558 (1953)

70. G. Jura, D. Fraga, G. Maki and J.H. Hildebrand, Proc. Nat.Acad.Sci. U.S., 39, 19,(1953)

71 V.K. Semenchenko and V.P. Skripov. Zhur Fiz.Khim., 29, 194,(1955)

72. I.R. Krichevski and Yu. V. Tsekhanskaya, Zhur Fiz.Khim., 30, 2315 (1956)

73. V.K. Semenchenko and M. Azimov, Zhur.Fiz.Khim., 30, 1821 (1956)

74. International Critical Tables, 3, 389 (1928)

75. C. Hudson, Z.Phys.Chem., 47, 113 (1903)

76. B. McEwan, J.Chem.Soc., 123, 2284 (1923)

77. R. Parvatiker and B. McEwan, J.Chem.Soc., 125, 1484 (1924)

78. W. Dolgolenko, Z.Phys.Chem., 62, 499 (1908)

79. E. Klobbie, Z.Phys.Chem., 24, 615 (1897)

CHAPTER TWO

THE THERMODYNAMICS OF CRITICAL BEHAVIOUR

2.1 Thermodynamic Functions

In this section the thermodynamic functions used to describe the conditions for the coexistence of several phases are developed. In practice it is usually convenient to define an equilibrium state in terms of the equilibrium values of the total pressure (p), the temperature (T), and the total number of moles of each component (n_i) in each of the phases of the system. With this choice of independent variables the equilibrium properties of any system are best correlated by means of the Gibbs Free Energy (G) and its partial derivatives with respect to the independent variables.

If we consider a single phase of this system in which the independent variables may all change, then the complete differential of G is,

$$dG = -S\,dT + V\,dp + \sum_i \mu_i\,dn_i \qquad (1),$$

where S and V are respectively the entropy and volume of the phase and μ_i is the chemical potential of the i th. component. As the free energy is a function of T, p, n_i

we can also write,

$$dG = \left(\frac{\partial G}{\partial T}\right)_{p,n_i} dT + \left(\frac{\partial G}{\partial p}\right)_{T,n_i} dp + \sum_i \left(\frac{\partial G}{\partial n_i}\right)_{T,p,n_j} dn_i \quad (2)$$

where constant n_j means that all the n values except n_i are constant. Comparing equations (1) and (2) enables the coefficients in equation (2) to be identified as,

$$\left(\frac{\partial G}{\partial T}\right)_{p,n_i} = -S \quad ,$$

$$\left(\frac{\partial G}{\partial p}\right)_{T,n_i} = V \quad , \qquad (3)$$

$$\left(\frac{\partial G}{\partial n_i}\right)_{T,p,n_j} = \mu_i \qquad \text{where } i \neq j \, .$$

When several phases are in equilibrium the values of T, p, μ_i are the same at all points in the system (assuming that gravitationally induced pressure gradients may be ignored).

The chemical potential of a component in a phase is a function of the mole fractions of all the components in that phase. For perfect solutions there is a simple relationship of the form [1,2],

$$\mu_i^{\alpha} = \mu_i^{o} + RT \ln x_i^{\alpha} \qquad (4),$$

where μ_i^{α} is the chemical potential of i in phase α , and where μ_i^{o} is the chemical potential of pure i and is a function only of temperature and pressure. For an imperfect solution we have,

$$\mu_i^{\alpha} = \mu_i^{\circ} + RT \ln a_i^{\alpha} \qquad (5),$$

where a_i^{α} is the activity of the i th component in phase α.

In order to write (5) in the same form as (4) we put,

$$\mu_i^{\alpha} = \mu_i^{\circ} + RT \ln x_i^{\alpha} \gamma_i^{\alpha} \qquad (6),$$

where γ_i^{α} is the activity coefficient ofthe i th component in phase α . If phases α and β are in equilibrium we have, necessarily,

$$\mu_i^{\alpha} = \mu_i^{\beta} \quad \text{whence,} \quad a_i^{\alpha} = a_i^{\beta} \quad \text{and} \quad x_i^{\alpha}\gamma_i^{\alpha} = x_i^{\beta}\gamma_i^{\beta} \quad (7).$$

In Guggenheim's notation an alternative form of (5) is used,

$$\mu_i^{\alpha} = RT \ln \lambda_i^{\alpha} \qquad (8),$$

where λ_i^{α} is the absolute activity of component i in phase α .

We have up to now been dealing exclusively with the equilibrium between liquid phases, but one of the equilibrium phases can be gaseous, and for such a phase it is more usual to express the chemical potential of any component in terms of its partial pressure. For a perfect gas mixture we have for component i in the vapour phase (v),

$$\mu_i^{v} = \mu_i^{+} + RT \ln p_i \qquad (9),$$

where μ_i^{+} is the standard chemical potential of i at one atmosphere pressure and is a function of temperature only, and p_i is the partial pressure of i measured in atmospheres. For any real gas we can now write,

$$\mu_i^{v} = \mu_i^{+} + RT \ln p_i^{*} \qquad (10),$$

where p_i^* is called the fugacity of component i in the vapour phase and is also measured in atmospheres. As the total pressure $p(= \sum_i p_i)$ tends to zero then $\frac{p_i^*}{p_i} \rightarrow 1$.

Equation (9) provides a method of determining the chemical potential of any component in solution. Thus if there is a vapour phase in equilibrium with the liquid phase (or phases), then the chemical potential of a component in the vapour is the same as that in the liquid. If the solution were perfect (this implies the existence of only one liquid phase) then the chemical potential of i is a linear function of the logarithm of its mole fraction x_i; but if deviations from ideality occur then some other way must be found to calculate the chemical potentials. Calculations based on the properties of the vapour phase can be used to obtain these chemical potentials, as the deviation from ideality of the vapour phase is small due to its low density. Interactions between molecules in the vapour phase will occur and the evaluation of these will lead to more accurate values of the chemical potentials; but even if these interactions cannot be determined the resulting error is usually small especially in the case of non-polar gases at low pressures.

The interactions in the gas phase are conveniently represented by an equation which shows how the vapour deviates from the ideal gas law. For a one component vapour the pressure may be expressed in terms of the volume by a virial equation of the form:

$$p = \frac{nRT}{V}\left(1 + \frac{nB}{V} + \frac{n^2C}{V^2} + \frac{n^3D}{V^3} + \cdots\right) \qquad (11),$$

where n is the number of moles of gas in volume V. If the vapour pressure is small it is usually sufficient to take account only of the second virial coefficient (B) and ignore third and higher virial coefficients (C,D etc.): one can then write for a one component vapour,

$$p = \frac{nRT}{V}\left(1 + \frac{nB}{V}\right) \qquad (12).$$

When we consider a mixture of two vapours equation (12) becomes,

$$p = (n_1 + n_2)\frac{RT}{V} + \frac{RT}{V^2}\left(B_{11}n_1^2 + 2B_{12}n_1n_2 + B_{22}n_2^2\right) \qquad (13),$$

where n_1 and n_2 are the numbers of moles of the two components in a volume V. B_{11} and B_{22} are the second virial coefficients for the pure species 1 and 2, and B_{12} is the mixed second virial coefficient, which is determined by the interactions between molecules of species 1 and molecules of species 2.

The chemical potentials of both the components are then given by,

$$\mu_1 = \mu_1^+ + RT \ln\left(\frac{n_1 RT}{V}\right) + 2RT\left(\frac{B_{11}n_1 + B_{12}n_2}{V}\right)$$

$$\mu_2 = \mu_2^+ + RT \ln\left(\frac{n_2 RT}{V}\right) + 2RT\left(\frac{B_{12}n_1 + B_{22}n_2}{V}\right) \qquad (14)$$

The fugacities are thus given by,

$$\ln p_1^* = \ln\left(\frac{n_1 RT}{V}\right) + 2\left(\frac{B_{11}n_1 + B_{12}n_2}{V}\right)$$

$$\ln p_2^* = \ln\left(\frac{n_2 RT}{V}\right) + 2\left(\frac{B_{12}n_1 + B_{22}n_2}{V}\right) \qquad (15)$$

If all the B terms were zero then the gas would be ideal and the fugacity would equal the vapour pressure. Equation (15) can thus be written in the form,

$$\ln \frac{p_1^*}{p_1^{id}} = 2\left(\frac{B_{11}n_1 + B_{12}n_2}{V}\right)$$

$$\ln \frac{p_2^*}{p_2^{id}} = 2\left(\frac{B_{12}n_1 + B_{12}n_2}{V}\right) \qquad (16)$$

2.2. The Thermodynamic Properties of Binary Liquid Mixtures

When one discusses the properties of liquid mixtures it is usual to express them in terms of the changes in the various extensive properties which occur when one mole of solution is formed from its components. For any such property, for example the free energy G, we can write the change on mixing x_1

moles of component 1 and $x_2(=1-x_1)$ moles of component 2 as,

$$g^M = g - x_1 g_1^\circ - x_2 g_2^\circ \qquad (17),$$

where g^M is the molar free energy of mixing, g is the molar free energy of the solution of composition x_1, and g_1° and g_2° are the molar free energies of the pure components. For a perfect solution the free energy of mixing is g^{Mid}, and a new quantity g^E can be defined as the excess of the free energy of mixing of an actual solution over that of a perfect solution.

$$g^E = g^M - g^{Mid} \qquad (18)$$

For perfect solutions the various properties can be written in terms of the mole fraction of the components as,

$$\text{(a)} \quad g^{Mid} = x_1 RT \ln x_1 + x_2 RT \ln x_2$$

$$\text{(b)} \quad s^{Mid} = -(x_1 R \ln x_1 + x_2 R \ln x_2) \qquad (19)$$

$$\text{(c)} \quad h^{Mid} = 0$$

$$\text{(d)} \quad v^{Mid} = 0$$

Combining equations (17, (18) and (19) the excess quantities may be written as,

$$\text{(a)} \quad g^E = g - x_1(\mu_1^\circ + RT \ln x_1) - x_2(\mu_2^\circ + RT \ln x_2)$$

$$\text{(b)} \quad s^E = s - x_1(s_1^\circ - R \ln x_1) - x_2(s_2^\circ - R \ln x_2)$$

$$(c)\quad h^E = h^M = h - x_1 h_1^\circ - x_2 h_2^\circ \qquad (20)$$

$$(d)\quad v^E = v^M = v - x_1 v_1^\circ - x_2 v_2^\circ$$

In the previous section the chemical potential of a component in solution was expressed in the form

$$\mu_1 = \mu_1^\circ + RT \ln x_1 \gamma_1 \qquad (6)$$

so g may be expressed as

$$g = x_1(\mu_1^\circ + RT \ln x_1 \gamma_1) + x_2(\mu_2^\circ + RT \ln x_2 \gamma_2) \qquad (21)$$

and (20a) now becomes

$$(a)\quad g^E = x_1 RT \ln \gamma_1 + x_2 RT \ln \gamma_2 \qquad (22)$$

The molar excess entropy, enthalpy and volume of mixing can be similarly expressed as

$$(b)\quad s^E = -\left(\frac{\partial g^E}{\partial T}\right)_{p,x} = -RT\left[x_1\left(\frac{\partial \ln \gamma_1}{\partial T}\right)_{p,x} + x_2\left(\frac{\partial \ln \gamma_2}{\partial T}\right)_{p,x}\right]$$
$$-R(x_1 \ln \gamma_1 + x_2 \ln \gamma_2)$$

$$(c)\quad h^E = -T^2\left(\frac{\partial (\frac{g^E}{T})}{\partial T}\right)_{p,x} = -RT^2\left[x_1\left(\frac{\partial \ln \gamma_1}{\partial T}\right)_{p,x} + x_2\left(\frac{\partial \ln \gamma_2}{\partial T}\right)_{p,x}\right]$$

$$(d)\quad v^E = \left(\frac{\partial g^E}{\partial p}\right)_{T,x} = RT\left[x_1\left(\frac{\partial \ln \gamma_1}{\partial p}\right)_{T,x} + x_2\left(\frac{\partial \ln \gamma_2}{\partial p}\right)_{T,x}\right]$$

2.3 Vapour - Liquid Equilibria

The free energy of mixing of a binary liquid mixture can be computed from analysis of the vapour pressure isotherms

for the vapour in equilibrium with the liquid. If data is available for adjacent temperatures then the entropy and the enthalpy may also be calculated. Equation (14) gives the chemical potentials of the components of a binary vapour, and combining these with equation 20 (a), the excess free energy of mixing is obtained in the form

$$g^E = x_1\left\{ \mu_1^+ + RT \ln c_1 RT + 2\ RT(B_{11}c_1 + B_{12}c_2) - \mu_1^\circ - RT \ln x_1 \right\} \quad (23)$$
$$+ x_2\left\{ \mu_2^+ + RT \ln c_2 RT + 2\ RT(B_{12}c_1 + B_{22}c_2) - \mu_2^\circ - RT \ln x_2 \right\}$$

where c_1 and c_2 represent the concentrations of the components 1 and 2 in the vapour in equilibrium with the solution of composition x_1. The relationship between μ^+ and μ° is

$$\mu_1^\circ = \mu_1^+ + RT \ln c_1^\circ RT + 2RT\ B_{11}c_1^\circ \quad (24)$$
$$\mu_2^\circ = \mu_2^+ + RT \ln c_2^\circ RT + 2RT\ B_{22}c_2^\circ$$

where c_1° and c_2° represent the vapour concentrations of the two components respectively, when they are in equilibrium with the pure liquids at temperature T.

Equation (23) now becomes

$$g^E = x_1\left\{ RT \ln \left(\frac{c_1}{c_1^\circ x_1}\right) + 2RT(B_{11}c_1 + B_{12}c_2 - B_{11}c_1^\circ) \right\} \quad (25)$$
$$+ x_2\left\{ RT \ln \left(\frac{c_2}{c_2^\circ x_2}\right) + 2RT(B_{12}c_1 + B_{22}c_2 - B_{22}c_2^\circ) \right\}$$

When virial coefficients can be neglected (25) may be written as,

$$g^E = x_1 RT \ln\left(\frac{p_1}{x_1 p_1^o}\right) + x_2 RT \ln\left(\frac{p_2}{x_2 p_2^o}\right) \qquad (26) \quad ,$$

where p_i^o is the vapour pressure of the pure component i,

Since $\left(\frac{\partial g^E}{\partial T}\right)_{p,x} = -s^E$, the excess entropy of mixing can be determined from vapour-liquid equilibrium data at two or more temperatures. The heat of mixing can also be calculated by the relationship, $h^E = -T^2 \left(\frac{\partial\left(\frac{g^E}{T}\right)}{\partial T}\right)_{p,x}$.

This procedure can lead to large errors in the calculated values of h^E and s^E because the variation of g^E with temperature $\left[\left(\frac{\partial g^E}{\partial T}\right)_{p,x} = -s^E\right]$ is usually small even though Ts^E may be comparable with g^E; and it is often more accurate to determine the heat and excess free energy of mixing independently at one temperature and then calculate the excess entropy by the identiy, $g^E = h^E - Ts^E$.

The Gibbs-Duhem equation relates the slope of the chemical potential isotherms (μ_1, x_1) and (μ_2, x_1), and can be used to provide a check upon the calculated free energy. The equation is,[3]

$$x_1\left(\frac{\partial \mu_1}{\partial x_1}\right)_{T,p} + x_2\left(\frac{\partial \mu_2}{\partial x_1}\right)_{T,p} = 0 \qquad (27);$$

and at any point on the free energy isotherm the chemical potentials must obey the relationship,

$$\left(\frac{\partial \mu_1}{\partial x_1}\right)_{T,p} \Big/ \left(\frac{\partial \mu_2}{\partial x_1}\right)_{T,p} = \frac{-x_2}{x_1} \qquad (28)$$

The check may also be applied by making a plot of $\ln\left(\frac{\gamma_1}{\gamma_2}\right)$ against mole fraction and finding the area under the curve; this should theoretically be zero[4]. This is easily proved as

$$\frac{g^E}{RT} = x_1 \ln\gamma_1 + x_2 \ln\gamma_2 \qquad 22(a),$$

whence

$$\frac{1}{RT}\left(\frac{\partial g^E}{\partial x_1}\right)_{T,p} = \left[x_1\left(\frac{\partial \ln\gamma_1}{\partial x_1}\right)_{T,p} + x_2\left(\frac{\partial \ln\gamma_2}{\partial x_1}\right)_{T,p}\right] + \ln\left(\frac{\gamma_1}{\gamma_2}\right)$$

The term in brackets is, by the Gibbs-Duhem equation, zero.

Therefore

$$\frac{1}{RT}\left(\frac{\partial g^E}{\partial x_1}\right)_{T,p} = \ln\left(\frac{\gamma_1}{\gamma_2}\right)$$

The excess free energy of mixing at $x_1 = 1$ and $x_1 = 0$ is

also zero, so

$$\int_{x_1=0}^{x_1=1} \frac{1}{RT}\left(\frac{\partial g^E}{\partial x_1}\right)_{T,p} = \frac{1}{RT}\left[\, g^E(x=1) - g^E(x=0)\right]$$

$$= 0 = \int_{x_1=0}^{x_1=1} \ln\left(\frac{\gamma_1}{\gamma_2}\right) dx_1 \qquad (29)$$

2.4 Critical Behaviour

In applying thermodynamics to critical phenomena it must be remembered that a system near its critical point shows large internal fluctuations, due to the small variation of free energy with composition; so the use of thermodynamics to describe what are in effect inhomogeneous systems must be carefully considered. These fluctuations decrease rapidly as the system moves away from the critical point, so even if thermodynamic methods are not applied to the immediate neighbourhood of the critical point, they can still be used to elucidate the onset of critical behaviour.

The first thermodynamic condition we have to consider relates to the stability of a binary liquid phase with respect to diffusion. Let there be a movement of the two components of the solution between two separate regions in the solution; this gives rise to a small amount of

heterogeneity. In order that the original solution should be stable, the partial differential of the affinity of a movement with respect to the amount of movement must be less than zero. In the case of a binary mixture this condition may be expressed as

$$\left(\frac{\partial^2 g}{\partial x^2}\right)_{T,p} > 0 \qquad (30)$$

while at the critical point, indicated by subscript c,

$$\left(\frac{\partial^2 g}{\partial x^2}\right)_{T_c,p_c} = 0 \text{ at } x_c \qquad (31).$$

The curves of μ against x at constant temperature tend to flatten out as the critical point is approached from the one phase region. At the critical point there is a point of inflexion so that,

$$\left(\frac{\partial^3 g}{\partial x^3}\right)_{T_c,p_c} = 0 \text{ at } x_c \qquad (32).$$

In the Gibbsian treatment of the critical point the next order differential, $\left(\frac{\partial^4 g}{\partial x^4}\right)_{T_c,p_c}$, is positive, but according to Zimm[5], this and all the other higher derivatives should be zero at the critical point. In the theories of Mayer[6,7] and Rice[8,9,10,], the

chemical potential isotherm (μ, x) contains a horizontal portion.

If the excess free energy of mixing is written in the form,

$$g^E = g - x_1(\mu_1^\circ + RT \ln x_1) - x_2(\mu_2^\circ + RT \ln x_2) \qquad (20)(a),$$

then the condition for the stability of a binary liquid phase can be written in terms of the excess free energy of mixing as

$$\frac{1}{RT}\left(\frac{\partial^2 g^E}{\partial x^2}\right)_{T,p} > -\frac{1}{x(1-x)} \qquad (33)$$

At the critical temperature T_c

$$\frac{1}{RT_c}\left(\frac{\partial^2 g^E}{\partial x^2}\right)_{T_c,p} \geq -\frac{1}{x(1-x)} \qquad (34),$$

where the equality identifies the mole fraction or the range of mole fractions at the critical point. We can now represent the passage from a one phase to a two phase system as the movement of a series of isotherms

$$\left\{\frac{1}{RT}\left(\frac{\partial^2 g^E}{\partial x^2}\right)_{T,p}, x\right\}$$

towards and into the unstable region bounded by $\frac{-1}{x(1-x)}$.

At an upper critical point (x_u, T_u) the approach to the two phase region results from decreasing the temperature,

so,

$$\frac{\partial}{\partial T}\left[\frac{1}{RT}\left(\frac{\partial^2 g^E}{\partial x^2}\right)_{T,p}\right] > 0 \text{ at } (x_u, T_u) \qquad (35)$$

this inequality leads to

$$\left(\frac{\partial^2 h^E}{\partial x^2}\right)_{T_u,p} < 0; \quad \left(\frac{\partial^2 s^E}{\partial x^2}\right)_{T_u,p} < \frac{R}{x_u(1-x_u)} \qquad (36)$$

For a lower critical point (x_l, T_l)

$$\left(\frac{\partial^2 h^E}{\partial x^2}\right)_{T_l,p} > 0; \quad \left(\frac{\partial^2 s^E}{\partial x^2}\right)_{T_l,p} > \frac{R}{x_l(1-x_l)} \qquad (37)$$

If, furthermore [11] g^E, h^E and s^E maintain the same sign for all values of x at a given temperature, it follows that at an upper critical point

$$g^E > 0; \quad h^E > 0; \quad s^E > 0 \text{ or } < 0 \text{ but satisfying (36) .. (38),}$$

at a lower critical point

$$g^E > 0; \quad h^E < 0; \quad s^E < 0 \text{ but satisfying (37) .. (39).}$$

These conditions may be summarised by saying that upper critical behaviour is related to large positive deviations of the free energy of mixing and enthalpy of mixing from ideality, while lower critical behaviour results from sufficiently large negative deviations of the entropy of mixing from ideality[11].

2.5 The Transition through the Critical Region

The condition for the stability of a binary liquid phase, $\left(\frac{\partial^2 g}{\partial x^2}\right)_{T,p} > 0$, can be used to study the formation

of two phases from an initially single phase system as the temperature is altered. In a closed system at constant temperature and pressure the stable phase distribution corresponds to a minimum of Gibbs Free Energy (G). Thus, if the free energy of a system is decreased by the formation of a new phase, then that phase will appear spontaneously. On the other hand if the free energy is decreased by the elimination of a phase, then that phase will spontaneously disappear. These conditions can best be illustrated in terms of figure 2.1, which shows several possible ways in which the molar free energy ($g_{T,P}$) of a homogeneous liquid phase can depend upon composition. For each curve in figure 2·1 the states of the system which correspond to a minimum value of the free energy will now be defined.

Figure 2.1. Curve 1. In this case the molar free energy of a homogeneous solution is a continuous function of the mole fraction, such that the curvature, $\left(\frac{\partial^2 g}{\partial x_2^2}\right)_{T,p}$, is greater than zero for all values of x_2. Let us consider a system containing X_2 moles of component 2 initially

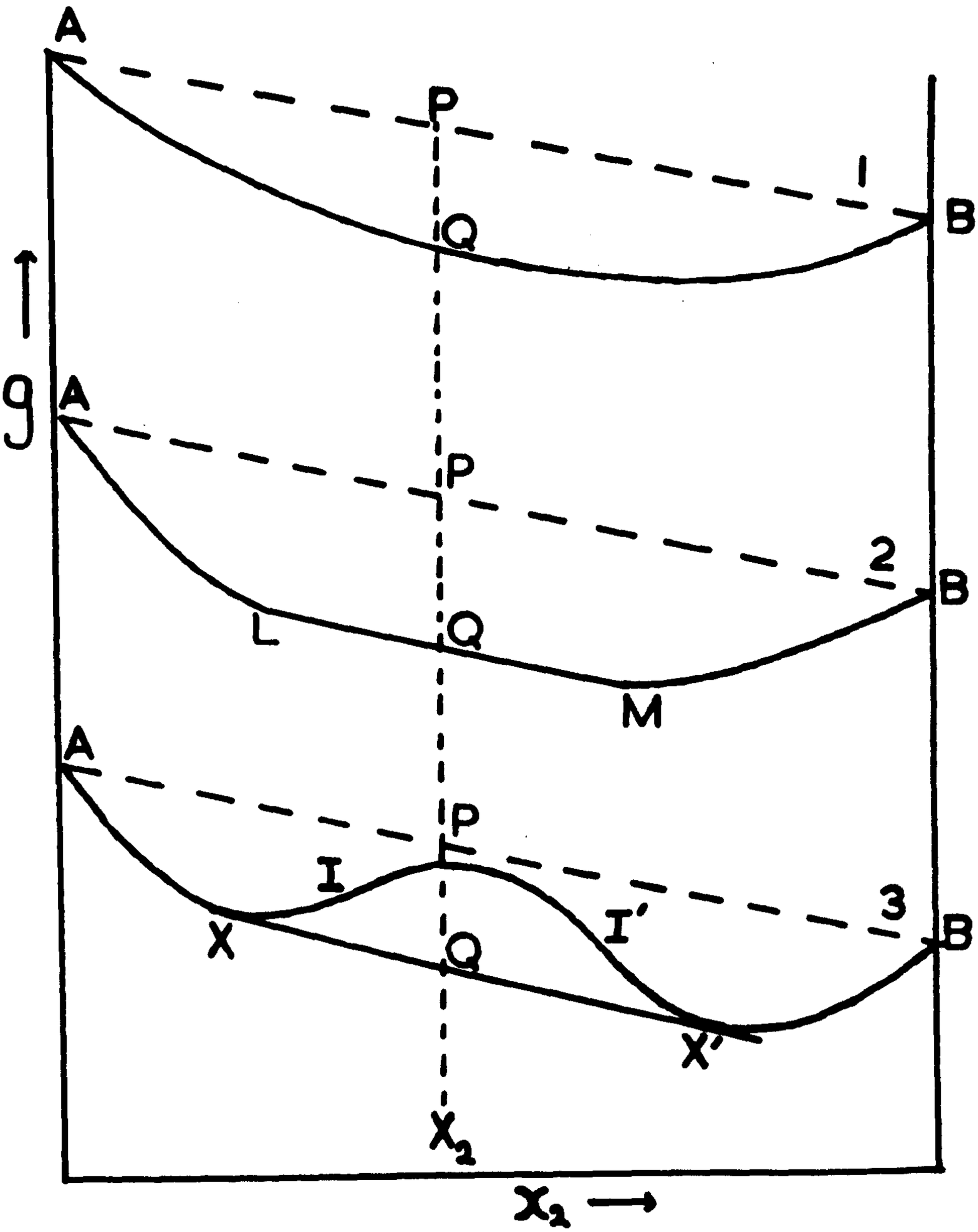

FIGURE 2·1 FREE ENERGY ISOTHERMS IN THE CRITICAL REGION OF A BINARY LIQUID SYSTEM

separated from $(1-X_2)$ moles of component 1. The molar free energy of this system is represented in curve 1 by a point P on the line AB, where A and B denote the molar free energies of the pure components. If the two phases are placed in contact, passage of components across the phase boundary will occur until both the phases have a composition given by X_2. The molar free energies of the two phases will approach each other from A and B along the curve, and the mean molar free energy of the two phase system will fall from P to Q. Mutual solution will occur spontaneously and will continue as long as the free energy of the system decreases. Thus the two phases will form a homogeneous phase represented by Q; and it follows that any state of this system which contains two liquid phases in contact must be unstable. Therefore the stable state of a binary liquid system, for which $\left(\frac{\partial^2 g}{\partial x^2}\right)_{T,p} > 0$ for all values of x, is a single liquid phase.

Curve 2. Curve ALMB represents the molar free energy of a homogeneous binary solution in which $\left(\frac{\partial^2 g}{\partial x_2^2}\right)_{T,p}$ is greater than zero in the ranges AL and MB and identically

equal to zero in the range LM. When the two components exist as separate phases, $1-X_2$ moles of component 1 and X_2 moles of component 2, the molar free energy of the system is equal to P. As solution occurs the molar free energies of the two phases move towards L and M as the free energy of the system falls from P to Q. Let us now consider further progress of the system towards Q. The free energy of the system will remain constant at Q while the molar free energies of the two phases converge on Q. Thus over the whole of the passage from L and M to Q, the free energy of the system remains constant; so while there has been no driving force making this change occur there has likewise been nothing to prevent it. Consequently states of the system might be recognised which are not homogeneous but do not contain two liquid phases separated by a distinct boundary. In this composition range molecular fluctuations can produce large changes of localised composition and density; for such changes, providing they are not too large, cannot lead to an increase in the free energy. We recall that in section 1.3, critical opalescence was explained in terms of changes in the refractive index produced by molecular fluctuations of composition or density.

Curve 3. In this case the curve consists of three distinct regions: along AXI the curvature is positive, at I it is zero and between I and I′ it is negative, at I′ it is again zero and between I′ and B it is positive. As before we consider a system initially consisting of the pure components in different phases, and whose molar free energy is given by point P: As solution occurs the molar free energies of the two phases change along the curves AXI and BX′I′: the free energy of the system as a whole decreases from P along the line PQ, attains a minimum value at Q (when the compositions of the phases are X and X′) and then increases along QP. The stable state of the system, corresponding to the minimum of the free energy, is therefore represented by two coexisting phases of compositions X and X′. The points X and X′ are the points of contact of a common tangent to the curve, such that the chemical potential of each component is the same in both phases. We may also note that the curves XI and X′I′ represent one phase states metastable with respect to the system containing two phases (X and X′) in contact.

The formation of two liquid phases from an initially homogeneous system on the alteration of temperature or

pressure must occur by a change in the free energy isotherms from uninflected to inflected curves. We shall consider here two possible ways in which the transition through the critical region occurs. Let us assume that the transition from free energy curves of the type 3 to those of type 1 takes place on decreasing the temperature at constant pressure: that is the binary liquid system shows lower consolute behaviour.

In the classical or van der Waals' transition the points X, I, X', I' converge on to a single point on the critical free energy VS. mole fraction isotherm. Above T_c the system consists of two liquid phases in equilibrium; at T_c the compositions of the two phases become identically equal to x_c, the unique point on the critical isotherm where both $\left(\frac{\partial^2 g}{\partial x^2}\right)_{T_c,p_c}$ and $\left(\frac{\partial^3 g}{\partial x^3}\right)_{T_c,p_c}$ are zero. Below T_c the system contains one homogeneous stable phase. The classical transition is not the only way in which free energy curves of type 3 can change to those of type 1. For example, on decreasing the temperature, the points X and X' approach each other but fail to meet before I and I' converge on X and X' respectively. In this case the

system is transformed into a state where molecular fluctuations prevent the formation of a homogeneous state, but cannot maintain two distinct phases in equilibrium. A free energy curve of type 3 is transformed into type 2 at the critical temperature T_M. As the temperature is lowered LM gradually shortens, and is finally eliminated as X and X' converge on to a unique point on the isotherm at Tc. A transition of this kind leads to a solubility diagram with a horizontal section at T_M capped by a region extending to Tc, in which a single but unhomogeneous phase exists.

2.6. Effects of Temperature and Pressure on Miscibility

The equilibrium set up between two phases of a binary liquid system has been discussed by Rice [9], who obtained equations expressing the effects of both temperature and pressure upon the miscibility. His thermodynamic argument for the case of a binary liquid mixture under a pressure greater than its vapour pressure (i.e. two liquid phase equilibrium) may be summarised as follows.

Let us consider two liquid phases (α, β) in equilibrium, and calculate how small changes of chemical potentials of the components (1,2) occur as results of changes of

temperature, pressure and mole fraction. This can be expressed for component 1 in phase α :

$$\mu_1^\alpha = f(T, p, x_1^\alpha)$$

$$\therefore \quad d\mu_1^\alpha = \left(\frac{\partial \mu_1^\alpha}{\partial T}\right)_{p,x_1^\alpha} dT + \left(\frac{\partial \mu_1^\alpha}{\partial p}\right)_{T,x_1^\alpha} \cdot dp + \left(\frac{\partial \mu_1^\alpha}{\partial x_1^\alpha}\right)_{T,p} dx_1^\alpha \quad \ldots(40)$$

This equation may be written as

$$\text{(i)} \quad d\mu_1^\alpha = -s_1^\alpha \cdot dT + v_1^\alpha \, dp + \left(\frac{\partial \mu_1^\alpha}{\partial x_1^\alpha}\right)_{T,p} \cdot dx_1^\alpha \qquad (41),$$

where $\left(\frac{\partial \mu_1^\alpha}{\partial T}\right)_{p,x_1^\alpha} = -s_1^\alpha$ (the partial molar entropy of component 1 in phase α), and $\left(\frac{\partial \mu_1^\alpha}{\partial p}\right)_{T,x_1^\alpha} = v_1^\alpha$ (the partial molar volume of component 1 in phase α). There are necessarily three more equations of this type. Thus

$$\text{(ii)} \quad d\mu_2^\alpha = -s_2^\alpha \cdot dT + v_2^\alpha \cdot dp + \left(\frac{\partial \mu_2^\alpha}{\partial x_2^\alpha}\right)_{T,p} \cdot dx_2^\alpha,$$

$$\text{(iii)} \quad d\mu_1^\beta = -s_1^\beta \, dT + v_1^\beta \, dp + \left(\frac{\partial \mu_1^\beta}{\partial x_1^\beta}\right)_{T,p} \cdot dx_1^\beta, \qquad (41)$$

$$\text{(iv)} \quad d\mu_2^\beta = -s_2^\beta \, dT + v_2^\beta \, dp + \left(\frac{\partial \mu_2^\beta}{\partial x_2^\beta}\right)_{T,p} \cdot dx_2^\beta$$

For each two component phase the Gibbs-Duhem equation must also be satisfied, and this gives two further equations,

$$\text{(i)} \quad x_1^{\alpha}\left(\frac{\partial \mu_1^{\alpha}}{\partial x_1^{\alpha}}\right)_{T,p} = x_2^{\alpha}\left(\frac{\partial \mu_2^{\alpha}}{\partial x_2^{\alpha}}\right)_{T,p}$$

$$\text{(ii)} \quad x_1^{\beta}\left(\frac{\partial \mu_1^{\beta}}{\partial x_1^{\beta}}\right)_{T,p} = x_2^{\beta}\left(\frac{\partial \mu_2^{\beta}}{\partial x_2^{\beta}}\right)_{T,p} \qquad (42)$$

As equilibrium exists between the two phases we have,

$$\text{(i)} \quad \mu_1^{\alpha} = \mu_1^{\beta}$$

$$\text{(ii)} \quad \mu_2^{\alpha} = \mu_2^{\beta} \qquad (43)$$

and therefore

$$\text{(i)} \quad d\mu_1^{\alpha} = d\mu_1^{\beta}$$

$$\text{(ii)} \quad d\mu_2^{\alpha} = d\mu_2^{\beta} \qquad (44)$$

Combining equation (44)(i) with equations (41)(i) and (iii), and equation (44)(ii) with equations (41)(ii) and (iv), gives

$$\text{(i)} \quad -(s_1^{\alpha} - s_1^{\beta})dT + (v_1^{\alpha} - v_1^{\beta})dp + \left(\frac{\partial \mu_1^{\alpha}}{\partial x_1^{\alpha}}\right)_{T,p} dx_1^{\alpha} - \left(\frac{\partial \mu_1^{\beta}}{\partial x_1^{\beta}}\right)_{T,p} dx_1^{\beta} = 0$$

$$\text{(ii)} \quad -(s_2^{\alpha} - s_2^{\beta})dT + (v_2^{\alpha} - v_2^{\beta})dp + \left(\frac{\partial \mu_2^{\alpha}}{\partial x_2^{\alpha}}\right)_{T,p} dx_2^{\alpha} - \left(\frac{\partial \mu_2^{\beta}}{\partial x_2^{\beta}}\right)_{T,p} dx_2^{\beta} = 0 \qquad \text{,...(45)}$$

Equation (45)(ii) may be modified by means of the Gibbs-Duhem equations (42)(i) and (ii) so that,

$$-(s_2^{\alpha} - s_2^{\beta})dT + (v_2^{\alpha} - v_2^{\beta})dp + \frac{x_1^{\alpha}}{x_2^{\alpha}}\left(\frac{\partial \mu_1^{\alpha}}{\partial x_1^{\alpha}}\right)_{T,p} dx_2^{\alpha} - \frac{x_1^{\beta}}{x_2^{\beta}}\left(\frac{\partial \mu_1^{\beta}}{\partial x_1^{\beta}}\right)_{T,p} dx_2^{\beta} = 0 \qquad (46)$$

The relationships, $dx_2^{\alpha} = -dx_1^{\alpha}$ and $dx_2^{\beta} = -dx_1^{\beta}$, enable equation (46) to be written,

$$-(s_2^{\alpha} - s_2^{\beta})dT + (v_2^{\alpha} - v_2^{\beta})dp - \frac{x_1^{\alpha}}{x_2^{\alpha}}\left(\frac{\partial \mu_i^{\alpha}}{\partial x_1^{\alpha}}\right)_{T,p} dx_1^{\alpha} + \frac{x_1^{\beta}}{x_2^{\beta}}\left(\frac{\partial \mu_i^{\beta}}{\partial x_1^{\beta}}\right)_{T,p} dx_1^{\beta}$$

$$= 0 \qquad (47)$$

Eliminating $\left(\frac{\partial \mu_i^{\alpha}}{\partial x_1^{\alpha}}\right)_{T,p} dx_1^{\alpha}$ between equations 45 (i) and (47) leads to,

$$0 = -\left[(s_1^{\alpha} - s_1^{\beta}) + \frac{x_2^{\alpha}}{x_1^{\alpha}}(s_2^{\alpha} - s_2^{\beta})\right] dT + \left[(v_1^{\alpha} - v_1^{\beta}) + \frac{x_2^{\alpha}}{x_1^{\alpha}}(v_2^{\alpha} - v_2^{\beta})\right] dp$$

$$+ \frac{x_1^{\beta} - x_1^{\alpha}}{x_1^{\alpha} x_2^{\beta}}\left(\frac{\partial \mu_i^{\beta}}{\partial x_1^{\beta}}\right)_{T,p} dx_1^{\beta} \qquad (48),$$

while eliminating $\left(\frac{\partial \mu_i^{\beta}}{\partial x_1^{\beta}}\right)_{T,p} dx_1^{\beta}$ between the same equations leads to ,

$$0 = -\left[(s_1^{\alpha} - s_1^{\beta}) + \frac{x_2^{\beta}}{x_1^{\beta}}(s_2^{\alpha} - s_2^{\beta})\right] dT + \left[(v_1^{\alpha} - v_1^{\beta}) + \frac{x_2^{\beta}}{x_1^{\beta}}(v_2^{\alpha} - v_2^{\beta})\right] dp$$

$$+ \frac{x_1^{\beta} - x_1^{\alpha}}{x_2^{\alpha} x_1^{\beta}}\left(\frac{\partial \mu_i^{\alpha}}{\partial x_1^{\alpha}}\right)_{T,p} dx_1^{\alpha} \qquad (49)$$

Let us assume that $x_1^{\alpha} > x_1^{\beta}$ and therefore $x_2^{\alpha} < x_2^{\beta}$. A decrease in the 'miscibility gap' $(x_1^{\alpha} - x_1^{\beta})$ implies that dx_1^{α} is negative and dx_1^{β} is

positive. For constant pressure equation (48) gives,

$$\left[(s_1^{\alpha} - s_1^{\beta}) + \frac{x_2^{\alpha}}{x_1^{\alpha}} (s_2^{\alpha} - s_2^{\beta})\right] dT < 0 \qquad (50),$$

and (49) gives,

$$\left[(s_1^{\alpha} - s_1^{\beta}) + \frac{x_2^{\beta}}{x_1^{\beta}} (s_2^{\alpha} - s_2^{\beta})\right] dT > 0 \qquad (51)$$

Rearranging equation (51)

$$\left[-\frac{x_1^{\beta}}{x_2^{\beta}} \frac{x_2^{\alpha}}{x_1^{\alpha}} (s_1^{\alpha} - s_1^{\beta}) - \frac{x_2^{\alpha}}{x_1^{\alpha}} (s_2^{\alpha} - s_2^{\beta})\right] dT < 0 \qquad (52)$$

and adding equations (52) and (50) gives

$$(s_1^{\alpha} - s_1^{\beta})\left(1 - \frac{x_1^{\beta}}{x_2^{\beta}} \frac{x_2^{\alpha}}{x_1^{\alpha}}\right) dT < 0 \qquad (53)$$

Now $1 - \frac{x_1^{\beta} x_2^{\alpha}}{x_2^{\beta} x_1^{\alpha}}$ is $+ve$,

so $$(s_1^{\alpha} - s_1^{\beta})\, dT < 0 \qquad (54)$$

If the system is to show a U.C.T. the miscibility gap decreases with increasing temperature so $(s_1^{\alpha} - s_1^{\beta}) < 0$, which means that the molar entropy of component 1 increases with dilution.

In the case of a L.C.T. dT is $-ve$ so $(s_1^{\alpha} - s_1^{\beta}) > 0$,

which means that the molar entropy decreases on dilution.

The effect of pressure may be similarly considered: if the miscibility gap decreases at constant temperature ,

$$(v_1^{\alpha} - v_1^{\beta})\, dp > 0 \qquad (55)$$

If the gap decreases with increase of pressure the molar volume must decrease on dilution.

2.7. Effect of Impurity on Miscibility

A great many experiments have been carried out to test the effect of a third component upon the phase diagram, and it has been found that these effects are often unexpectedly large[9]. For example the addition of 3% of sodium chloride to the critical mixture of phenol and water raised the critical temperature by almost 40°C, while in a similar case a 1% solution of sodium oleate lowered the critical temperature by 20°C. These are examples of the two types of impurity which can affect a phase diagram: the first is a substance which is more soluble in one of the pure components than in the other and is not absorbed at the interface; and the second is a substance which is nearly insoluble in both of the pure components, but is strongly absorbed at the interface.

Let us consider [10] a two phase liquid system of two principal components, A and B, and a small amount of impurity, C. We shall designate the phase richer in A by the prime (^{1}), and the phase less rich in A by the double prime (^{11}). The chemical potentials, which are

common to both phases, are given without primes.

The Gibbs-Duhem equation must be satisfied by each phase,

$$\text{(i)}\quad x_A^1\, d\mu_A + x_B^1\, d\mu_B + x_C^1\, d\mu_C = 0$$
$$\text{(ii)}\quad x_A^{11}\, d\mu_A + x_B^{11}\, d\mu_B + x_C^{11}\, d\mu_C = 0 \qquad (56)$$

When the concentration of impurity is very low, the activity coefficient of the impurity is independent of concentration, so we can write,

$$d\mu_C = RT\, d \ln x_C^{1} = RT\, d \ln x_C^{11} \qquad (57)$$

Substituting equation (57) into equations (56) and solving for $d\mu_A$ and $d\mu_B$ we obtain,

$$\text{(i)}\quad d\mu_A = \frac{RT(x_B^{1}\, dx_C^{11} - x_B^{11} dx_C^{1})}{x_B^{11} x_A^{1} - x_A^{11} x_B^{1}}$$
$$\text{(ii)}\quad d\mu_B = \frac{RT(x_A^{11} dx_C^{1} - x_A^{1}\, dx_C^{11})}{x_A^{11} x_A^{1} - x_A^{11} x_B^{1}} \qquad (58)$$

Let us now suppose that component C is much more soluble in component A and phase (^{1}) than in component B and phase (^{11}), so that the signs of $d\mu_A$ and $d\mu_B$ are determined by the terms containing dx_C^{1}. Equation (58) reduces to,

$$\text{(i)}\quad d\mu_A = \frac{-RTx_B^{11} dx_C^{1}}{x_B^{11} x_A^{1} - x_A^{11} x_B^{1}}$$
$$\text{(ii)}\quad d\mu_B = \frac{RTx_B^{11} dx_C^{1}}{x_B^{11} x_A^{1} - x_A^{11} x_B^{1}} \qquad (59)$$

$x_B^{11} x_A^{1} - x_A^{11} x_B^{1}$ must be positive, since $x_A^{1} > x_A^{11}$ and $x_B^{11} > x_B^{1}$, so $d\mu_A$ is negative and $d\mu_B$ is positive.

Let us suppose that we had not allowed transfer of material between the phases while adding dx_c^{1} to one phase and dx_c^{11} to the other. Since dx_c^{11} is very small there would have been practically no change in μ_A and μ_B in phase $(^{11})$. The decrease in μ_A and the increase in μ_B therefore arise from the transfer of component A from phase $(^{11})$ to phase $(^{1})$, or from the transfer of component B from phase $(^{1})$ to phase $(^{11})$ or both. Thus the effect of an impurity, which is preferentially soluble in one of the principle constituents, is to decrease the mutual solubility.

Rice also considered an impurity of the second type, and derived an equation for the effect of a surface active impurity on the interfacial tension.

$$d\gamma \cong - \Gamma_c \, d\mu_c \qquad (60)$$

This equation shows the change in surface tension (γ) on the addition of a small amount of impurity. Γ_c is the surface excess of the impurity. The chief effect is a lowering of the surface tension between the two phases, causing an increased mutual solubility of the two components.

This equation may also be applied to an impurity of the first type, where the surface excess of the impurity with respect to the phase in which it is more soluble is negative. This gives rise to an increase in γ and a decrease in the mutual solubility of the components.

2.8. Correlation of Free Energy of Mixing and Miscibility

The nature of the free energy-composition isotherms of a binary liquid system decides the way in which that system will behave, particularly with respect to the possibility of phase separation. The shape of the miscibility curve can be calculated from a knowledge of the dependence of the free energy on composition and temperature, in both the one and two liquid phase states of the system. Copp and Everett [12] have calculated the miscibility curve of the system methyldiethylamine+water from free energy of mixing data; and Kohler [13] has performed the reverse calculation on the system triethylamine+water and obtained the free energy of mixing from the coexistence curve. Copp and Everett found that the excess free energy of the system methyldiethylamine+water can be expressed as a function of mole fraction, such that one term varies linearly with temperature while the remainder are temperature independent.

The excess free energy of a binary liquid mixture may be expressed conveniently in the form,

$$\frac{g^E}{RT} = x(1-x)\left[A + B(1-2x) + C(1-2x)^2 + D(1-2x)^3 + \ldots\right] \qquad (61),$$

where all the coefficients A,B,C,D may depend upon temperature. It was found that A approximates to a linear function of temperature, while the remaining coefficients are temperature independent: thus for this system equation (61) may be written,

$$\frac{g^E}{RT} = A(T)\, x(1-x) + \phi(x) \qquad (62)$$

It thus follows that the heat of mixing should be a symmetrical parabolic function of x, while the asymmetry in the behaviour of the system can be attributed to entropy effects.

Copp and Everett analysed data for the system methyldiethylamine + water at 47°C. They fitted the experimental data by the equation,

$$\phi = x(1-x)\left[0.250(1-2x) + 0.460(1-2x)^2 + 0.810(1-2x)^2(1-x)^6\right] \qquad (63),$$

where x is the mole fraction of methyldiethylamine, and where $(1-x)^6$ can be written as $\frac{1}{2^6}\left[1+(1-2x)\right]^6$ and is therefore a function of (1-2x). The free energy isotherms were then calculated for various values of A, and the

compositions of the equilibrium phases plotted as a function of A. The instability diagram (corresponding to I and I' in figure 2.1) was also found by the relationship $\frac{I}{RT}\left(\frac{\partial^2 g^E}{\partial x^2}\right)_{T,P} = \frac{-1}{x(1-x)}$. Figure 2.2. shows the calculated instability curve (1), the calculated coexistence curve (2), and the experimentally determined coexistence curve (3), plotted as functions of A and of temperature. The correlation between A and temperature was obtained by determining the free energy curves at several temperatures. The agreement between curves (2) and (3) is reasonable. The general shape and position of the critical point is predicted, but the experimental curve is much flatter than the calculated one. This may be due to an incorrect value for the dependence of A upon temperature in the critical region, or to insufficiently precise free energy values.

Kohler [13] described a method by which it is possible to calculate the free energy of a binary liquid system from the miscibility curve. The method consists of writing down the conditions for the coexistence of two phases and carrying out an integration along the miscibility curve.

If x^{I} and x^{II} are the mole fractions of one of the components in the two equilibrium phases then,

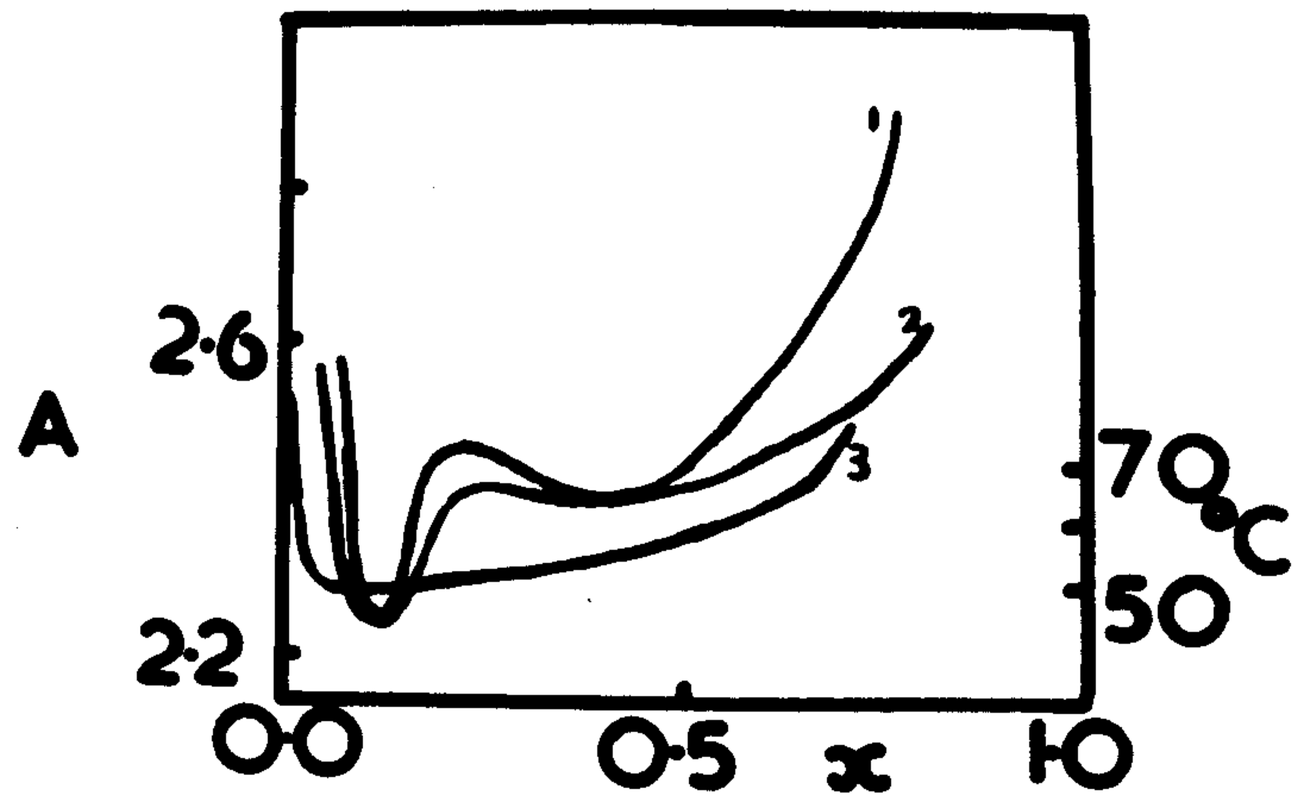

FIGURE 2·2 PHASE DIAGRAM OBTAINED FROM EQUATION 63 IN TERMS OF 'A'
CURVE 1: INSTABILITY CURVE
CURVE 2 COEXISTENCE CURVE
CURVE 3 OBSERVED COEXISTENCE CURVE - TEMPERATURE SCALE ON RIGHT

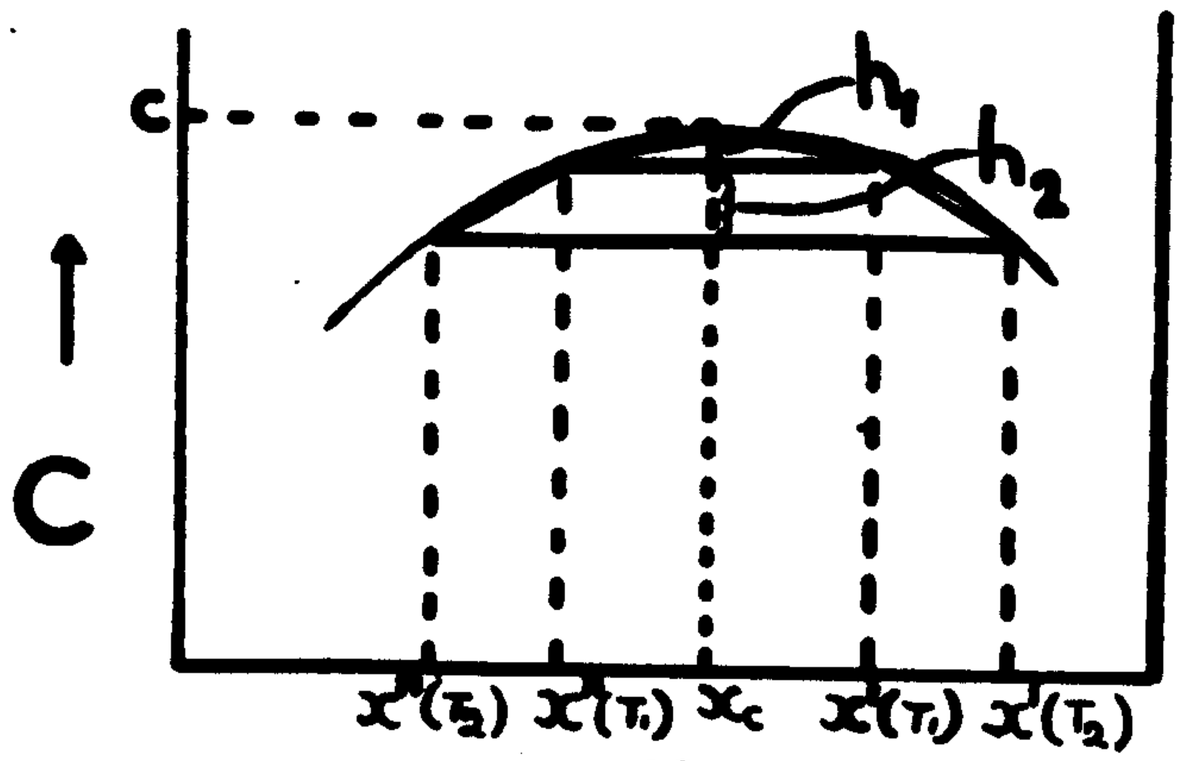

FIGURE 2·3 C AS $\overrightarrow{x}$ A FUNCTION OF MOLE FRACTION

$$\left|\frac{\partial g^M}{\partial x}\right|_{x^1} = \left|\frac{\partial g^M}{\partial x}\right|_{x^{11}} \tag{64}$$

and $$\left|\frac{\partial g^M}{\partial x}(1-x) + g^M\right|_{x^1} = \left|\frac{\partial g^M}{\partial x}(1-x) + g^M\right|_{x^{11}} \tag{65}$$

Equations (64) and (65) arise from the condition that the compositions of the equilibrium phases are given by the points of contact of a common tangent to the free energy curve. The free energy of mixing, g^M, can be expressed as

$$g^M = RT\left[x \ln x + (1-x)\ln(1-x)\right] + g^E_{T_c} - s^E(T-T_c), \tag{66}$$

where we have assumed that the excess entropy of mixing is independent of temperature.

We initially make the assumption that $s^E = 0$. This approximation will not give rise to large errors if the temperature T is near T_c or if the excess entropy is small. Let C be the value of $(\partial g^M/\partial x)$ along the miscibility curve; this function depends upon T and x along the miscibility curve and is the same for the two equilibrium phases. Equation (66) can now be written

$$\frac{\partial g^E_{T_c}}{\partial x} = -RT \ln \frac{x}{1-x} + C\ , \tag{67}$$

and equation (67) is valid along the miscibility curve. Substituting for g^M from equation (66) into equation (65) and eliminating $g^E_{T_c}$ by the integration of (67), we have

$$\int_{x^{II}}^{x^{I}} C\,dx - C\,(x^{I}-x^{II}) = RT\left[x^{II}\ln x^{II} + (1-x^{II})\ln(1-x^{II})\right.$$

$$\left. -x^{I}\ln x^{I} - (1-x^{I})\ln(1-x^{I})\right]$$

$$-\int_{x^{I}}^{x^{II}} RT \ln \frac{x}{1-x}\,dx \qquad (68)$$

The difference between the two terms on the righthand side of this equation is that in the first term T is the temperature of the equilibrium (x^{I},x^{II}) phases, while in the second term T varies along the miscibility curve. As long as the temperature of the equilibrium phases is not far removed from the critical point, then the % change in T in the second term is unimportant, and the righthand side of the equation becomes zero. C is therefore the same for all temperatures, and in particular is the same as the slope of the g^{M} curve at the critical point (c). The error involved in putting the righthand side of equation (68) equal to zero is less than that due to the assumption $S^{E} = 0$.

c can now be obtained from equation (67),

$$0 = \int_{0}^{1} \frac{\partial g^{E}_{Tc}}{\partial x}\,dx = \int_{0}^{1} -RT \ln \frac{x}{1-x}\,dx + c \qquad (69),$$

where the integration of the term on the righthand side of equation (69) is carried out along the miscibility curve. If this integration cannot be carried to one end of the

concentration interval, then a value of $g^E_{T_c}$ must be known for one mole fraction. $g^E_{T_c}$ can now be found by integration of equation (67).

If the approximation $s^E_T = 0$ is not made then equation (66) may be written as

$$\frac{\partial g^E_{T_c}}{\partial x} = -RT \ln \frac{x}{1-x} + C + (T-T_c) \frac{\partial s^E_{T_c}}{\partial x} \qquad (70)$$

Experimentally determined heats of mixing can be combined with the excess free energy values previously obtained to give $s^E_{T_c}$. Substituting for g^M from equation (66) into equation (65) and eliminating g^E_T by the integration of (70) we have

$$\int_{x^{11}}^{x^1} C dx - C(x^1-x^{11}) = RT\left[x^{11} \ln x^{11} + (1-x^{11}) \ln (1-x^{11}) - x^1 \ln x^1 - (1-x^1) \ln (1-x^1)\right] - \int_{x^1}^{x^{11}} RT \ln \frac{x}{1-x}\, dx - \int_{x^1}^{x^{11}} (T_c-T) \frac{\partial s^E_{T_c}}{\partial x} dx - (T_c-T)(s^E_{T_c x^1} - s^E_{T_c x^{11}}) \qquad (71)$$

The left-hand side of equation (71) is the area between the C curve and the horizontal lines in figure 2.3. The right-hand side is calculated for the range $x^1_{T_1}$ to $x^{11}_{T_1}$, where T_1 is near T_c: this enables the height h_1 of the triangle to be calculated. Starting at c we thus obtain

the points $x^{1}_{T_1}$ and $x^{11}_{T_1}$ on the curve. The integral from $x^{1}_{T_2}$ to $x^{11}_{T_2}$ is now found and is the previous triangle plus a trapezium. The lengths of the top and bottom parallel sides of the trapezium are known, and thus its height h_2 calculated and the C-curve further constructed. The shape of the curve is thus known with respect to an indefinite c. The total area under the C-curve can be calculated, and hence the position of c found, by the use of equation (70)

$$0 = \int_0^1 \frac{\partial g^{E}_{T_c}}{\partial x}\, dx = \int_0^1 -RT \ln \frac{x}{1-x}\, dx + \int_0^1 C\, dx + \int_0^1 (T-T_c)\, \frac{\partial s^{E}_{T_c}}{\partial x}\, dx \qquad (72),$$

where $\int_0^1 C\, dx$ is the area under the C curve. Once the C curve has been constructed, the excess free energy of mixing can be obtained by integrating equation (70) along the solubility curve.

By this method Kohler obtained the excess free energy of mixing of the system triethylamine + water at the critical temperature in the range 0.0 - 0.5 mole fraction of amine.

REFERENCES FOR CHAPTER TWO

1. I. Prigogine and R. Defay, Chemical Thermodynamics, translated by D.H. Everett, Longmans, (1954)

2. E.A. Guggenheim, Thermodynamics, North Holland Publishing Company, (1950)

These two books have been used a great deal in preparing this chapter, and I shall only indicate their use when a point of sufficient interest warrants a reference.

3. Reference 1, page 71.

4. E.F.G. Herington, Nature, 160, 610, (1947)

5. B.H. Zimm, J. Chem. Phys., 19, 1019, (1951)

6. J.E. Mayer and S.F. Harrison, J.Chem.Phys., 6, 87, (1938)

7. S.F. Harrison and J.E. Mayer, J.Chem.Phys., 6, 101, (1938)

8. O.K. Rice, J.Chem.Phys., 15, 314, (1947)

9. O.K. Rice, Chem.Rev., 44, 69, (1949)

10. O.K. Rice, J.Phys.Coll.Chem.,54, 1293, (1950)

11. J.L. Copp and D.H. Everett, Dis.Farad.Soc., 15, 182,(1953)

12. J.L. Copp and D.H. Everett, Trans.Farad.Soc.,53,9,(1957)

13. F. Kohler, Monat für Chem, 88, 388, (1957)

CHAPTER THREE

SOLUTION MODELS IN THE CRITICAL REGION

3.1. Introduction

I intend to devote the major part of this chapter to a discussion of the nature of interactions between molecules, and to the determination, from simple solution models, of the conditions necessary for the formation of critical points in binary liquid systems. It is doubtful whether statistical mechanics or thermodynamics can be applied to a solution at its critical point, because molecular fluctuations become so large that a statistical average of any property can be of uncertain value. We need not however deny ourselves the use of these methods to determine the changes in any solution on the approach to the critical region, as we are here dealing either with a homogeneous phase or with two phases in equilibrium, and the molecular fluctuations are usually very small. Consequently while I shall develop and use several theories of solution, we cannot expect to learn much from them concerning the critical point. An an example of this it has been shown (1) that most binary liquid miscibility

curves fit an equation of the form $Tc-T \propto (x^1-x^{11})^3$ (the difference between the critical temperature and the temperature of phase separation is proportional to the cube of the difference in composition of the two phases), but all simple solution models when applied to the critical solution point predict a quadractic instead of cubic relationship.

Theoretical treatment of the critical point began with the formulation of the van der Waals' equation of state, in which the critical point appears as a singularity defined by $\left(\frac{\partial p}{\partial v}\right)_{T_c} = 0$ and $\left(\frac{\partial^2 p}{\partial v^2}\right)_{T_c} = 0$. When the van der Waals equation is combined with a premise due to Maxwell [2], that the vapour-liquid tie lines cut off equal areas in the loops of the p-V isotherms, it can be deduced that the coexistence curve is of a parabolic form. In the following sections I shall consider the application to the critical point of several theories of binary liquid solutions; and in the final section I shall discuss Mayer's theory of condensing systems, which leads to a non-classical view of the vapour liquid critical point.

3.2. Forces between Molecules in Solution

In order to discuss the behaviour predicted by

theoretical models of solutions, it is necessary to deal briefly with the intermolecular forces which occur in the liquid state. The following types of forces can be recognised [3,4]: (1) forces between permanent dipoles; (2) forces between permanent and induced dipoles; (3) London dispersion forces [5,6]; (4) repulsive forces; (5) forces leading to the formation of an electron pair, covalent bonds; (6) coulombic forces between ions; (7) metallic forces. Coulombic and metallic forces do not occur in solutions of nonelectrolytes and need not be discussed.

(1) The interaction energy (ε) between two permanent dipoles (j_1, j_2) depends upon their relative orientations and the cube of the inverse of the distance (r) between their centres.

$$\varepsilon = \frac{-j_1 j_2}{r^3} \left[2 \cos\theta_1 \cos\theta_2 - \sin\theta_1 \sin\theta_2 \cos(\phi_1 - \phi_2) \right]$$

θ and ϕ are polar coordinates giving the orientations of the dipoles and r is the distance between them.

Boltzmannian statistics are applicable in this case and give the interaction energy averaged over all possible relative orientations as,

$$\bar{\varepsilon} = \frac{-2 j_1^2 j_2^2}{3 r^6 kT}$$

In a condensed phase, where steric and other factors prevent free rotation, this equation is inadequate. The dipole interaction known as the 'hydrogen bond' is such a case.

Forces can also occur between dipoles and quadrupoles ($\varepsilon \propto \frac{1}{r^4}$), and between pairs of quadrupoles ($\varepsilon \propto \frac{1}{r^5}$).

(2) The induction effect occurs when a molecule with a permanent dipole (j_1) induces a dipole in another molecule as a result of the polarisability of the latter (α_2). The energy is found to be proportional to $\frac{\alpha_2 j_1^2}{r^6}$

(3) The interactions between non-polar molecules are known as London dispersion forces. London [5,6] suggested that molecules, which do not contain permanent dipoles, possess oscillating dipoles caused by the movement of the nuclei and electrons. Internal electronic oscillations in one molecule induce further oscillations in its neighbours, and as these will always be in phase there is a resultant attraction. London related the interaction energy to the polarisabilities of the molecules according to,

$$\varepsilon = \frac{-3\alpha_1\alpha_2}{2r^6} \cdot \frac{h\nu_{o,1} \cdot h\nu_{o,2}}{h\nu_{o,1} + h\nu_{o,2}}$$

where ν_0 is the characteristic frequency of the molecule in its unperturbed state, and $h\nu_0$ is approximately equal to the ionisation energy of the molecule.

(4) When intermolecular distances are only a few times the molecular diameter, short range repulsive forces become significant. It is possible to represent the repulsive potential by an equation of the form

$$\varepsilon = \frac{k_1}{r^n}$$

Lennard-Jones [7] predicted some aspects of the behaviour of real gases by assuming an interaction potential of the form,

$$\varepsilon = \frac{k_1}{r^{12}} - \frac{k_2}{r^6} ,$$

and this agrees with the interaction potential calculated for helium by the use of wave mechanics [8].

(5) The question whether or not covalent bonds make a significant contribution to interaction energies in solutions was at one time a source of great controversy [9,10]. Dolezalek [9] had tried to explain all interactions in solution as due to the formation of chemical bonds, but his theory was violently attacked by van Laar[10]. There

is no doubt that certain solution interactions may be regarded as the formation of a new chemical species, but to suggest that all interactions may thus be accounted for is obviously incorrect.

3.3. The Hydrogen Bond

Under certain circumstances the hydrogen atom can interact with two atoms instead of only one, so that it may be considered to form a bond between these atoms. This bond is called the hydrogen bond, and it is considered to be of a predominately ionic character because it is only formed between the most electronegative elements [11]. Dipoles, in which hydrogen is linked to nitrogen, oxygen or fluorine, exert effects upon other nitrogen, oxygen or fluorine atoms far greater than one would expect from the magnitude of their moments. The effects of hydrogen bonding are particularly noticed in the boiling points of NH_3, H_2O and HF; these boiling points are remarkably high for molecules of such low molecular weight, especially when compared with the boiling points of similar hydrides (e.g. PH_3, H_2S and HCl respectively).

The hydrogen bond is due to the interaction of a hydrogen atom attached to a highly electronegative atom, with another highly electronegative atom.

Thus the hydrogen atom may be considered to have been partially stripped of its electron, so enabling it to form an electrostatic bond with an electronegative atom. The bond may be written thus,

$$-X\overset{\delta-}{\text{——}}H\overset{\delta+}{\cdots\cdots}Y\overset{\delta-}{\text{——}}R\overset{\delta+}{\quad},$$

or in the case where Y is an ion,

$$-X\overset{\delta-}{\text{——}}H\overset{\delta+}{\cdots\cdots}Y^{-}\quad.$$

It is therefore an extreme example drawn from the wider class of dipole-dipole or dipole-ion interactions. The unique ability of hydrogen to form such a strong bridge is due to the fact that, of all the atoms electropositive with respect to X, its nucleus (in the X-H bond) is shielded by the least number of electrons. Only in this case can an electronegative atom or ion Y approach the dipole so closely that a strong electrostatic union is formed. The evidence for accepting this interpretation of hydrogen bonding may be summarised as follows:

(1) Hydrogen bonding is restricted in the main to systems where X and Y are F, O or N atoms; that is for atoms which are highly electronegative.

(2) The dissociation energy of a hydrogen bond increases

with the electronegativities of the atoms X and Y and decreases with their distance apart.

(3) The hydrogen atom remains closely bound to the atom X when the bond is formed. The possible exception to this is F...H-F. The most important evidence in support of the view that hydrogen bonding is electrostatic in origin and does not involve protonic resonance, comes from an analysis of the infra-red absorption spectra of ice [11]. In ice each oxygen atom is surrounded tetrahedrally by four other oxygen atoms at a distance 2.76Å. If hydrogen bonding were due to protonic resonance between two oxygen atoms, then the most favourable position of the hydrogen atom would be half way between the oxygen atoms. It is actually found that the length of the O-H bond is approximately normal i.e. $\sim$ 1Å. This means that each oxygen atom is surrounded by two hydrogen atoms at $\sim$ 1.0Å and two at $\sim$ 1.7Å, and the water molecule retains its identity. Pauling [11,12] showed that this ice model is consistent with a crystal containing N atoms having $(3/2)^N$ configurations of equal energy. This leads to a theoretical value of $R\ln(3/2) = 0.81$ cals.deg^{-1}mole^{-1} for the residual entropy of ice at 0°K. The experimental

values are 0.82 cals.deg^{-1}.mole^{-1} for ordinary ice and 0.77 cals.deg^{-1}.mole^{-1} for heavy ice; this agreement with the theoretical value provides strong support for the postulated structure involving hydrogen bonds, with the hydrogen nucleus unsymmetrically placed between two oxygen atoms.

In certain types of solutions hydrogen bonding is very important, and it is known to be able to cause negative excess entropies and lower consolute temperatures. Theoretical treatments of binary liquid solutions related to the cell and lattice models mostly assume molecular rotations to be uninhibited. These treatments are thus inapplicable to solutions containing hydrogen bonds and showing lower consolute temperatures. In hydrogen bonded mixtures rotations are not free and adjacent molecules can assume preferred orientations. In the case of amines in water the molecules have highly asymmetric force fields. Water and both primary and secondary amines can partially donate and accept protons to give hydrogen bonds, whereas tertiary amines can only accept. Thus all the hydrogen atoms forming hydrogen bonds in the system triethylamine + water come from the water, which must act as an acid to the amine, while to adjacent water molecules it can act

as both an acid and a base.

3.4. The Regular Solution

The name 'regular solution' was invented by Hildebrand [13] to describe mixtures whose experimental behaviour showed certain regularities. He showed that for certain binary solutions the relationship $RT \ln \gamma_2 = Bx_1^2$ sufficed to account for such properties as heats of mixing and critical temperatures, where B is a function of temperature only. Heitler [14] had previously derived this equation by assuming a lattice structure for the solution and examining the probability of the various arrangements of the molecular species. Hildebrand described the behaviour of a regular solution in terms of the entropy of mixing: 'A regular solution is one involving no entropy change when a small amount of one of its components is transferred to it from an ideal solution of the same composition, the total volume remaining unchanged.' Guggenheim [15] then defined a 'strictly regular solution' as, any mixture of molecules satisfying all the conditions for forming an ideal mixture except that the interchange energy W (to be defined later) is not zero. The molecules are assumed to be sufficiently alike in size and shape to be interchangeable

on a lattice, but the entropy of mixing is now dependent upon the interchange energy. Only if the interchange energy is zero or very small will the solution have zero excess entropy of mixing.

Let us consider [16] a binary mixture composed of $N_A (= N(1-x))$ molecules of A and $N_B (= Nx)$ molecules of B on a lattice of N sites with a co-ordination number of z. As each molecule has z nearest neighbours there will be $\frac{1}{2}zN$ nearest neighbour pairs. Such pairs are of three kinds, namely, AA, BB, and AB. Let us denote the number of AB pairs in a given configuration by zX, then the number of A contacts which are used in A.A pairs is $zN_A - zX$ and so the number of A.A pairs is $\frac{1}{2}z(N_A - X)$. If the energy relative to infinite separation of an AA contact is ϵ_{AA}, that of a BB contact is ϵ_{BB}, and that of an AB contact ϵ_{AB}, the total energy of the system can be written as

$$U = \tfrac{1}{2}z(N_A - X)\,\epsilon_{AA} + \tfrac{1}{2}z(N_B - X)\,\epsilon_{BB} + zX\,\epsilon_{AB}$$

$$= \tfrac{1}{2}zN_A\,\epsilon_{AA} + \tfrac{1}{2}zN_B\,\epsilon_{BB} + \tfrac{1}{2}zX\left\{2\epsilon_{AB} - \epsilon_{AA} - \epsilon_{BB}\right\}$$

The energy of the pure unmixed components is

$$\tfrac{1}{2}zN_A\,\epsilon_{AA} + \tfrac{1}{2}zN_B\,\epsilon_{BB}$$

and so the change on mixing is

$$U^M = \tfrac{1}{2}zX(2\epsilon_{AB} - \epsilon_{AA} - \epsilon_{BB}) \quad .$$

W, the interchange energy, is defined by,

$$W = \tfrac{1}{2}z(2\epsilon_{AB} - \epsilon_{AA} - \epsilon_{BB}) \ ,$$

so $U^M = XW$.

If $\bar{X}$ is the equilibrium value of X then,

$$U^M = \bar{X}W \quad .$$

The problem now concerns the determination of $\bar{X}$, and we shall start with the simplest case, the zeroth approximation.

The zeroth approximation assumes a random distribution of the two types of molecules on the lattice. Thus the average value of X is given by

$$\bar{X}^2 = (N_A - \bar{X})(N_B - \bar{X})$$

$$\therefore \bar{X} = \frac{N_A N_B}{N_A + N_B} = Nx(1-x)$$

The energy of mixing is now given by

$$U^M = Nx(1-x)W \ ,$$

and its value per mole is

$$u^M = N_o x(1-x)W,$$

where N_o is Avogadro's number.

The entropy of mixing is ideal, so the free energy of mixing becomes

$$f^M = N_o x(1-x)W + RT(x\ln x + (1-x)\ln(1-x))$$

The condition for critical mixing is $\left(\frac{\partial^2 g^M}{\partial x^2}\right)_{T_c,p_c} = 0$,

and as the difference between the Gibbs and Helmholtz free energies is very small for condensed phases, we have $\left(\frac{\partial^2 f^M}{\partial x^2}\right)_{T_c,p_c} = 0$. This leads to

$$0 = -2N_oW + \frac{RT_c}{x_c(1-x_c)}$$

$$\therefore \quad x_c^2 - x_c + \frac{RT_c}{2N_oW} = 0 \quad ,$$

where x_c, T_c defines the critical point.

The condition for this equation to have one solution is

$$2RT_c = N_oW \quad \text{or} \quad T_c = \frac{W}{2k} \qquad \text{at } x_c = \tfrac{1}{2} \, .$$

The chemical potentials of the two components are given by,

$$\mu_A - \mu_A^o = RT \ln \frac{N_A}{N_A+N_B} + \frac{N_B^2}{(N_A+N_B)^2} N_oW$$

$$\mu_B - \mu_B^o = RT \ln \frac{N_B}{N_A+N_B} + \frac{N_A^2}{(N_A+N_B)^2} N_oW$$

As the magnitude of W/kT increases, so do the deviations from Raoult's law. The activity curves plotted as a function of mole fraction lie above or below the straight line corresponding to Raoult's law according as W is positive or negative. When W/kT = 2 the activity curves have a point of horizontal inflexion at $x = \frac{1}{2}$. For

higher values of W/kT the curves have a maximum or minimum; the system will then split into two phases over a given composition range in order to minimise the free energy. The molar free energy of mixing is symmetrical about $x = \frac{1}{2}$, so the compositions of the two equilibrium phases are given by the condition $\left(\frac{\partial f^M}{\partial x}\right)_T = 0$. The equation of the miscibility curve becomes,

$$\ln \frac{x}{1-x} = (2x-1) \frac{W}{kT}$$

For regions in which T is just less than T_c, i.e. W/kT is a little greater than 2, this equation reduces to

$$(2x-1)^2 = \frac{3W}{2kT_c^2} \cdot (T_c - T);$$

which implies a parabolic coexistence curve in the region of the critical point instead of the cubic form which is usually observed with binary liquid systems.

The assumption of the zeroth approximation that complete randomness occurs on mixing cannot be strictly correct. It is obvious that as $W/kT \rightarrow 0$, $\overline{X}$ will tend to the random value $\frac{N_A N_B}{N_A + N_B}$, but that at a finite temperature $\overline{X}$ will be greater or less than this depending upon whether W is negative or positive. The zeroth approximation can

be improved by assuming that $\bar{X}$ does depend upon W/kT, and this is done in the first or quasi-chemical approximation.

In the quasi-chemical approximation the equilibrium value of X is given by,

$$\bar{X}^2 = (N_A-\bar{X})(N_B-\bar{X})e^{-2W/zkT}.$$

$2W/z$ is the energy change on the formation of two AB pairs from an AA pair and a BB pair, and the equation is of the form to be expected if the nearest neighbour pairs were gaseous molecules in equilibrium. The free energy is then obtainable, and the critical temperature is given by,

$$T_c = \frac{W}{k} \frac{1}{z\ln[z/(z-2)]}$$

For a body-centred cubic lattice $z=8$ and $T_c = W/2.301k$, while for a face-centred cubic lattice $z=12$ and $T_c = \frac{W}{2.188k}$.

If $z \to \infty$ the zeroth approximation is recovered. The quasi-chemical approximation was introduced without any support other than the analogy with the law for gaseous equilibria. A method which leads exactly to the same results consists of calculating the total number of configurations in terms of the number of pairs, assuming

that one pair does not affect any other. The partition function is then obtained and when it is replaced by its maximum term the quasi-chemical approximation is exactly reproduced.

The essential basis of the first approximation is the hypothesis of the non-interference of pairs. The hypothesis is obviously false in the case of a normal close-packed lattice, and for such a lattice a better approximation would be to consider triangular triplets or tetrahedral quadruplets of sites. In the case of the systems of triangles the critical temperature is given by(16)

$$T_c = \frac{2W}{zk \ln\left(\frac{z+1}{z-3}\right)} ,$$

which may be compared with the first approximation of

$$T_c = \frac{W}{zk \ln\left(\frac{z}{z-2}\right)}$$

In the case of quadruplets of sites(16),

$$\eta_c^3 - \eta_c^2 + \eta_c = \frac{z}{z-4} ,$$

$$\eta_c = e^{W/zkT_c} .$$

The values obtained for W/kT_c from the various approximations

are given in the following table for the case of face-centred cubic lattice ($z = 12$).

Approximation	W/kT_c
zeroth	2
first (pairs)	2.1878
triplets	2.2063
quadruplets	2.2288

Kirkwood [17] suggested that it was in principle possible to evaluate $\ln \Omega$ (the logarithm of the partition function) to any degree of accuracy as a power series in W/zkT. The value for f^M is

$$\frac{f^M}{RT} = (1-x)\ln(1-x) + x\ln x + x(1-x)\frac{W}{kT} - \frac{z}{2}\left\{\frac{1}{2!}\left(\frac{2W}{zkT}\right)^2 + \frac{1}{3!}\left(\frac{2W}{zkT}\right)^3 + \frac{1}{4!}\left(\frac{2W}{zkT}\right)^4 + \cdots\right\}$$

The evaluation of the coefficients becomes increasingly difficult as the series is ascended. $\frac{W}{kT_c}$ can be expressed as a series in $\frac{1}{z}$:

$$\frac{W}{kT_c} = 2\left\{1 + \frac{1}{z} + \frac{4}{3}\frac{1}{z^2} + \left(2 + \frac{y}{z}\right)\frac{1}{z^3} + \left(\frac{16}{5} + \frac{4y}{z}\right)\frac{1}{z^4} + \cdots\right\}$$

where y is a constant depending upon the lattice. If we make $z \to \infty$ the zeroth approximation is regained, and if

terms in y/z are omitted we obtain the first approximation. The disadvantage of this method is that the convergence of a series expansion in $\frac{1}{z}$ is too slow to lead to a precise value of T_c; but it does show that, whatever the true value may be, the quasi-chemical approximation is more accurate than the zeroth approximation.

3.5. Regular Solutions and Solubility Parameters

In 1906 van Laar [18,19] developed a treatment of the vapour pressures of binary liquid mixtures based upon the van der Waals equation for the mixture and the pure components. The relation between the van der Waals "a" for the mixture and a_A and a_B for the pure components is,

$$a = n_A^2 a_A + 2n_A n_B \; a_{AB} + n_B^2 a_B \; ,$$

where n_A and n_B are the numbers of moles of pure A and pure B respectively and a_{AB} represents the interaction between unlike molecular species. The van der Waals "b" is given by the relation

$$b = n_A b_A + n_B b_B$$

The heat of mixing is then,

$$H^M = n_A \frac{a_A}{b_A} + n_B \frac{a_B}{b_B} - \frac{a}{b}$$

If the intermolecular forces are essentially dispersion forces, the interaction constant is of the form [20]

$$a_{AB} = \sqrt{a_A \; a_B} \quad ,$$

and we then obtain for the heat of mixing,

$$H^M = \frac{n_A n_B b_A b_B}{n_A b_A + n_B b_B} \left(\frac{a_A^{\frac{1}{2}}}{b_A} - \frac{a_B^{\frac{1}{2}}}{b_B} \right)^2$$

Thus the heat of mixing can only be zero if $a_A^{\frac{1}{2}}/b_A = a_B^{\frac{1}{2}}/b_B$, which implies that the two components must have approximately the same critical pressures since $Pc = {}^{8a}/_{27b^2}$. Van Laar and Lorenz [21] improved this equation by substituting molar volumes, v_A and v_B, for the constants b_A and b_B.

$$H^M = \frac{n_A n_B v_A v_B}{n_A v_A + n_B v_B} \left(\frac{a_A^{\frac{1}{2}}}{v_A} - \frac{a_B^{\frac{1}{2}}}{v_B} \right)^2$$

This equation was further modified by Scatchard [22] in order to remove terms in a and replace them by terms in $v\Delta E$ (where ΔE is the latent heat of vaporisation). Volume fractions ($\phi A, \phi B$) were also introduced,

$$H^M = (n_A v_A + n_B v_B) \left[\left(\frac{\Delta E_A}{v_A} \right)^{\frac{1}{2}} - \left(\frac{\Delta E_B}{v_B} \right)^{\frac{1}{2}} \right]^2 \phi_A \phi_B$$

Solubility parameters may be defined as

$$\delta_A = \left(\frac{\Delta E_A}{v_A} \right)^{\frac{1}{2}}$$

so we can now write,

$$H^M = \left(n_A v_A + n_B v_B\right) \left[\delta_A - \delta_B \right]^2 \quad \phi A \phi B$$

This equation was also derived by Hildebrand and Wood [23] by integrating the intermolecular potentials between pairs of molecules throughout the liquid. The critical temperature corresponding to such a mixture is given by,

$$4RT_c = (v_A + v_B) \ (\delta_A - \delta_B)^2$$

Hildebrand and Cochran [24] determined the critical temperatures of mixtures of perfluoromethylcyclohexane with various liquids, and obtained reasonable agreement between theory and experiment. Brusset and Bono [25] proposed that, instead of terms in $(\delta_A - \delta_B)$, we should have $K(\delta_A - \delta_B)$, where K is calculated so that the correct value of the critical temperature is obtained. The variation of δ with temperature is found in terms of the coefficient of expansion.

3.6. Conformal Solutions

The object of any theory of solutions is to derive the thermodynamic functions of a given mixture from the forces between the molecules. The regular solution theory has been quite successful in accounting for the properties of many liquid mixtures, but several of its assumptions are clearly unsatisfactory. Firstly it seems unrealistic to take account only of nearest neighbour interactions, as intermolecular forces vary continuously with distance. Secondly one cannot make the assumption that the internal degrees of freedom are unaffected by mixing. And thirdly the regular solution theory takes no account of volume changes on mixing, and consequently ignores entropy effects associated with these volume changes. Longuet-Higgins [26] considered that a new approach to the theory of solutions was justified, and consequently developed his theory of conformal solutions.

The theory of conformal solutions is primarily applicable to solutions of similar molecules showing small deviations from ideality. The determination of the conditions for the occurence of a critical solution

point is therefore beyond its scope, so I shall only briefly discuss the assumptions and the results of the theory. The three main assumptions made by Longuet-Higgins were,

1) The intermolecular energy in any configuration is the sum of bimolecular terms, one for every pair of molecules in solution.

2) The mutual potential energy of a molecule of species L_A and one of the species L_B at a distance r is given by the expression,

$$U_{AB}(r) = f_{AB}\ Uoo\ (g_{AB}, r)\ ,$$

where Uoo is the mutual potential energy of some reference species Lo, and f_{AB} and g_{AB} are constants depending only on the nature of L_A and L_B. f_{AB} and g_{AB} are the ratios of the coordinates of the position of minimum interaction energy between a molecule L_A and a molecule L_B to those of the reference species: $f_{AB} = \frac{\epsilon^*_{AB}}{\epsilon^*_{oo}}$, $g_{AB} = \frac{r^*_{AB}}{r^*_{oo}}$. Where the superscripts * denote the position of minimum potential energy on the energy-intermolecular distance curve.

3) It is possible to find a reference species Lo such that the various constants f_{AB} and g_{AB} are close to unity.

Assumption (2) limits the theory to mixtures of spherical molecules (not necessarily equal in size), and to non-spherical molecules of the same size and shape.

Assumption (3) implies that the intermolecular forces are approximately the same for all pairs of components.

The development of the theory consists of comparing a solution with a reference solution of isotopes in the same concentrations. The probability of any distribution of the molecules is taken as the same as in the perfect solution of isotopes. These assumptions lead to the evaluation of the basic thermodynamic excess functions.

$$g^E = Eo \sum_{A<B} x_A x_B d_{AB}$$

$$s^E = -\left(\frac{\partial Eo}{\partial T}\right)_p \sum_{A<B} x_A x_B d_{AB}$$

$$h^E = \left\{ Eo - T\left(\frac{\partial Eo}{\partial T}\right)_p \right\} \sum_{A<B} x_A x_B d_{AB}$$

$$v^E = \left(\frac{\partial Eo}{\partial p}\right)_T \sum_{A<B} x_A x_B d_{AB}$$

The quantity d_{AB} is a constant for each pair of components,

$$d_{AB} = 2f_{AB} - f_{AA} - f_{BB}$$

and Eo is the configurational energy of the reference species at the same temperature and pressure. The theory of conformal solutions leads to the same dependence of excess free energy on composition as the zeroth approximation of the regular solution. It also makes certain predictions concerning the volume of mixing, which is beyond the scope of the regular solution theory.

A striking consequence of the expressions for the excess functions is that they are proportional to each other. The excess functions can be shown to be either all positive or all negative. More refined theories show that these excess functions are not necessarily all of the same sign, and the study of these inversions of sign can give interesting indications about intermolecular forces.

Perhaps the main relevance of the Conformal Solution theory to the present work is that it forms a basis for extensions of the cell model [27], and these extensions can be used to make predictions concerning the occurence of critical mixing.

3.7. The Cell Model of Liquids.

Any molecule in a liquid is surrounded by a number of

nearest neighbours and so may be considered to move in a cell formed by these nearest neighbours. In order to set up a partition function for a molecule in its cell it is necessary to assume that the number of nearest neighbours of the molecule is effectively constant, and that the actual cell field does not depart significantly from the average cell field. The potential energy of a molecule may be calculated as a function of position in its cell from the various interactions with its neighbours: the simplest approximation for the position of the neighbouring molecules is that they are each at the centre of their respective cells. [28,29,30,31]

Prigogine has developed the theory in the case of binary liquid solutions. [31,32] His first treatment assumed that the minima in the interaction energies occur at the same distance (r^*), but have different values (ϵ^*_{AA}, ϵ^*_{BB}, ϵ^*_{AB}). Then the configuration partition function for each molecule, referred to an energy zero at the cell centre, is

$$\psi_A = \int_{Cell} e^{-(w_A(r) - w_A(0))/RT} 4\pi r^2 dr ,$$

$$\psi_B = \int_{Cell} e^{-(w_B(r) - w_B(0))/RT} 4\pi r^2 dr ,$$

where $w_A(r)$ is the energy of a molecule of kind A at a distance r from the centre of its cell. The configurational partition function for the whole assembly of $N(= N_A + N_B)$ particles is then given by

$$\Omega = \frac{N!}{N_A!N_B!} (\psi_A)^{N_A}(\psi_B)^{N_B} e^{-\frac{1}{kT}\{N_A w_A(o) + N_B w_B(o)\}}$$

The excess free energy of mixing is

$$\frac{F^E}{NkT} = x_A\left[-\ln \frac{\psi_A}{\psi_A^o} + \frac{1}{2kT}\{w_A(o) - w_A^o(o)\}\right]$$

$$+ x_B\left[-\ln \frac{\psi_B}{\psi_B^o} + \frac{1}{2kT}\{w_B(o) - w_B^o(o)\}\right]$$

where the superscript o refers to pure A or B, while terms without the superscript refer to the solution. Thus the problem reduces to finding values for w and ψ. Prigogine considered two approximations for w(r). For solids the molecule can be considered to behave as a harmonic oscillator, but for the range of densities corresponding to the liquid state the potential well is an adequate approximation. The potential well model is based on the following assumptions regarding w(r),

$$w(r) - w(o) = 0 \qquad 0 < r < (a - \sigma)$$

$$w(r) - w(o) = +\infty \qquad (a - \sigma) < r,$$

where a is the distance between nearest neighbours and σ is

the molecular diameter. The values of the excess functions obtained in this case are,

$$\frac{U^E}{U^*} = 2.03\, RT \left\{ \frac{1}{\langle \epsilon^* \rangle} - \frac{x_A}{\epsilon^*_{AA}} - \frac{x_B}{\epsilon^*_{BB}} \right\},$$

$$g^E = -1.442 \left(\epsilon^*_{AB} - \frac{\epsilon^*_{AA} + \epsilon^*_{BB}}{2} \right) x_A x_B - 5.3\, RT \frac{U^E}{U^*}$$

$$h^E = -1.442 \left(\epsilon^*_{AB} - \frac{\epsilon^*_{AA} + \epsilon^*_{BB}}{2} \right) x_A x_B + 5.3\, RT \frac{U^E}{U^*}$$

$$s^E = 10.6\, R \frac{U^E}{U^*}$$

where $\langle \epsilon^* \rangle = x_A^2 \epsilon^*_{AA} + 2 x_A x_B \epsilon^*_{AB} + x_B^2 \epsilon^*_{BB}$, $U^* = \frac{r^{*3}}{\gamma}$

and γ is a numerical factor depending upon the geometrical arrangement of the molecules.

We can now consider a few typical cases which may arise.

(a) Dispersion forces ($\epsilon^{*2}_{AB} = \epsilon^*_{AA} \epsilon^*_{BB}$). The correction to the critical temperature, as calculated from the zeroth approximation of the regular solution, is small for the potential well approximation. The potential well approximation increases the critical temperature, while the quasi-chemical approximation to the regular solution tends

to lower it.

(b) Association of one of the species ($\epsilon^*_{BB} >> \epsilon^*_{AA}$, $\epsilon^*_{BB} >> \epsilon^*_{AB}$)

The potential well approximation predicts a critical temperature close to that predicted by the quasi-chemical approximation of the regular solution, and lower than that predicted by the zeroth approximation.

(c) Association in solution ($\epsilon^*_{AB} > \epsilon^*_{AA}$, $\epsilon^*_{AB} > \epsilon^*_{BB}$). In this case one might expect a lower consolute temperature because the excess entropy of mixing is negative. When the model is considered, it is found that the magnitude of the negative excess entropy is never large enough to produce a lower consolute temperature while the components remain liquid. This shows that Ono's [33] results, which were thought to have shown a lower consolute temperature from the variation of free volume with composition, are not correct, as the L.C.T. would not occur in the liquid regions of the phase diagram.

3.8. Solution Models showing Lower Consolute Temperatures

From the discussion in the previous section it appears that a solution model using only spherically symmetrical forces cannot show a lower consolute point in the condensed region; for this phenomenon to occur other causes for the

lowering of the entropy of mixing must be found. A large negative excess entropy can be attributed in part to a decrease in the effective number of particles present in solution by the interaction between these particles, and also by the restriction of the rotation of particles by specific interactions. The thermodynamic requirements for a lower consolute point may be summarised as follows:[34]

(1) large negative excess entropy;

(2) small negative heat of mixing;

(3) the excess heat capacity, if positive, to be smaller than some critical value.

These generalisations are limited by the assumption that the various excess thermodynamic functions maintain the same sign for all values of x.

Copp and Everett [34] examined the behaviour of a solution for which the excess free energy of mixing is parabolic with respect to composition. For a large number of systems g^E is roughly symmetrical about $x = 0.5$ even though there may be marked asymmetry in h^E and s^E. According to the zeroth approximation to the regular solution theory the critical value of g^E is $RT/2$ at $x = 0.5$. We can now consider a one phase system, given by (g^E_o, T_o) in figure

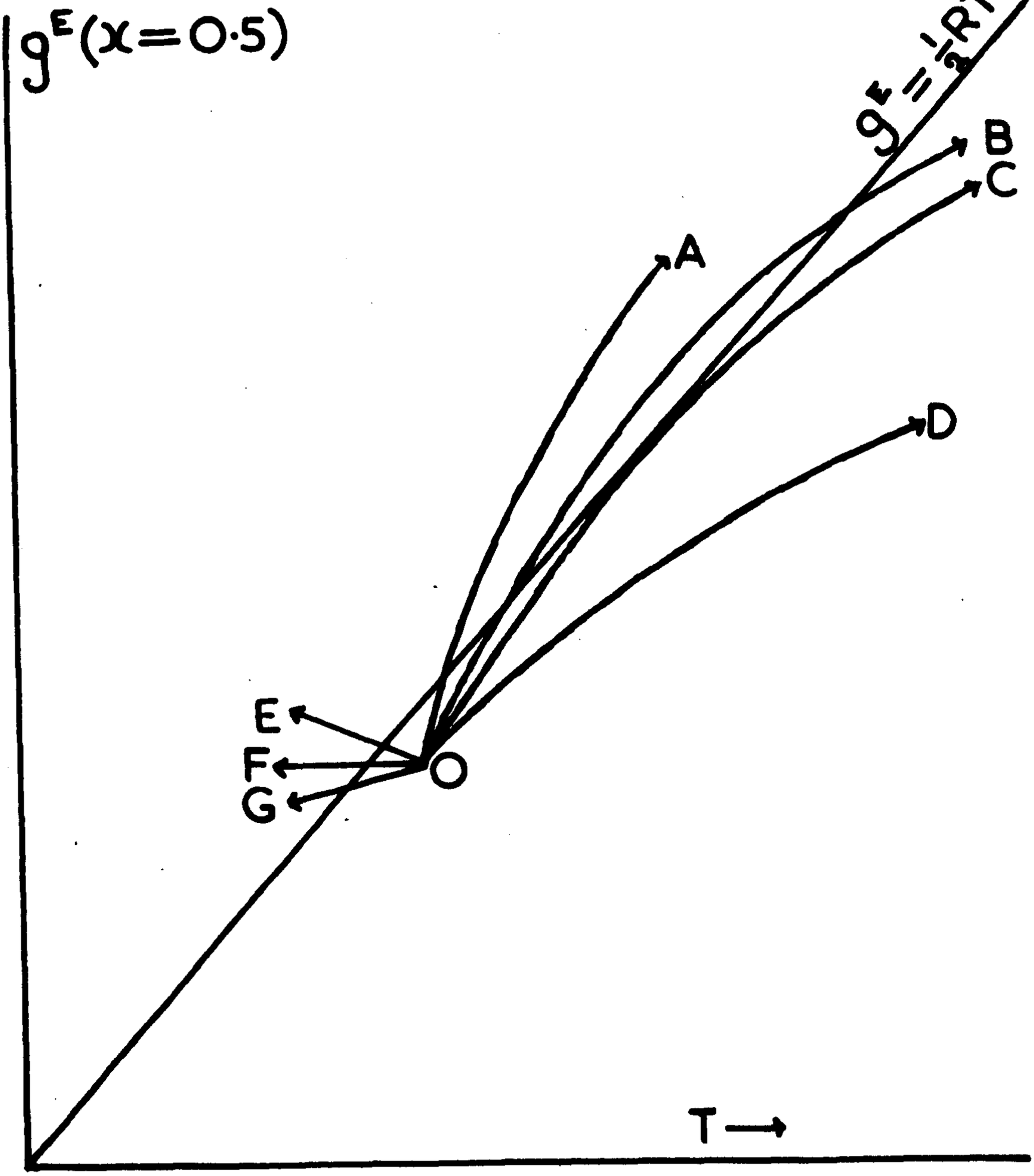

FIGURE 3·1 ILLUSTRATING HOW THE VARIATION OF $g^E(x=0.5)$ WITH TEMPERATURE LEADS TO THE FORMATION OF PHASE DIAGRAMS, STARTING AT O

3.1, potentially able to separate into two phases on increase of temperature. The excess entropy of mixing is negative so g^E will increase with temperature, however if c_p^E is positive (which is very probable as below a L.C.T. $h^E<0$ and above a U.C.T. $h^E>0$) then s^E increases with increase of temperature and the slope of g^E decreases. The curvature of g^E will be greater the larger the value of c_p^E compared with s_o^E, and may be large enough to prevent g^E reaching its critical value. This is illustrated in figure 3.1 where $g^E(x=0.5)$ is drawn as a function of T for four values of the ratio s_o^E/cp. System A will have a lower consolute temperature, B a closed loop, and D will not show phase separation. For system C, where the excess free energy curve just touches the critical line, no bulk phase separation will be expected, although turbidity of the solution might be observed over a short temperature range. On the other hand any system at O, having an excess entropy greater than $-R/2$, will, on lowering the temperature, separate into two phases e.g. OE, OF(corresponding to the zeroth approximation of the regular solution) and OG.

In order that a solution model should show lower consolute behaviour the molecular interactions must depend

upon the relative orientations of the molecules. While cases have been cited in which no orientation dependent interactions occur (33,35) they probably do not correspond to physically realisable conditions. Parling and Eyring [35] suggested that if the lattice co-ordination number of a solution fell from say 12 to 4 with a few degrees rise in temperature then it might be possible for a lower consolute temperature to be formed. Barker and Fock [36] calculated the phase behaviour of a number of models in which the molecular interactions depend on relative orientation. They found that one model shows upper and lower critical solution temperatures in the manner of the nicotine+water system. Another shows the kind of behaviour observed with partially miscible solids in which compound formation occurs, while a third, representing a mixture of two hydroxy compounds shows only a U.C.T. In order to obtain a closed solubility loop the heats of mixing must be positive at higher temperatures and negative at lower temperatures. This is possible if the interaction between unlike molecules is repulsive for a majority of relative orientations and attractive for a few. At higher temperatures the orientations will be nearly random, and the repulsive

interactions will give a positive heat of mixing; while at lower temperatures the attractive orientations will be favoured and may give rise to a negative heat of mixing. Barker and Fock assumed that the two species of molecule (A, a) each carry one strongly polar group (Q,q) and Z-1 non polar groups (P,p). The energies of such groups are set out below; they do not represent total interaction energies but E_1 for example is the difference between the energy of a P-p contact and the arimethic mean of P-P and p-p contacts.

Contacts	Interaction Energies
P-P, P-Q, Q-Q	0
p-p, p-q, q-q	0
P-p	E_1, positive or repulsive
P-q, Q-p, Q-q	E_2, negative or attractive.

They based their calculations on the methods outlined in a previous paper by Barker [37], using Bethe's quasi-chemical approximation. They found that for values of $m(= -E_2/E_1)$ less than a certain value the solution showed both upper and lower consolute points at $x = 0.5$. They plotted the coexistence curves for certain values of m and $Z = 4$ and 6.

3.9. Mayer's Theory of the Critical Region

Mayer first introduced his theories concerning the shape of the activity isotherms and of the coexistence curve in a series of papers which dealt with the statistical mechanics of condensing systems. [38,39,40]. In the first of these papers he showed that the method commonly used in statistical mechanics to obtain the second virial coefficient, if followed through completely for higher virial coefficients, leads to equations predicting the existence of a condensed phase. In the second paper Mayer and Harrison developed a more concise method of handling the equations, and showed that the equations predicted the existence of some unexpected phenomena in the region of the critical point. In the third paper they considered the practical results of their theory and the experimental evidence in favour of it.

The partition function was obtained by integrating the negative exponential of the sum of the kinetic and potential energies divided by kT over the 3N momenta and 3N spacial co-ordinates.

$$\Lambda = \frac{1}{N!h^{3N}} \iint \cdots \int e^{-\frac{1}{kT}\left(\sum_{i=1}^{N} \frac{p_i^2}{2m} + V(r_i)\right)} dp_{x_1} \cdots dp_{z_N} dr_1 \cdots dr_N$$

where $\gamma_i = x_i, y_i, z_i$, and $p_i^2 = p_{x_i}^2 + p_{y_i}^2 + p_{z_i}^2$

$V(\gamma_i)$ is the total potential energy of the gas in a given configuration. The integration over the momentum space is easily carried out and there remains the integration over the configuration space of N particles

$$\Lambda = \left(\frac{2\pi mkt}{h^3}\right)^{\frac{3N}{2}} \frac{\Lambda_{conf}}{N!}$$

where $\Lambda_{conf.} = \int\int\cdots\int e^{-V(\gamma_i)/kT} \, d\gamma_i \ldots d\gamma_N$,

and where $d\gamma_i = dx_i \, dy_i \, dz_i$. The potential energy $V(\gamma_i)$, is regarded as the sum of $\frac{N(N-1)}{2}$ possible pairs, and so the integrand can be written as the product of this number of terms.

$$\Lambda_{conf.} = \int\int\cdots\int_{N \geq i > j \geq 1} \prod e^{-v(r_{ij})/kT} d\gamma_i \ldots d\gamma_N$$

where $v(r_{ij})$ represents the interaction energy between molecules i and j, and $e^{-v(r_{ij})/kT}$ can be written as $1 + f_{ij}$. Then

$$\Lambda_{conf.} = \int\int\cdots\int \left[1 + \sum_{i>j} f_{ij} + \sum f_{ij} f_{i'j'} + \cdots\right] d\gamma_i \ldots d\gamma_N$$

If in any term in the expansion a molecule is not bound to any other molecule then it is a free molecule (this means that it does not occur anywhere as a subscript in the

product). If, in a given term, f_{ij} occurs and i and j do not occur again, then these are referred to as a cluster of two molecules. If i is bound to j and j is bound to k, whether i is bound to k or not, we than have a cluster of three molecules. In general if l molecules are bound together directly or indirectly, but none of them is bound to any molecule not occuring in the group, we then say that they form a group of l molecules in that particular term.

Mayer and Harrison then collected all terms characterised by having the same number m_1 clusters of one molecule, m_2 clusters of two molecules and m_ℓ clusters of ℓ molecules. They introduced a quantity b_ℓ, the integral over a single cluster defined by:

$$b_\ell = \frac{1}{V \ell!} \int\int \cdots \int \sum_{\ell \geq i > j \geq 1} \prod f_{ij} \, d\tau_1 \ldots d\tau_\ell$$

where V is the total volume.

$\frac{\Omega_{conf}}{N!}$ now becomes $\frac{\Omega_{conf}}{N!} = \sum_{m_\ell} \prod_{\ell} \frac{(N v b_\ell)^{m_\ell}}{m_\ell!}$

where v is the average molecular volume.

The logarithm of $\frac{\Omega_{conf}}{N!}$ can now be replaced with sufficient accuracy by its largest term. The b_ℓ integrals are

expressed in terms of normalised integrals β_k , which are the integrals over the configuration space of k+1 particles, each particle being connected to any other by more than a single path. The pressure of the gas can now be obtained from the simple relationship:

$$\frac{p}{kT} = \left(\frac{\partial}{\partial V}(\ln \Omega)\right)_T$$

$$\therefore \frac{p}{kT} = \rho - \sum_{k \geq 1} \frac{k}{k+1} \beta_k \rho^{k+1} \text{ , where } \rho = \frac{N}{V}$$

and in which $\frac{k}{k+1}\beta_k$ is the (k+1)th virial coefficient. One can deduce that

$$\left[\frac{\partial\left(\frac{p}{kT}\right)}{\partial \rho}\right]_T = 1 - \sum_k k \beta_k \rho^k$$

At any given temperature the density is less than or equal to the densities given by the three conditions [41].

(A) $S = \sum_k k \beta_k \rho^k$ becomes singular

(B) $S = \sum_k k \beta_k \rho^k = 1$

(C) $p \geq$ vapour pressure.

Condition (C) is not required as it is always satisfied if the density is less than or equal to the densities given by (A) and (B).

Mayer developed his theory in terms of the manner in

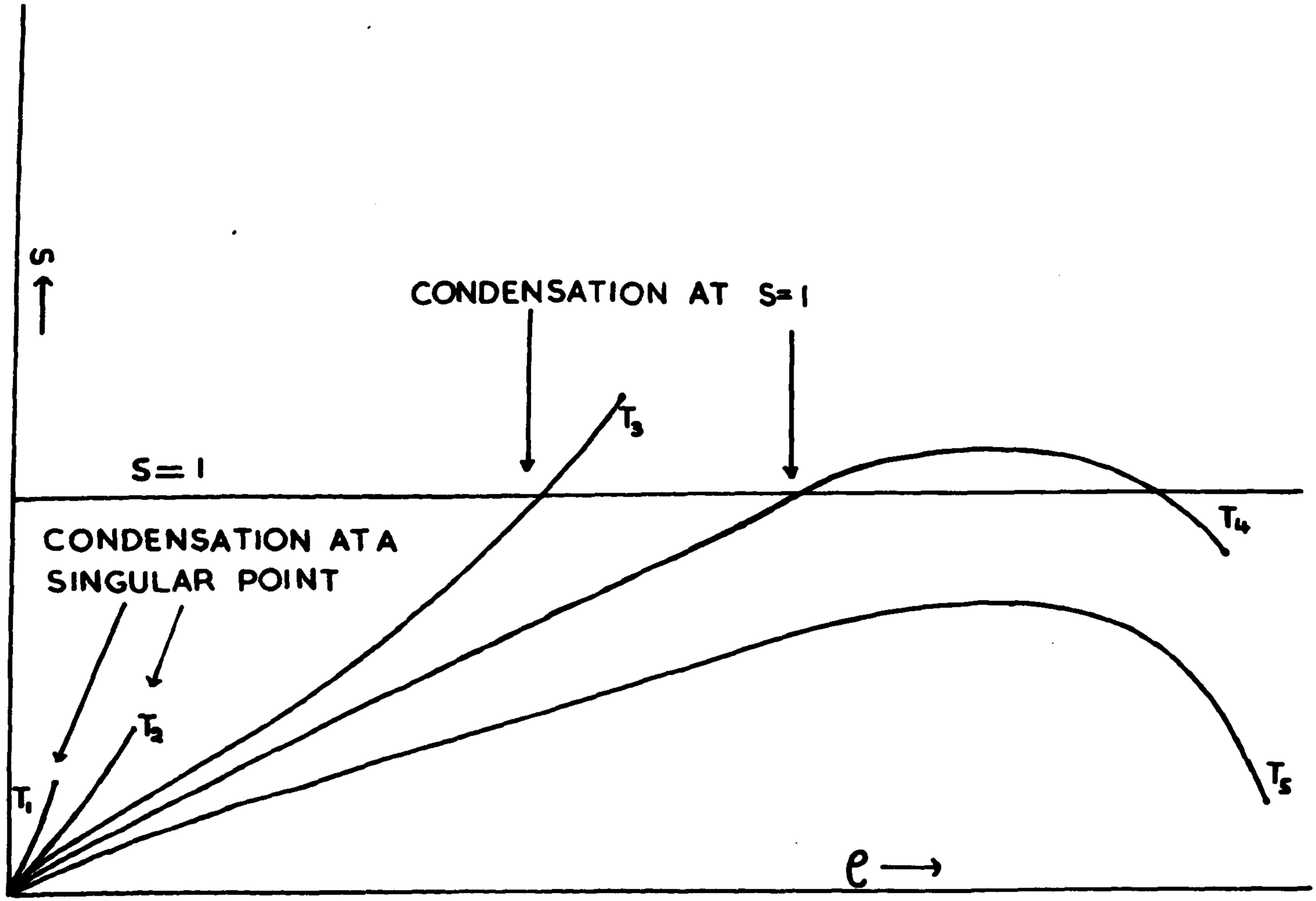

FIGURE 3·2 $S=\sum_k k\beta_k \rho^k$ AS A FUNCTION OF DENSITY AT DIFFERENT TEMPERATURES

which S depends upon density at different temperatures. Figure 3.2 shows S as a function of density at five different temperatures. At a sufficiently low temperature (T_1) the initial slope is positive and relatively steep. The condition for the singularity (A) occurs at low density when the value of S is small; condensation occurs at the density of this singularity, and as the density is low the deviation of the vapour from ideality is small. At a higher temperature (T_2) the inital slope of S as a function of density is less, but the singularity occurs at a much higher density. At this density, corresponding to the saturated vapour, the vapour shows a larger deviation from the perfect gas. At a temperature (T_5) above the critical temperature, S first increases with density but never reaches unity and decreases rapidly at high densities.

We have to decide what happens in the temperature range T_2 to T_5. At the critical point $\left(\frac{\partial P}{\partial \rho}\right)_T = 0$ so $S = 1$. The classical van der Waals' case is only achieved when the singularity and $\left(\frac{\partial S}{\partial \rho}\right)_T = 0$ both occur at $S = 1$. These conditions demand a relationship between the β_k coefficients which does not seem possible, so Mayer advanced a theory which does not make such exacting demands. The first

critical point occurs between T_2 and T_3 when S becomes singular at the point S = 1. The condition $\left(\frac{\partial S}{\partial \rho}\right)_T = 0$ does not occur at this temperature T_m. The next critical temperature T_c occurs when $\left(\frac{\partial S}{\partial \rho}\right)_T = 0$ and S = 1, but a singularity does not appear at this point. Thus to summarise,

at T_m S = 1 S becomes singular

at T_c S = 1 $\left(\frac{\partial S}{\partial \rho}\right)_T = 0$

Below T_m (figure 3.3) the p-V isotherms show discontinuous changes of slope at the phase boundaries. At T_m the interfacial tension disappears, and above this temperature there will be no visible meniscus between condensed and dispersed phases. Between T_m and T_c the isotherms are continuous but have zero slope in the shaded region; above T_c they are never horizontal. In the range T_m to T_c the limits of the shaded area are decided by the intercepts of the S - curves with the line S = 1; an isothermal compression of the system in this shaded region will correspond to a uniform increase in density throughout the whole system at constant pressure.

Alternative theories of the critical region have been put forward which either modify or completely reject that

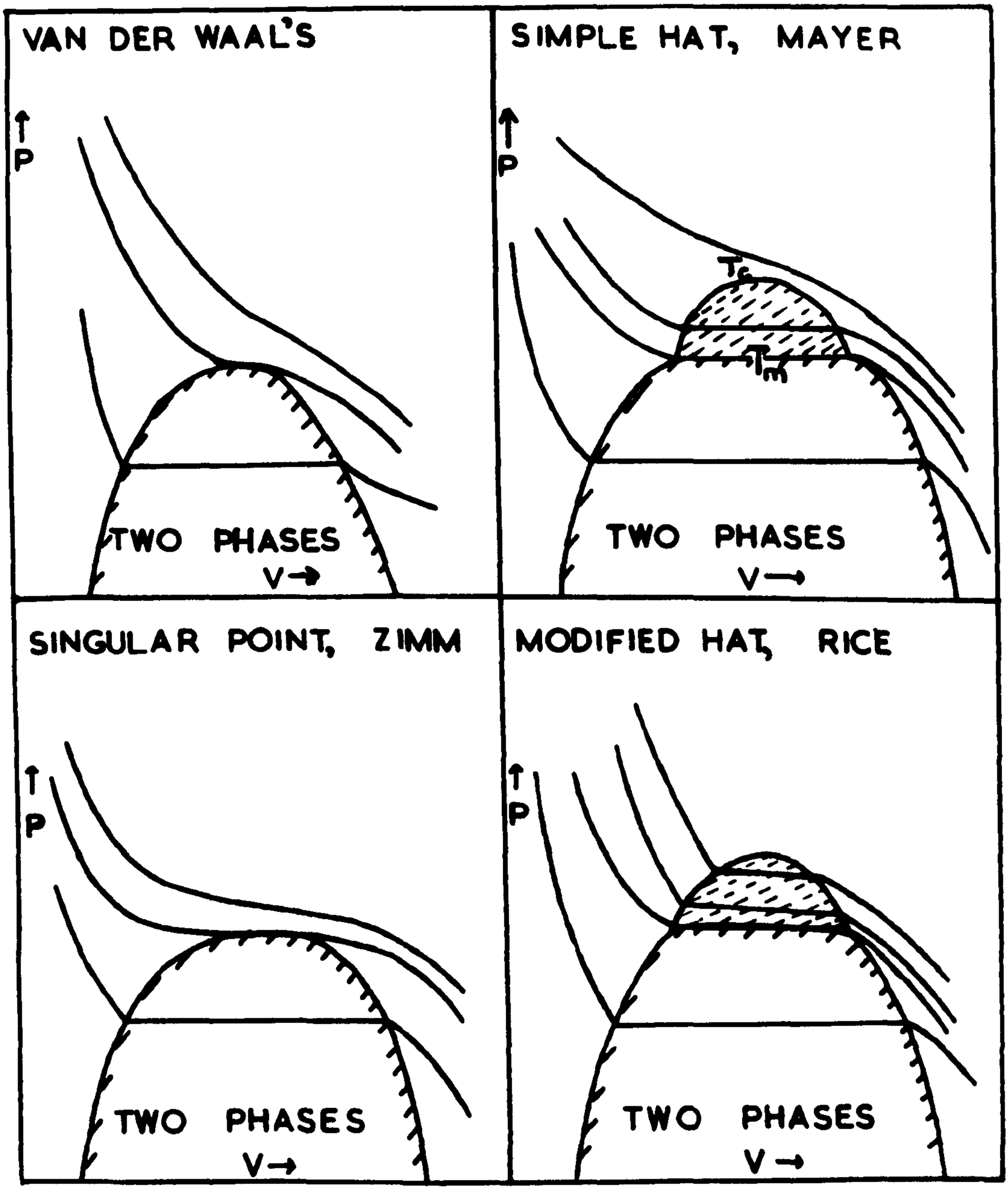

FIGURE 3·3 GRAPHICAL REPRESENTATION OF FOUR THEORIES OF THE CRITICAL REGION

of Mayer. Zimm [42] has put forward an argument in which the critical point is a singularity on a pressure-volume isotherm, given by $\left(\frac{\partial^n p}{\partial V^n}\right)_T = 0$ for all real positive values of n. Zimm showed that if the critical point is such a singularity, then the Mayer theory of condensation leads to a single critical temperature and the anomalous region is no longer predicted. Mayer [43] pointed out that Zimm's argument did not appear to be final, but that it was at least as plausible as Mayer's own original argument. Rice's theory [44,45,46] predicts a critical region in which the top of the phase diagram is flat, but above which the isotherms have small but definite slopes. He obtained his results by a consideration of the effect of surface tension on the size of a molecular cluster in the vapour. The phase diagrams and activity isotherms resulting from these four theories of the critical region are shown in figure 3.3.

It is difficult to decide which of these theories shows the best agreement with the available experimental evidence. The shapes of phase diagrams and critical isotherms were discussed in the first chapter, and despite the large amount of experimental data few definite conclusions can be drawn. If a choice had to be made between the various theories, I feel that Rice's treatment corresponds most closely to physical reality.

REFERENCES FOR CHAPTER THREE

1. O.K. Rice, J. Chem. Phys., 23, 164, (1955)
2. See for example: J.R. Partington, 'An Advanced Treatise on Physical Chemistry', Longmans, (1949), Vol.1., p.676
3. J.H. Hildebrand and R.L. Scott, 'The Solubility of Nonelectrolytes', Rheinhold, New York, (1950), p. 48
4. H. Margenau, Rev.Mod.Phys., 11, 1, (1939)
5. F. London, Trans.Farad.Soc., 33, 19 ,(1937)
6. idem, J.Phys.Chem., 46, 305, (1942)
7. J.E. Lennard-Jones, Proc.Roy.Soc., A112, 214, (1926)
8. J.C. Slater, Phys.Rev., 32, 349, (1928)
9. F. Dolezalek, Z. Phys.Chem., 64, 727, (1908)
10. J.J. van Laar, Z.Phys.Chem., 72, 723, (1910)
11. L. Pauling, 'The Nature of the Chemical Bond', O.U.P., (1950), p.284
12. L. Pauling, J.Am.Chem.Soc., 57, 2680, (1935)
13. J.H. Hildebrand, Proc.Natl.Acad.Sci., 13, 267, (1927)
14. W. Heitler, Ann.d. Phys., 80, 629, (1926)
15. E.A. Guggenheim, Proc.Roy.Soc., A148, 304, (1935)
16. E.A. Guggenheim, 'Mixtures', O.U.P., (1952), chapter IV.
17. J.G. Kirkwood, J.Chem.Phys., 6, 70, (1938)

18. J.H. Hildebrand and R.L. Scott, 'The Solubility of Nonelectrolytes', Rheinhold, (New York), (1950), chapter 7.

19. J.J. van Laar, Z. Physik,Chem., 72, 723, (1910)

20. I. Prigogine and R. Defay, Chemical Thermodynamics, trans. D.H. Everett, Longmans, Green and Co., (1954) p. 395

21. J.J. van Laar and R. Lorenz, Z.Anorg. Allgem.Chem., 146, 42, (1925)

22. G. Scatchard, Chem.Rev., 8, 321, (1931)

23. J.H. Hildebrand and S.E.Wood, J.Chem.Phys., 1, 817, (1933)

24. J.H. Hildebrand and D.R.F. Cochran, J.Am.Chem.Soc., 71, 22, (1949)

25. H. Brusset and D. Bono, 'Changements de Phases', Société de Chimie Physique, Paris (1952), p.125

26. H.C. Longuet-Higgins, Proc.Roy.Soc., A205, 247, (1951)

27. I. Prigogine, 'The Molecular Theory of Solutions', North Holland Publishing Co., Amsterdam, (1957),Chapter IX

28. J.E. Lennard-Jones and A.F. Devonshire, Proc.Roy.Soc., A163, 53, (1937)

29. idem, ibid, A165, 1, (1938)

30. R. Fowler and E.A. Guggenheim, 'Statistical Thermodynamics', C.U.P. (1956), p.336

31. Ref. (27), chapters VII, VIII

32. I. Prigogine 'Changements de Phases', Société de Chimie Physique, Paris, (1952), p 95

33. S. Ono, Memoir Fac.Eng.Kyushu Univ., 12, 2, (1950)

34. J.L. Copp and D.H. Everett, Dis.Farad.Soc;, 15, 185, (1953)

35. R.B. Parling and H. Eyring, Chem.Rev., 44, 47, (1949)

36. J.A. Barker and W. Fock, Dis.Farad.Soc., 15, 188, (1953)

37. idem, J.Chem.Phys., 20, 1526, (1952)

38. J.E. Mayer, J.Chem.Phys., 5, 74, (1937)

39. J.E. Mayer, and S.F. Harrison, J.Chem.Phys., 6, 87, (1938)

40. S.F. Harrison and J.E. Mayer, J.Chem.Phys., 6, 101, (1938)

41. J.E. Mayer, 'Changements de Phases', Société de Chimie Physique, Paris, (1952), p.35

42. B.H. Zimm, J.Chem.Phys., 19, 1019, (1951)

43. J.E. Mayer, J.Chem.Phys., 19, 1024, (1951)

44. O.K. Rice, J.Chem.Phys., 15, 314, (1947)

45. idem, Chem.Rev., 44, 69, (1949)

46. idem, J.Phys.Coll.Chem., 54, 1293, (1950)

CHAPTER FOUR

THE MISCIBILITY OF TRIETHYLAMINE AND WATER

4.1. Introduction

The system triethylamine+water has long been regarded as an interesting example of the group of systems which show lower consolute behaviour. This system has already been studied extensively [1,2,3,4], and some work has been performed on the related systems diethylamine+water [5] and methyldiethylamine+water [6]. Work on a similar series of systems has also been carried out by Andon, Cox and Herington [7,8,9,10,11,12]. They studied the systems formed by pyridine and the methylpyridines with water, and took particular interest in the conditions for the onset of phase separation.

Many liquid pairs show an upper consolute temperature but only a limited number show a lower consolute temperature, and these are restricted to mixtures of water or glycerol with secondary or tertiary amines, ketones or ethers. Obviously such systems have important structural properties in common, and it is fairly certain that one of these is the interaction between a nitrogen atom and a water molecule through a hydrogen bond [13]. The system triethylamine+water

is a convenient example of such a liquid pair as it shows a lower consolute temperature at 18.30°C. The systems methyldiethylamine+water and diethylamine+water have progressively higher L.C.T.'s. This is accounted for by the decrease of the solubility of a hydrocarbon group in water with increasing length. Pyridine and its homologues show all forms of behaviour from the complete miscibility of water with pyridine, to the closed miscibility loops formed by 2:3 and 2:4 dimethylpyridines [10]. Andon and Cox [7] studied the system 4 methylpyridine +water, and found that while the two components were completely miscible (contrary to the observations of Flaschner [14] which suggested a closed miscibility loop between 49°C and 153°C), critical opalescence without phase separation was observed over a certain range of composition and temperature. The divergence between the observations of Andon and Cox and those of Flaschner shows the important effect impurity can have upon the miscibility of liquids; this effect is particularly noticeable in the system triethylamine+water, the miscibility curve of which has an unusually small curvature in the region of the critical point.

4.2. Purification of the Experimental Materials.

a) Water

Distilled water was passed through an ion exchange resin containing the resins IR 120, for the removal of cations, and IRA 400 for the removal of anions. The treated water was then distilled at about 100 ml. per hour in an all-glass still and collected in a conductivity cell. The water could then be stored for use in a stock bottle or rejected if the conductivity were too high. The apparatus was kept free of carbon dioxide, and all connections with the atmosphere were made through soda-lime tubes. A continuous stream of carbon dioxide-free air was passed through the apparatus. The specific conductivity of the water so obtained was between 3 and 5×10^{-7} mohs.

b) Triethylamine

The material supplied contained up to 3% of impurity, the chief impurities being lower amines and water. The triethylamine was refluxed over, and then distilled from, a mixture of caustic potash pellets and para-toluenesulphonylchloride in order to dry it and remove lower amines. This process was repeated. As a final purification the amine was fractionated from metallic sodium through a close packed column of about

four theoretical plates. About 150 ml. of amine were refluxed in the all-glass apparatus and were collected at a reflux ratio of about 15:1. The middle third of the distillate was accepted, and this boiled under a pressure pmm. and at a temperature t°C given by the equation,

$$(t - 89.50 \pm 0.05) = 0.042\ (p-760)$$

This equation is due to Copp.[4]

4.3 Filling the Sample Tubes

We decided that the best method of filling the sample tubes was to distil quantities of the two components into a tube under vacuum. The apparatus used consists of a vacuum line connected to a rotary oil pump and a mercury diffusion pump. At intervals along the line five taps lead to B10 cones. Two large (100 cc) flasks with taps were used to store the liquids, and two smaller (25 cc) flasks with taps were used for weighing the quantities of liquids distilled. All these flasks were specially shaped to withstand freezing in liquid oxygen and were well washed with chromic acid and then with water before use. When the apparatus had been evacuated and found to be leakfree, a flask containing amine was connected into the line, frozen in liquid oxygen, and all the air pumped away. Most of the

air dissolved in the amine was removed by alternate freezing and melting of the amine and pumping the air away. One of the storage flasks was immersed in liquid air and the amine distilled into it, intermittently pumping away the air; this distillation between the flasks was repeated several times. Water was purified in a similar manner.

A sample tube was cleaned in chromic acid and washed with water; it was then connected to the vacuum line by its B10 cone, and evacuated. Both the small weighing flasks were filled - one with water and the other with amine - weighed, and reconnected to the line. The sample tube was immersed in liquid oxygen, and water and then amine distilled into it. The tube was then sealed off and the weighing flasks reweighed.

The chief difficulty encountered in filling the sample tubes resulted from the action of the amine vapour upon the Apiezon tap grease; unless careful watch was kept on the taps they would quickly 'streak' and so leak. Silicone tap grease was tried and this was hardly affected by the amine vapour, but the results obtained for the phase separation temperatures varied greatly due to the presence

of some of the grease in the sample tube. (The 'Wandering' of silicone grease around the system was noticed by the change of the contact angle of water in the storage flask.)

4.4. The Determination of the Miscibility Curve

The tubes containing the amine-water solutions were placed in a large glass tank of water. The tank was well stirred and could be heated by a carbon filament lamp placed behind it. The experiments were started at about 16°C and the tank was heated at a rate of about 0.01°C per minute; when nearing the phase separation temperature the rate of heating was decreased to 0.005°C per minute. The temperature at which each homogeneous mixture showed the first trace of forming a second phase (cf. section 1.3) was recorded with a precision of 0.01°C on the thermometer scale (the thermometer being protected from direct radiation from the lamp). When solutions in which the mole fraction of amine was greater than 0.4 were used, the exact onset of heterogeneity was difficult to determine, and it was only by experience and slow heating that the phase separation temperatures could be determined with an accuracy of 0.02°C. The results obtained are given in the following table.

PHASE SEPARATION TEMPERATURES FOR THE SYSTEM TRIETHYLAMINE + WATER

Mole fraction of amine	°C
0.021	20.41
0.043	18.49
0.054	18.43
0.065	18.32
0.073	18.30
0.078	18.30
0.081	18.29
0.091	18.31
0.094	18.32
0.107	18.35
0.126	18.41
0.139	18.46
0.167	18.70
0.218	19.21
0.219	19.20
0.261	19.63
0.264	19.68
0.270	19.73
0.277	19.95

Mole fraction of amine	°C
0.296	20.05
0.310	20.15
0.349	20.41
0.386	20.76
0.408	20.96
0.450	21.55
0.458	21.64
0.470	21.85
0.549	22.83

The results in this table are plotted in figure 4.1. Two comments can immediately be made upon the miscibility curve obtained. The first concerns the position of the lower consolute point. The maximum critical opalescence was observed in the solution $x_A = 0.073$, and this appears from the figure to coincide with the minimum of the miscibility curve (confirmation of this point will be given when the viscosity of the system is considered). The second comment concerns the point of inflexion which occurs in the region $x_A = 0.3$. Rothmund [2] obtained a horizontal section in the phase diagram extending from this point to $x_A = 0.6$, and Copp's [4] results show an uncertainty in

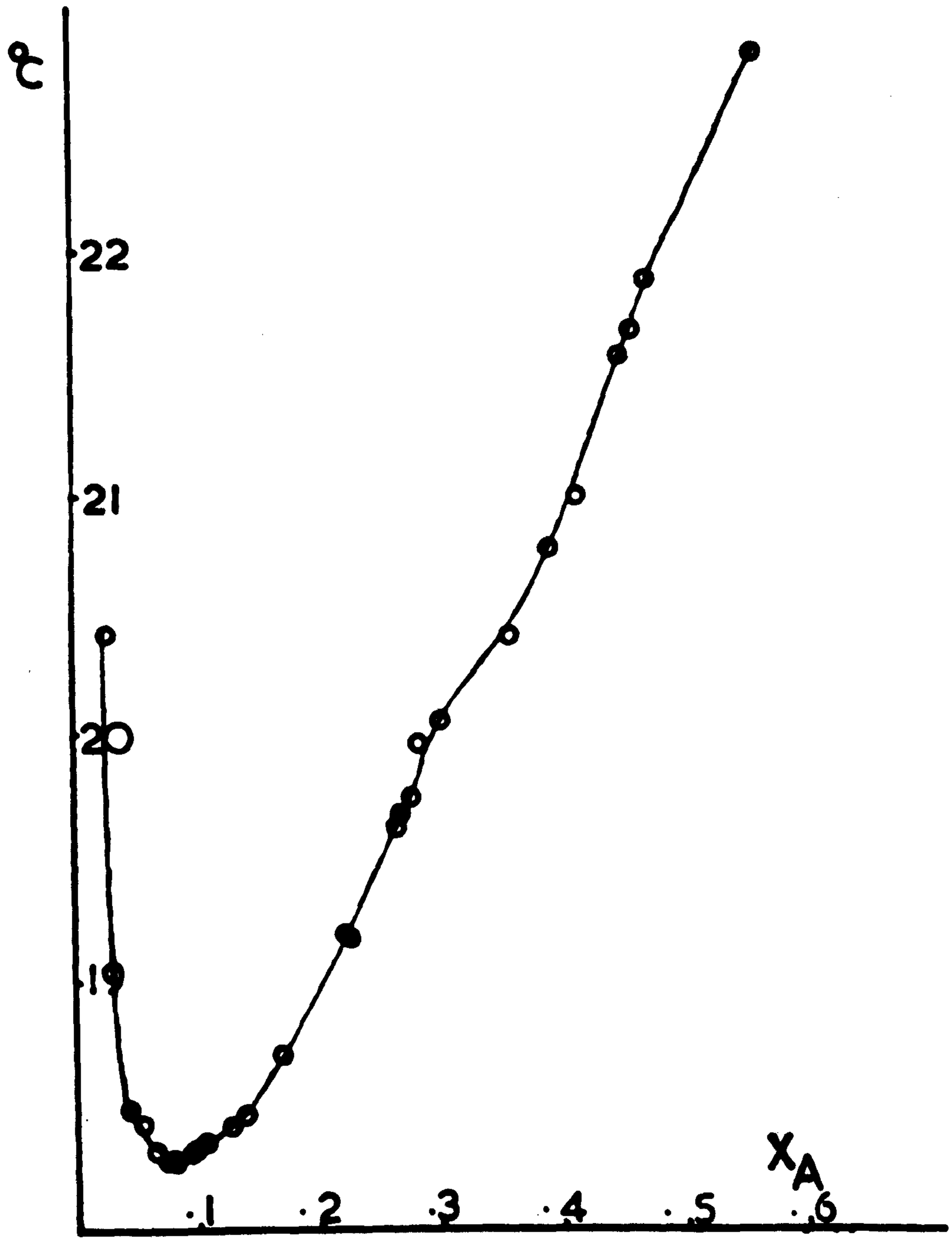

FIGURE 4·1 THE MISCIBILITY CURVE OF THE SYSTEM TRIETHYLAMINE + WATER

the region $x_A = 0.3$. Thus it appears that this point is at the start of a region characterised by conflicting observations of consolute behaviour, and it might be that small amounts of impurity greatly influence the phase separation temperature in this particular composition range.

4.5 Comparison with other work

The miscibility curves obtained by Guthrie [1], Rothmund [2], Roberts and Mayer [3], and Copp [4] are shown in figure 4.2. All these curves show the same critical mole fraction, except that obtained by Guthrie which is indeterminate. The values obtained for the L.C.T. vary from 18.27°C to 18.70°C. The later work of Kohler and Rice [15], which was published after the completion of this part of our work, does not show any noticeable impurity effects, although this cannot be said with absolute certainty as only two points were determined above $x_A = 0.25$ and these were not in the impurity sensitive region.

Figure 4.3 compares Kohler and Rice's curve with that obtained in the present work. Kohler and Rice took special care to remove all impurities, especially carbon dioxide, as this interacts with the solution. They also used silica tubes (actually only the part of the bulb in

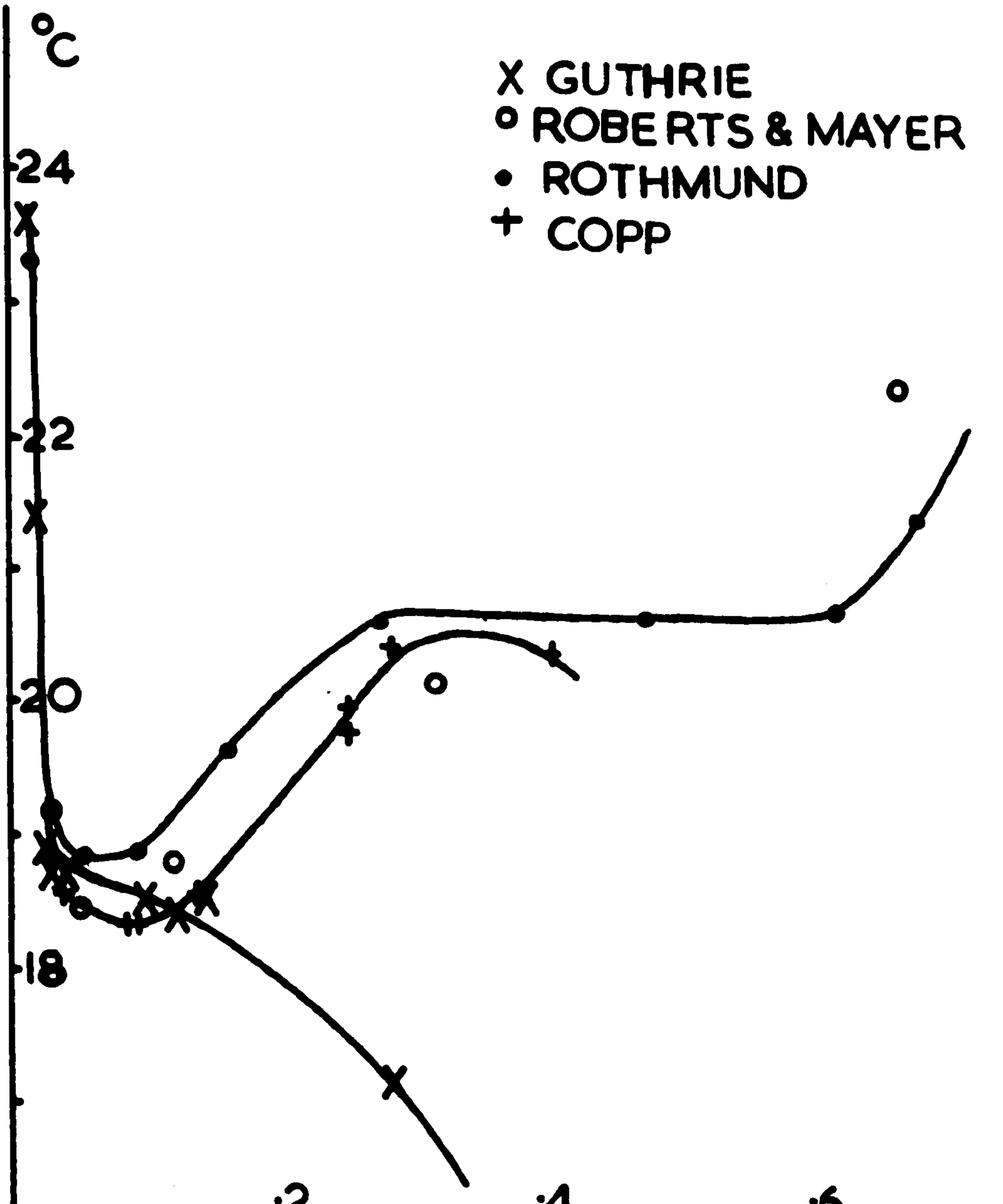

FIGURE 4·2 THE MISCIBILITY CURVE OF THE SYSTEM TRIETHYLAMINE + WATER DUE TO PREVIOUS WORKERS

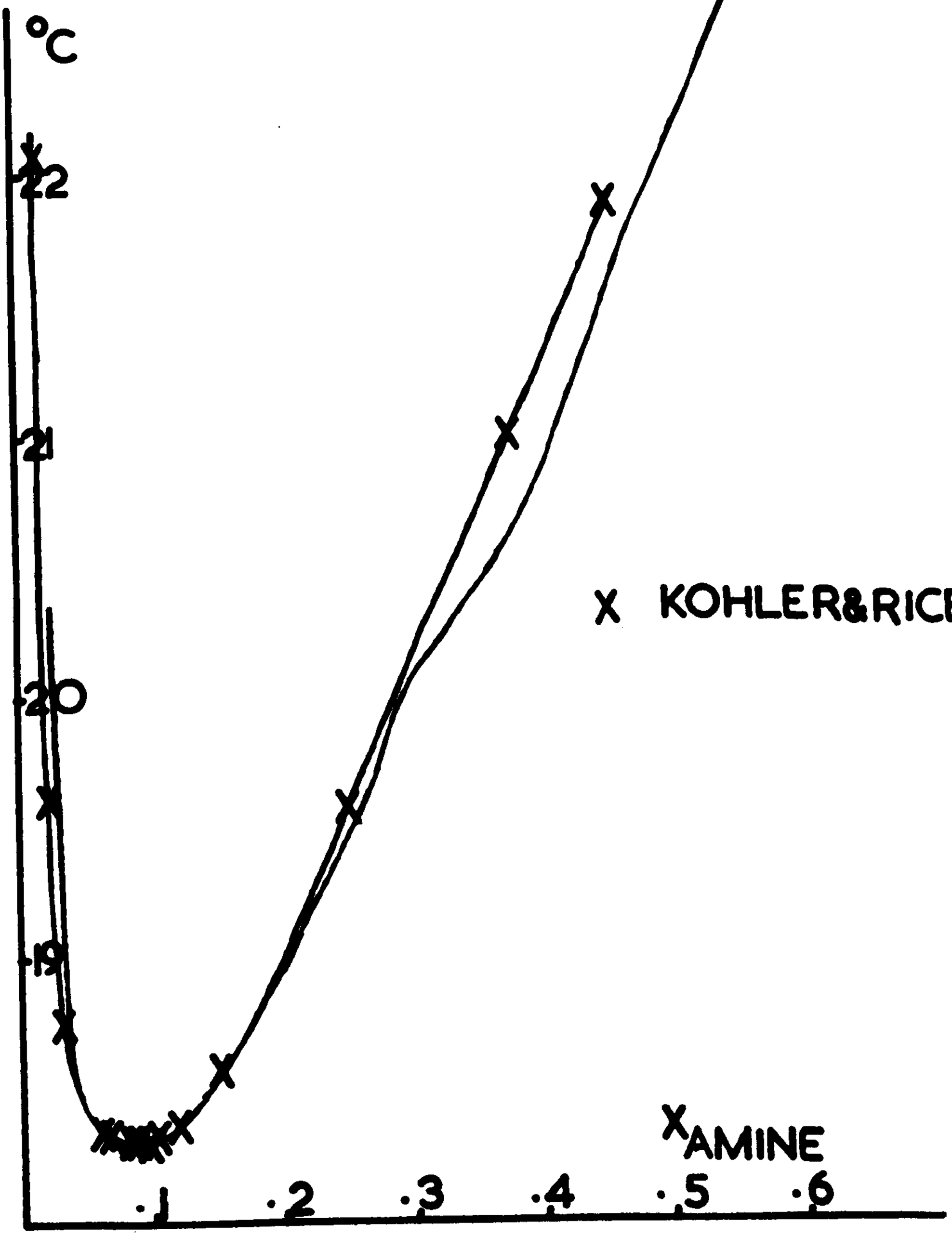

FIGURE 43 MISCIBILITY CURVES OF TRIETHYLAMINE AND WATER OBTAINED BY KOHLER AND RICE AND IN THIS WORK

contact with the liquid was silica, and the rest was pyrex) because the observed phase separation temperature of an amine-water solution in a pyrex bulb alters on standing. Kohler and Rice thermostated their sample tubes at 0.001°C intervals, and for solutions in the critical region the phase separation temperature could be obtained with an accuracy of 0.001°C. The absolute temperatures are accurate to 0.03°C. At the phase separation temperature turbidity occured and after a few hours two phases appeared. For solutions removed from the critical region the phase separation temperature was difficult to determine, and so it was approached from the two phase side. Here the sample was agitated by a magnetic stirrer, and the temperature at which the last traces of heterogeneity could be observed was noted.

4.6. The Effect of Impurity upon the Phase Separation Temperature

In the last section we discussed the results previously obtained for this system, and noted the large disagreements among them and with the present work. The obvious cause for disagreement between the various sets of results is the effect of impurity, so we decided to find the effect on the miscibility curve of a small amount of a third component.

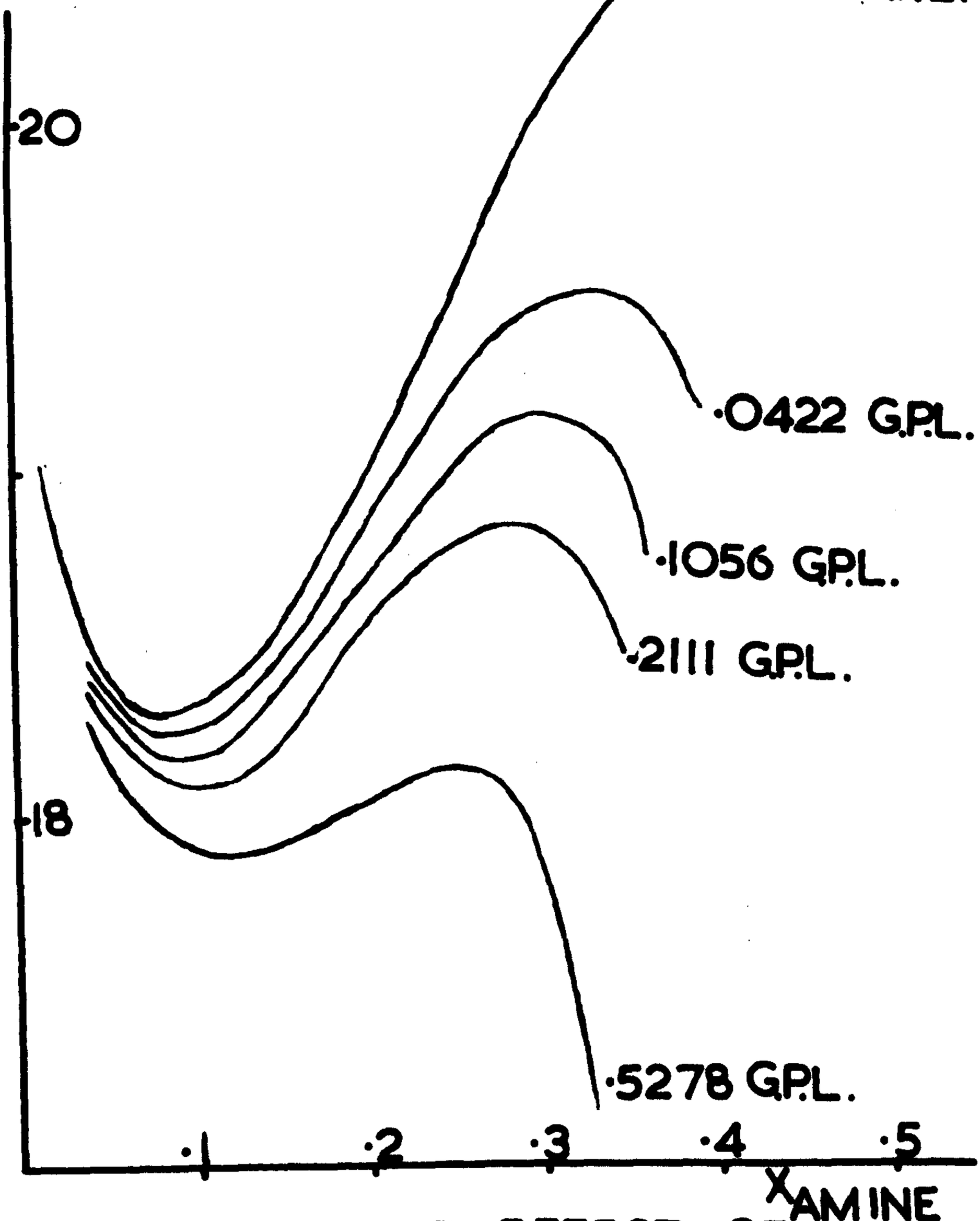

FIGURE 4·4 THE EFFECT OF IMPURITY-GM. SODIUM CARBONATE PER LITRE OF WATER-ON THE MISCIBILITY OF TRIETHYLAMINE AND WATER

The experiments were performed by making various solutions from triethylamine and sodium carbonate solution and finding their phase separation temperatures. The solubility curves obtained are plotted in figure 4.4. The chief region of interest is in the range $x_A = 0.25 - 0.30$: here the impurity produces a maximum in the curve and so explains the curious effects which have been observed in this region, especially the small but noticeable inflection occuring near $x_A = 0.30$ which was observed in this present work.

REFERENCES FOR CHAPTER FOUR

1. F. Guthrie, Phil.Mag., (5), 18, 22, (1909)
2. V. Rothmund, Z.Phys.Chem., 26, 433, (1898)
3. L.D. Roberts and J.E. Mayer, J.Chem.Phys., 9, 851, (1941)
4. J.L. Copp, Ph.D.Thesis, University of St. Andrews (1953)
5. R. Lattey, Phil.Mag., (6), 10, 398, (1905)
6. J.L. Copp and D.H. Everett, Trans.Farad.Soc., 53, 9, (1957)
7. R.J.L. Andon and J.D. Cox, J.Chem.Soc., 4061, (1952)
8. J.D. Cox, J.Chem.Soc., 4606, (1952)
9. R.J.L. Andon, J.D. Cox and E.F.G. Herington, Dis.Farad.Soc., 15, 169, (1953)
10. J.D. Cox, J.Chem. Soc., 3183, (1954)
11. R.J.L. Andon, J.D. Cox and E.F.G. Herington, J.Chem.Soc., 3188, (1954)
12. R.J.L. Andon, J.D. Cox and E.F.G. Herington, Trans.Farad. Soc., 53, 410,(1957)
13. J.O. Hirschfelder, D.P. Stevenson and H. Eyring, J.Chem.Phys. 5, 896, (1937)
14. O. Flaschner, J.C.S., 95, 668, (1909)
15. F. Kohler and O.K. Rice, J.Chem.Phys, 26, 1614, (1957)

CHAPTER FIVE

THE VISCOSITY OF THE SYSTEM TRIETHYLAMINE + WATER

5.1 Introduction

Semenchenko and Zorina [1,2,3] found that the viscosity of the system triethylamine + water shows a rapid increase as the critical point is approached. They also observed an apparent temperature dependent hysteresis in the viscosity. This hysteresis effect was found to be small in regions near the critical point, whilst in regions removed from the critical point, but still showing critical opalescence, the effect was great. This is the reverse of what one would expect if it were a true hysteresis, as maximum hysteresis should have occurred in the region of the critical composition (as in the case of the conductivity of triethylamine + water solutions cf. Chapter Six). Thus one must look for another explanation of these hysteresis effects, and the presence of impurity must be considered. When the effect of impurity upon the phase separation temperature was examined in Section 4.6, it was found to be most pronounced for regions away from the critical point; so the lowering of the phase separation temperature by impurity may cause the hysteresis effect.

The presence of impurity in the solutions used by Semenchenko and Zorina is indicated by the fact that the miscibility curve they obtained showed two minima and a maximum. However the present work is in general agreement with that of Semenchenko and Zorina concerning the shape of the individual viscosity vs. temperature curves in that they show a maximum at the phase separation temperature.

Similar work on the system triethylamine + water has been performed by both Kohler [4] and Tsakalotos [5]. Kohler measured the viscosities of nine solutions at 0,10, 18°C, as Tsakalotos had previously done for six solutions at 15°C; the maximum found in the two cases for the viscosity vs. mole fraction curve agrees well with that found in this work. A maximum was also noted by Tsakalotos in the system nicotine + water, and he remarked upon the fact that the viscosity at the maximum was eight times that of pure nicotine and thirty-five times that of water. Similar effects occur in the case of the system triethylamine + water, and can be attributed to the strong interaction between the two components in solution.

5.2 The Viscometer

In order to measure the viscosity under conditions

of maximum purity, and to avoid the loss of amine or water by evaporation, the determinations were carried out in a viscometer which had been filled and sealed in the absence of air. The liquids were prepared and the viscometer filled in a manner similar to that used for the sample tubes described in the previous chapter. As we had decided to fill the viscometer this way, a vessel had to be used which could be cooled in liquid air and which could also work with varying quantities of solution, because an exact amount of solution could not be distilled in each time as would have been required by a normal Ostwald type viscometer. The viscometer must also be recharged by inverting it.

After one failure the viscometer shown in figure 5.1 was used. In this viscometer there are two bulbs of approximately 2 $cm.^3$ each, joined by a 3 cm. piece of 5 mm. tubing with a mark halfway along it. Another 3 cm. piece of 5 mm. tubing halfway along which is another mark, extends from the bottom of the lower bulb. This is then connected to 7 mm. of 0.5 mm. capillary of uniform bore. Thus on inverting the viscometer the solution easily runs from the large lower bulb and fills the two smaller ones and the

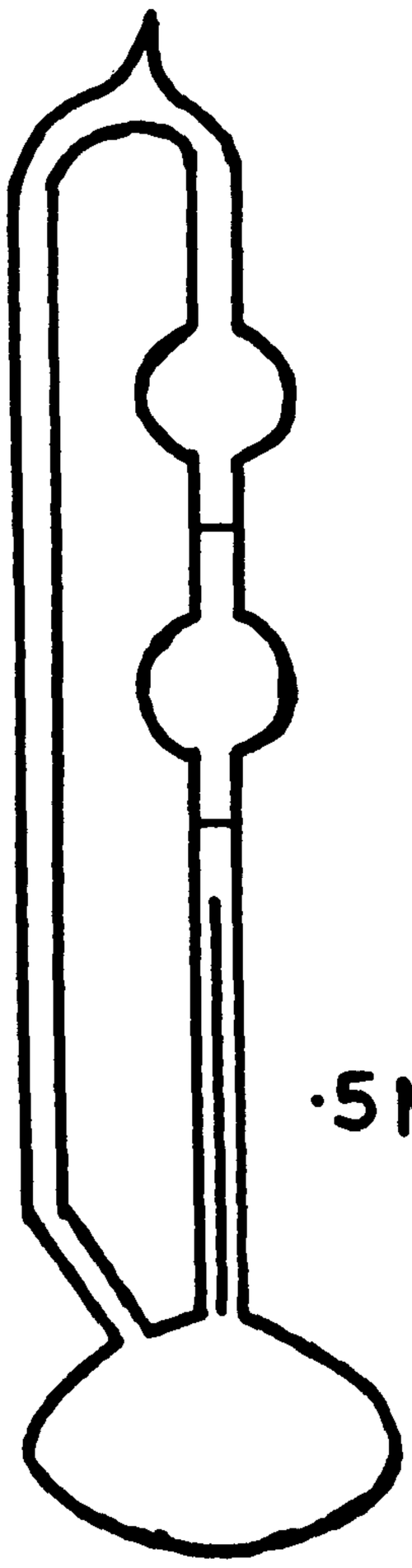

HALF SCALE

·5 MM CAPILLARY

FIGURE 5·1 THE VISCOMETER

capillary tube. Initially the viscometer was made with capillary tubing in place of the 3 mm. lengths of 5 mm. tubing, but it was found impossible to fill the viscometer satisfactorily on simple inversion, because of small bubbles of vapour formed in the capillary. Even though the graduation marks are on 5 mm. internal diameter tubing, the flow times could be accurately reproduced to 0.2 sec., which was about the limit of accuracy of the stop watch. The viscometer was filled by freezing the large bulb in liquid air and distilling air-free water and triethylamine into it. The viscometer was then sealed off.

5.3 Experimental

The viscometer was maintained at a constant temperature by operating it in a thermostatted tank. The tank contained twenty litres of distilled water and its temperature was controlled by means of a mercury-toluene regulator. Heating was provided by light bulbs placed around the glass tank, the bulbs being connected through a relay to the regulator. Cooling was provided by passing tap water through a glass spiral. The tank could be maintained at a temperature in the range 15 to 20°C with an accuracy better than 0.01°C, and its temperature was read to 0.01°C by means of a mercury

in glass thermometer which was protected from direct radiation by a metal shield.

The viscometer itself was fixed to a metal plate, which was pivoted about a bolt near the end of a holding bar, the bar being perpendicular to the axis of rotation. The bar was held vertically in the tank, and the viscometer could then be inverted and erected completely under the surface of the water in the tank. After inverting, the viscometer was arrested in the vertical position by means of a piece of metal protruding from the bar; and this was checked by setting the capillary tubing parallel to a plumb-line. The flow time for a given temperature was then recorded as the time necessary for the meniscus to travel between the two marks. Three consecutive readings agreeing within 0.2 sec. were obtained at each temperature. The flow time thus obtained multiplied by the density of the solution is proportional to the viscosity, with a constant depending only upon the viscometer. Flow times were measured at various temperatures from 15°C to just past the phase separation temperature for twelve solutions in the range of $x_A = 0.00 - 0.20$, and also for the pure liquids. Above 15°C readings were taken at up to half degree

intervals until the critical region was reached where they were taken at approximately 0.05°C intervals.

5.4 Results

From the experiment the flow times for the passage of a given volume of solution through the capillary were obtained. The viscometer was also calibrated with water, therefore, knowing the density of the solution, the viscosity of the solution can be compared with that of water at the same temperature. Thus if the times of outflow of equal volumes in the same apparatus are t_1 and tw (referring to water), then (6)

$$\frac{\eta_1}{\eta_w} = \frac{t_1 \rho_1}{t_w \rho_w}$$

where η is the viscosity and ρ the density.

The flow times were recorded and plotted against temperature. For all the solutions of composition near the critical there was a fall in the flow time with rising temperature until a minimum was reached. With further increase of temperature the viscosity reached a peak at the phase separation temperature, and then rapidly fell on the formation of two phases. The magnitude of this peak probably depended upon the temperature control in the region of the phase separation point, as at this point variations of only a fraction of a degree greatly affect the viscosity.

Figure 5.2 is a typical example of the viscosity vs. temperature curve obtained; while for solutions away from the critical region curves of the form of figure 5.3 were obtained.

The viscosities determined at 16.50°C are given in the following table. This temperature was chosen for comparison of results because it was intermediate in the investigated temperature interval, and also because it was well clear of the critical region. The viscosity of water used to calculate the results was obtained from the work of Swindells [7]. The viscosities are plotted against mole fraction in figure 5.4.

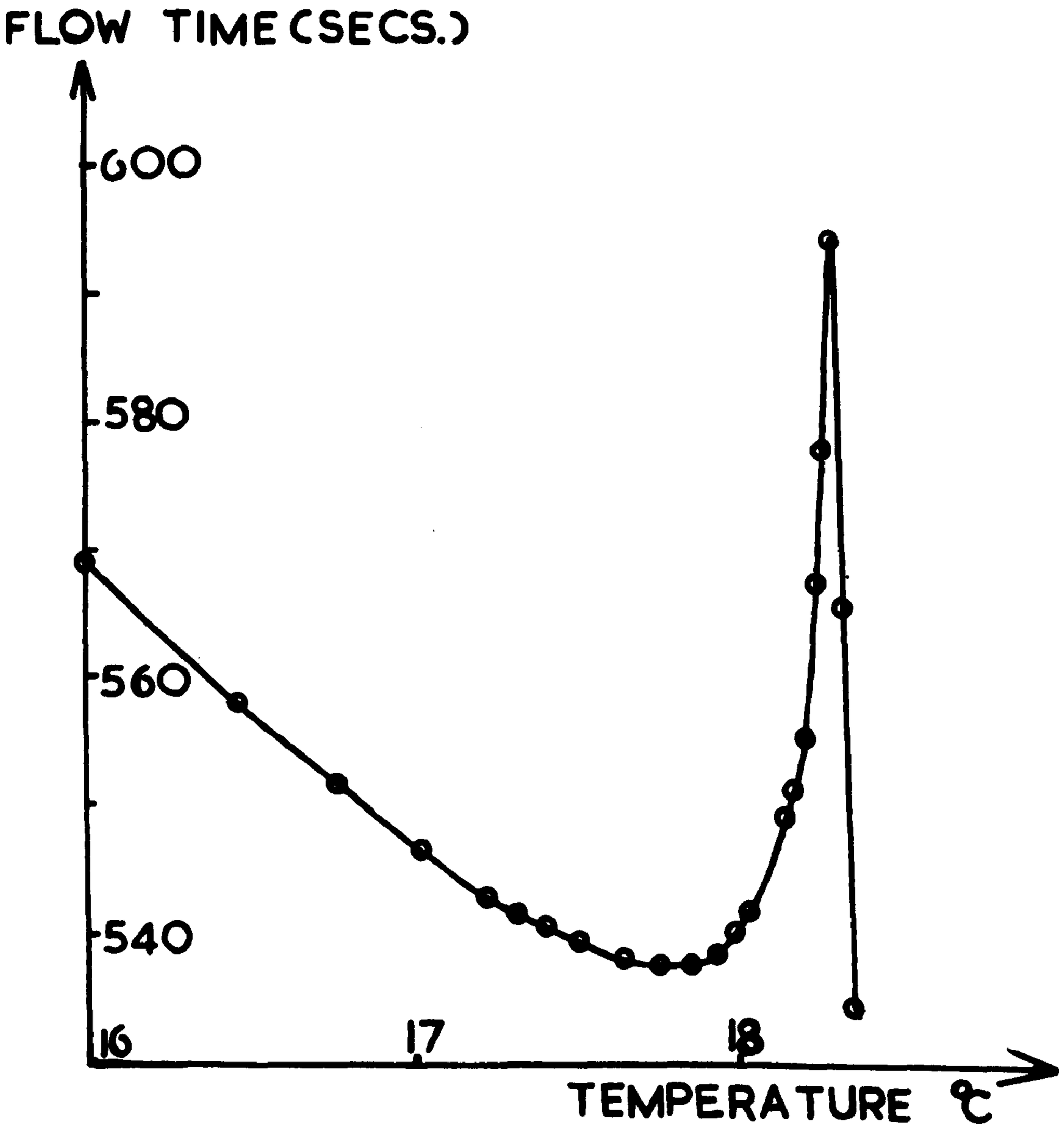

FIGURE 5·2 FLOW TIME-TEMPERATURE CURVE FOR MOLE FRACTION OF TRIETHYLAMINE $X_A = 0·0782$

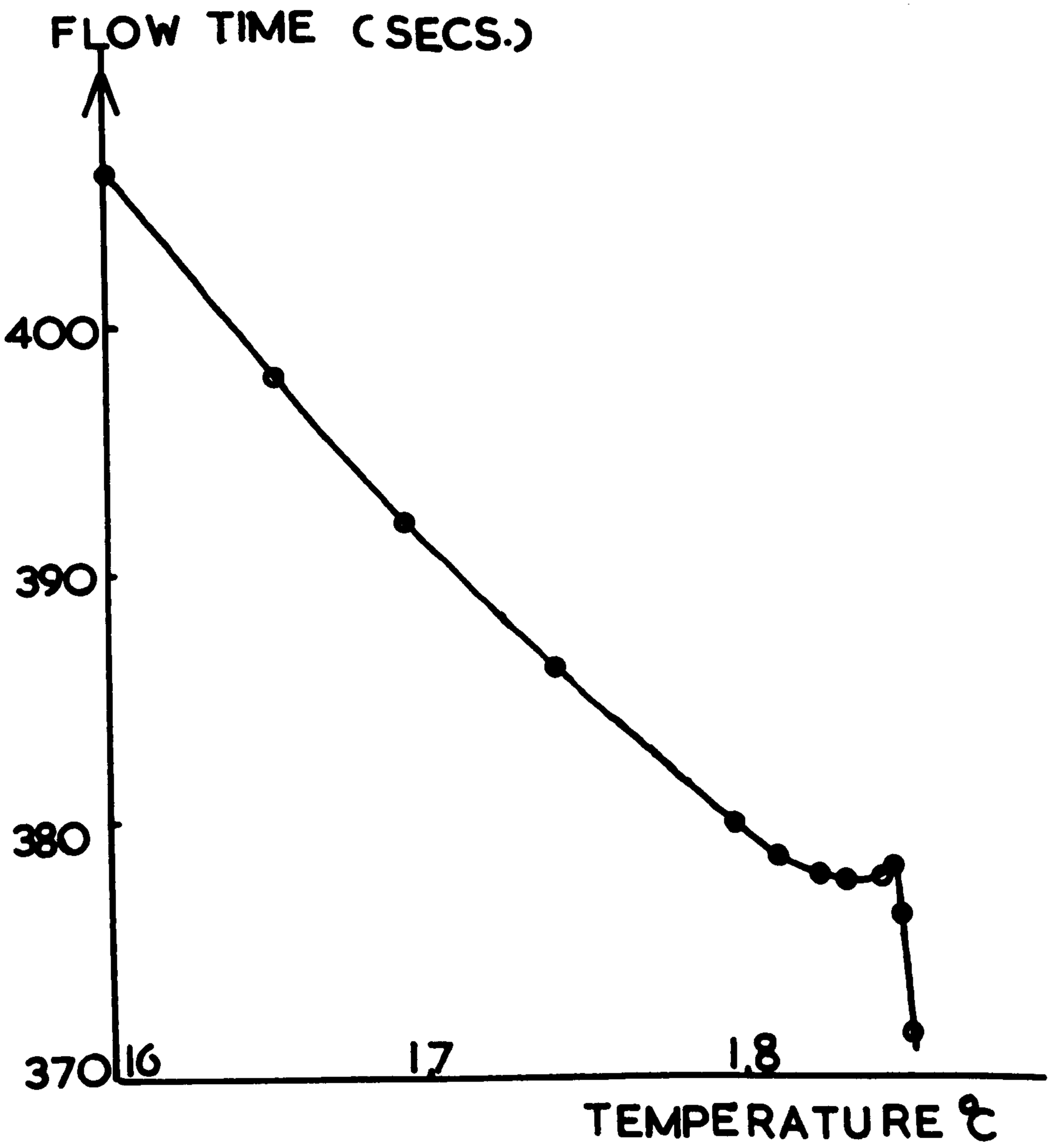

FIGURE 5·3 FLOW TIME–TEMPERATURE CURVE FOR MOLE FRACTION OF TRIETHYLAMINE $X_A = 0{\cdot}0433$

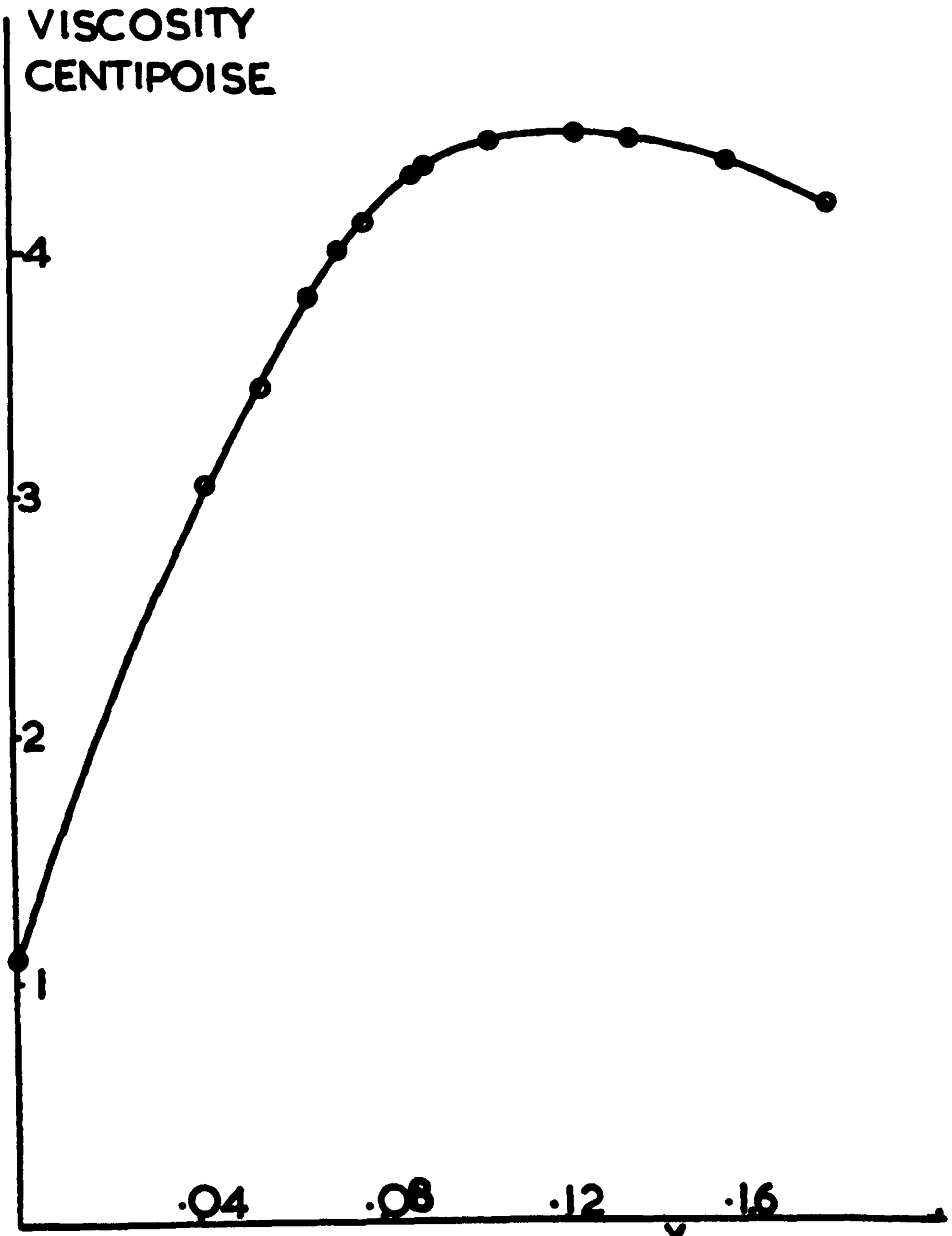

FIGURE 5·4 THE VISCOSITY AT 16·50°C OF THE TRIETHYLAMINE + WATER SYSTEM

Mole fraction of Triethylamine	Flow time at 16.50°C., sec.	Viscosity at 16.50°C., Cent ipoise
0.0000	138.7	1.0975
0.0433	398.2	3.025
0.0540	456.0	3.431
0.0653	509.8	3.796
0.0728	538.2	3.982
0.0782	556.5	4.098
0.0914	589.1	4.295
0.0942	595.9	4.335
0.1070	614.0	4.427
0.1255	627.4	4.457
0.1376	629.0	4.449
0.1584	620.2	4.334
0.1809	602.0	4.159
1.0000	66.3	0.384

5.5 Discussion of Results

We may remark upon the absence of hysteresis in the flow time vs. temperature curves. This is in contradiction to the observations of Semenchenko and Zorina, and I feel that the only way in which to explain the results of these workers is by assuming that their solutions contained impurity.

Figure 3.4 shows the viscosity of the system triethylamine + water plotted against mole fraction at 16.50°C. A maximum is obtained in the region $x_A = 0.13$. At this point the viscosity is four times that of water and twelve times that of triethylamine, and is six times the value one would expect if a perfect solution were formed. Thus one might consider that when triethylamine and water are mixed in the approximate ratio 1:6 a geometric condition is fulfilled which leads to large interactions between the molecules.

Figure 5.2 is a typical example of a flow time vs. temperature curve for a solution whose composition is near the critical. The rise in viscosity becomes large as the phase separation temperature is approached, and it is possible that the observed value of the viscosity at the phase separation temperature is less than the true value as a result of imperfect temperature control. As the viscosity

rises in this region critical opalescence reaches a maximum, and when the phase separation temperature is reached, opalescence is replaced by cloudiness and the viscosity rapidly falls. Hence on the basis of these results one may conclude that the change in the nature of the solution on approaching the critical point consists in the formation of a microheterogeneous state, and in further change in the degree of microheterogeneity. At the critical point the maximum possible degree of microheterogeneity is realised. It is likely that when these conditions are disturbed, there occurs a sudden fusion of molecular aggregates and a transition of the resultant microdispersed system into an ordinary dispersed system having milky cloudiness as its chief characteristic. One can also understand the existence of a critical region of concentrations in which viscosity peaks differing in height and sharpness are observed; the nearer the concentration is to the critical, the greater is the possibility that a large degree of microheterogeneity will develop, which corresponds to a higher viscosity.

If the height of the peak in the viscosity vs. temperature curves is indeed greatest for the critical composition, then one can use the viscosity data to obtain

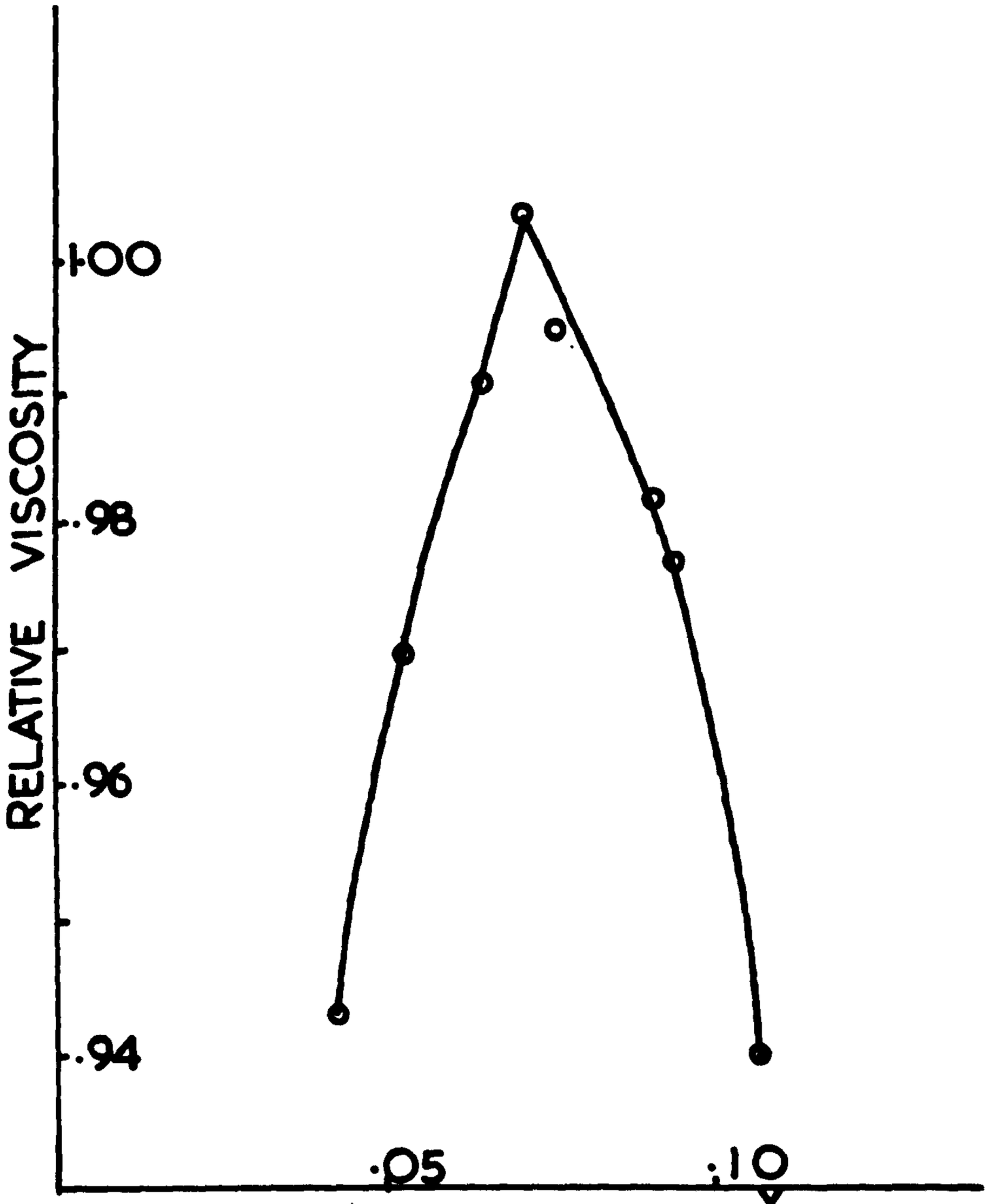

FIGURE 5·5 THE RELATIVE VISCOSITY AT ·10°C BELOW THE CRITICAL TEMP. TO THAT AT 16·50°C

a value for the critical composition. In figure 5.5 the heights of the various peaks are compared by plotting the value of the flow time at 0.10°C below the phase separation temperature divided by the value at 16.50°C against the mole fraction. It was necessary to take a temperature a little below the phase separation temperature to represent the height of the peak, due to the uncertainty of the actual height at the phase separation temperature. This figure clearly shows that the critical composition is $x_A = 0.073$.

REFERENCES FOR CHAPTER FIVE

1. V.K. Semenchenko and E.L. Zorina, Doklady Akad.Nauk. S.S.S.R., 73, 331, (1950)

2. idem. ibid, 80, 803, (1951)

3. idem, ibid, 84, 1191, (1952)

4. F. Kohler, Monat. für Chemie, 82, 913, (1951)

5. D.E. Tsakalotos, Z. Phys. Chem., 68, 36, (1909)

6. J.R. Partington, 'An Advanced Treatise on Physical Chemistry', Longmans, Green and Company, Vol. 2, page 75.

7. J.F. Swindells, J.Coll.Sci., 2, 177, (1947)

CHAPTER SIX

THE ELECTRICAL CONDUCTIVITY OF THE SYSTEM TRIETHYLAMINE + WATER

6.1. Introduction

Having observed that solutions of triethylamine and water show a viscosity maximum at $x_A = 0.13$, we decided to determine whether any other properties of the system show a similar maximum. The occurence of this maximum probably implies significant changes in the microscopic structure of the system as the mole fraction passes through $x_A = 0.13$. One would normally expect the electrical conductivity of the system to be sensitive to such structural changes, and this was therefore chosen as the next property to be studied.

At low concentrations triethylamine behaves as a weak electrolyte in water, the dissociation constant at $25^{\circ}C$ being 7.42×10^{-4} gm.ions litre^{-1} (1). This value, however, relates to solutions in which the mole fraction of amine was less than 0.0003. It seemed improbable that the triethylamine behaves as a simple weak electrolyte at higher concentrations, so in this work we set out to discover the behaviour of the conductivity in the range of mole fractions $x_A = 0.00 - 0\ 20$ and particularly in the critical region.

6.2 Apparatus

The conductivity cell is shown in figure 6.1. It consists of two platinum electrodes of 1.5 cm diameter coated to a black velvet-like finish by electrolysis of a 3% solution of chloroplatinic acid. The cell was washed with distilled water. Dilute sulphuric acid was then electrolysed in it, the current being reversed from time to time, in order to remove traces of chlorine and platinising liquid. After filling with the amine + water solution, the cell was placed in the thermostat, connected to the bridge, and surrounded by an earthed copper foil. The copper foil prevents direct radiation from the heater lights in the thermostat from heating the electrodes; it was also found to aid the attainment of a stable capacity value.

The conductivity bridge consists of a Wheatstone network incorporating a capacity balance and a Wagner earth arrangement. In general the bridge is similar to that used by Shedlovsky [2], and its circuit diagram is shown in figure 6.2. Two of the arms of the Wheatstone network are provided by Sullivan non-reactive screened 1000 ohm resistances. The variable third arm is a Sullivan and Griffiths non-reactive decade resistance box, with a maximum

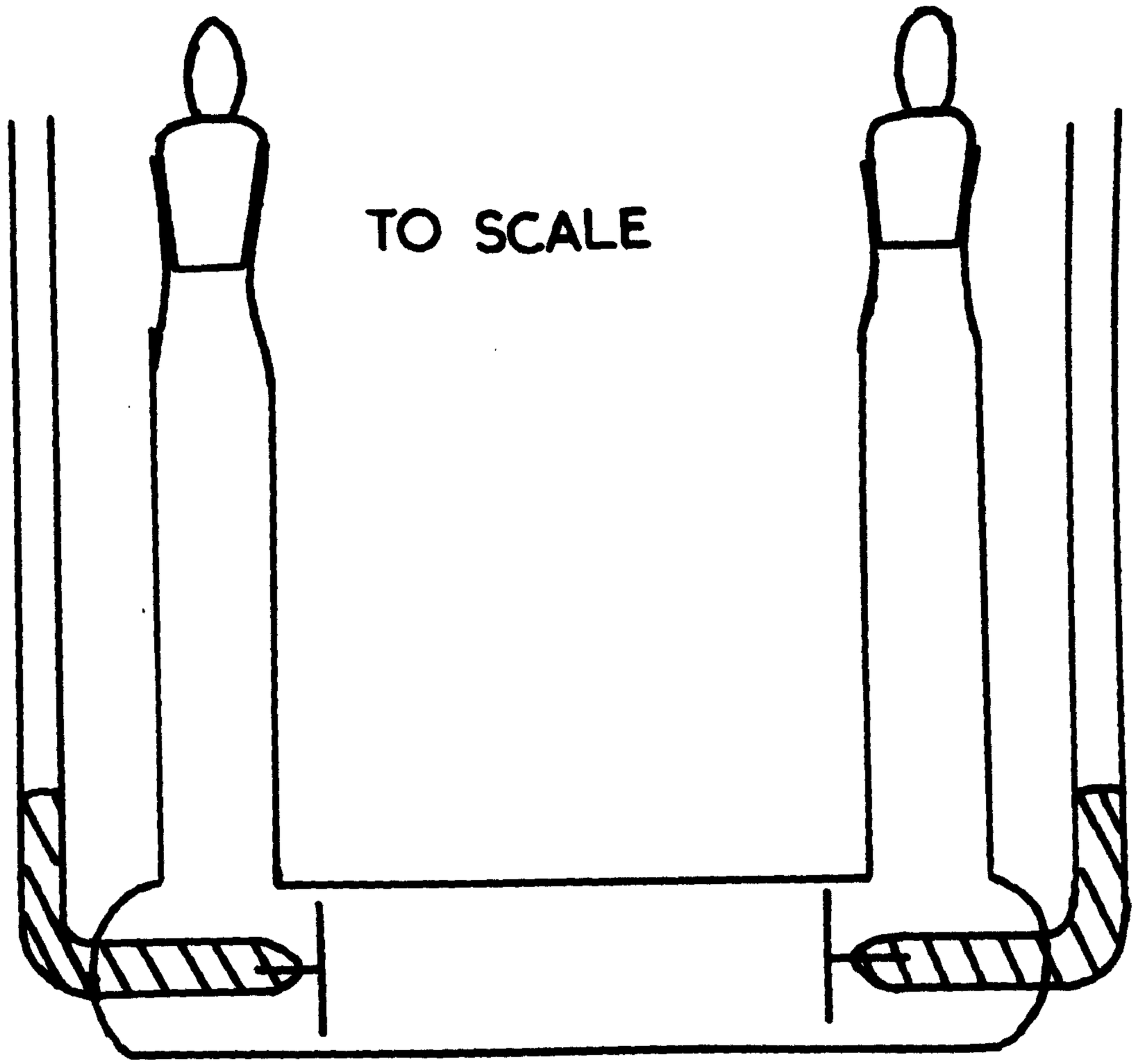

FIGURE 6·1 THE CONDUCTIVITY CELL

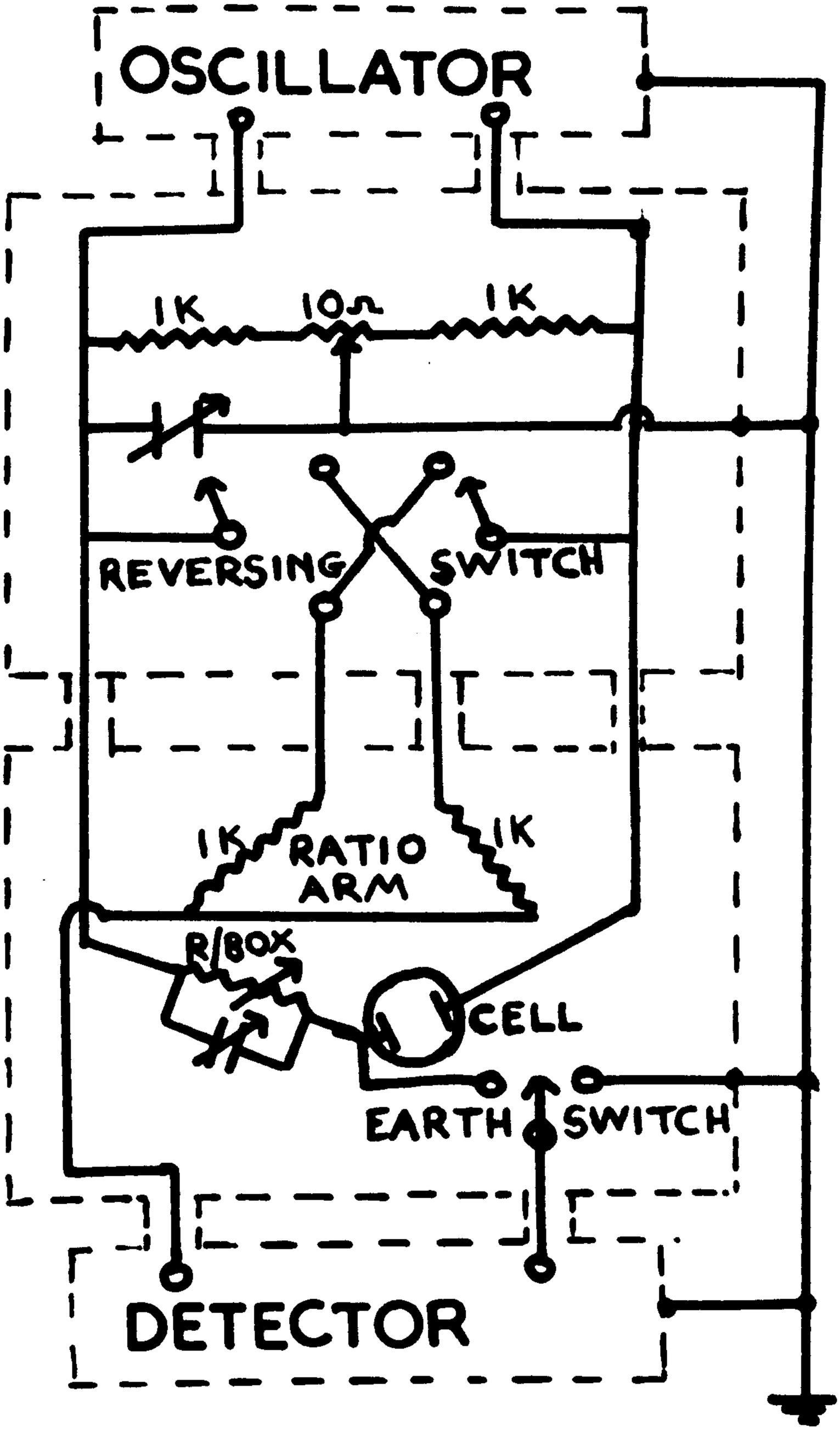

FIGURE 6·2 THE CONDUCTIVITY BRIDGE

reading of 11,111 ohms and capable of being read to 0.1 ohm. It is screened and compensated for reactance.

The A.C. oscillator was designed to produce a frequency of 1050 c. The output of this oscillator is taken through the primary coil of a 1:2 step-up transformer, the output of the secondary coil being led to the bridge by a screened two-core cable. The battery operated null detector incorporates a microammeter used for the approximate balancing of the bridge. A Cambridge 20 ohm spot galvanometer with an instrument rectifier can be switched in for the final adjustment of the balance point. The shielded leads from the cell and other bridge connections are taken to a Wagner-earth arrangement housed in a soft iron box. Two Sullivan 1000 ohm standard non-inductive resistances are connected together by a 10 ohm potentiometer whose contact arm is earthed. Two identical, variable air condensers of about 300 pf. capacity are used to balance out the cell reactance, one across the resistance box and the other across the corresponding Wagner earth ratio arm resistance.

A double pole double throw switch is used to reverse the bridge ratio arms when necessary. A brass knife switch connects the detector either to the bridge or to earth.

6.3 Experimental

The amine and water were both prepared as described in the previous section. Both were degassed by boiling and stored in glass vessels with tight fitting stoppers. The solutions were then prepared by weighing water and amine into a stoppered flask: solutions with amine concentrations below $x_A = 0.005$ were made by diluting stronger solutions with water. The cell was calibrated by means of a standard $^N/_{100}$ solution of KCl at 18.00°C. $^N/_{10}$ KCl (7.4552 g.p.l.) was diluted to give $^N/_{100}$ KCl and the resistance of the cell was found to be 1873.5 ohms: using the value of 0.0012205 ohm^{-1} cm^{-1} for the conductivity of $^N/_{100}$ KCl [3] we found a value of 2.288 cm^{-1} for the cell constant.

Values of the cell resistance for various mole fractions of amine in water were obtained in the temperature range 14-20°C. These readings were taken at approximately 0.50°C intervals, except in the cases of solutions near the critical point where readings were taken at much closer intervals. The temperature of the tank was again measured by a calibrated thermometer which can be read to 0.01°C. The sensitivity of the bridge depended upon the actual resistance of the solution, but it varied from about 0.02% for solutions

in the region x_A = 0.01 to 0.05% in the region x_A = 0.15.

6.4 Results

Figures 6.3 and 6.4 show examples of resistance vs. temperature curves obtained for solutions near to and removed from the critical mole fraction respectively. Figure 6.3 contains several approximately parallel curves. These were obtained by measuring the resistance of the solution up to the phase separation temperature, and then, after the formation of two phases, cooling the solution, shaking the cell to make the solution homogeneous, and repeating the procedure. The new curve obtained was parallel to, but displaced from, the original. If this effect were due to accumulation of impurities, then the resistances at any given temperature would be expected to move in one direction as the number of runs increased. This was not observed to be the case so the effect may be attributed to the absence of stirring, which is probably needed in order to obtain true equilibrium in a solution near its critical point. Figure 6.5 shows the specific conductivities at 16.50°C for solutions in the range x_A = 0.00 - 0.15. This contains a maximum at x_A = 0.0115.

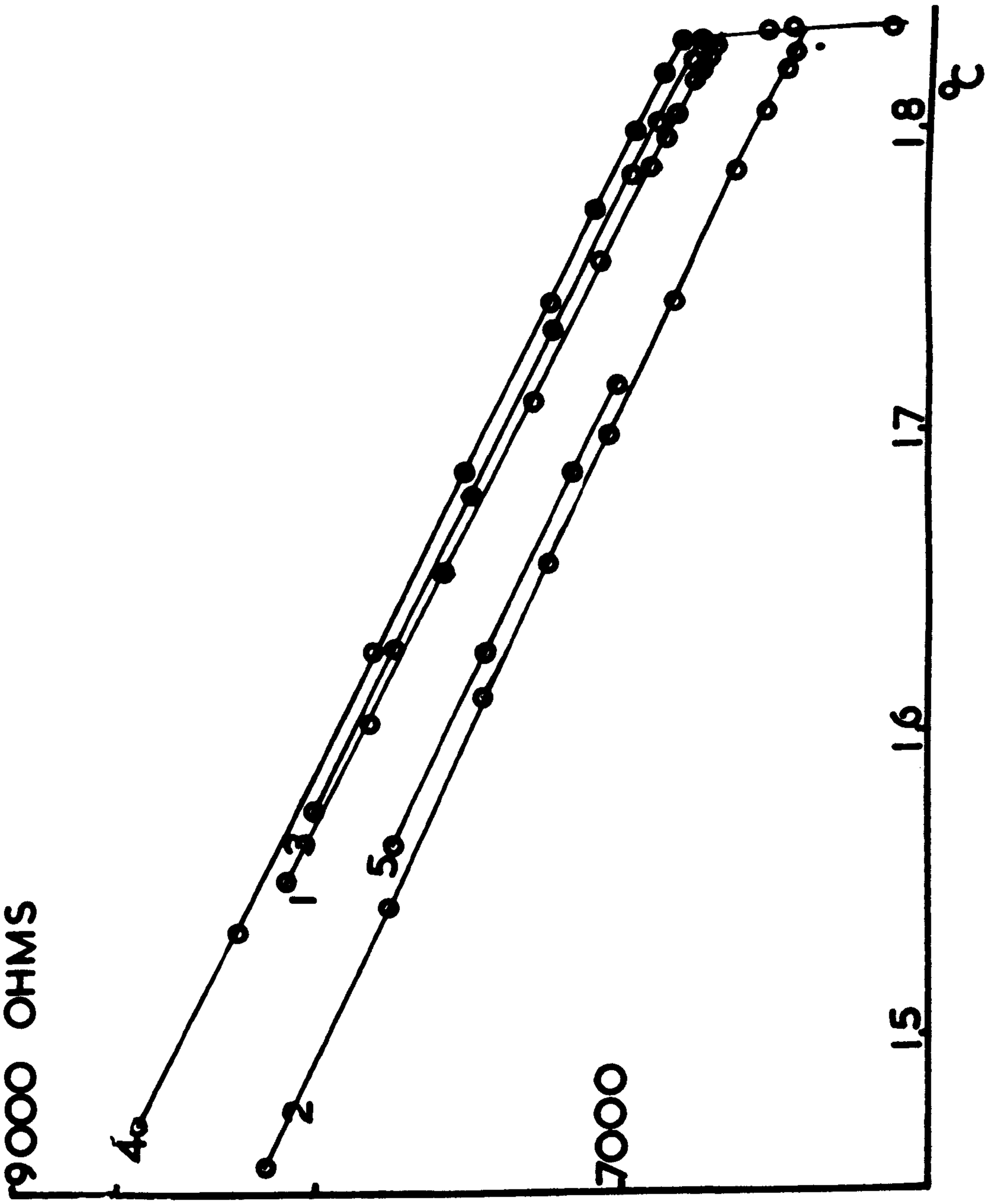

FIGURE 6·3 RESISTANCE-TEMPERATURE DIAGRAM FOR MOLE FRACTION OF TRIETHYLAMINE $X_A = 0.0926$

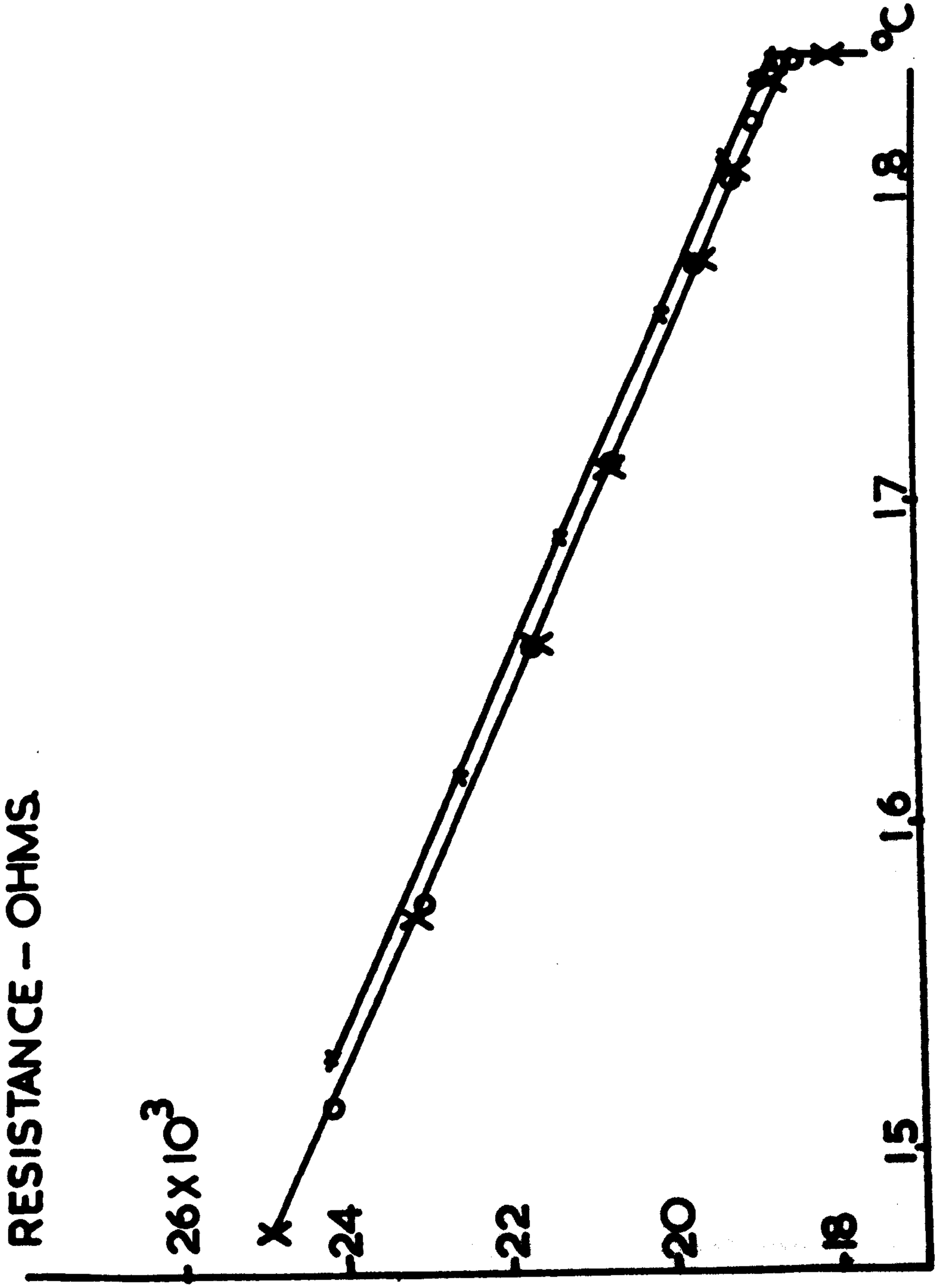

FIGURE 6·4 RESISTANCE-TEMPERATURE DIAGRAM FOR MOLE FRACTION OF TRIETHYLAMINE $X_A = 0.1350$

6.5 Discussion of Results

In all solutions examined the specific resistance shows an approximately linear dependence upon temperature. The specific resistance decreases with increasing temperature, until the phase separation temperature is reached. There is then a sharp fall in the resistance corresponding to the formation of two phases. This sharp fall past the phase separation temperature has no relevance as we were then determining the resistance of two phases instead of a uniform single phase.

The fact that the resistance is approximately a linear function of temperature for the solutions examined, and does not show any deviation in the critical region, deserves some discussion.

In most electrically conducting solutions the resistance depends directly upon the viscosity, so one would expect in the present system that solutions near the critical point might show a rise in resistance with increasing temperature due to the viscosity effect discussed in the previous chapter. This effect was not discovered so it appears that some other method of conduction occurs which is viscosity independent. Another interesting deduction from the

linearity of the resistance vs. temperature curves is that the occurence of molecular clustering in the critical region has no direct effect upon the conductivity. Consequently one must assume either that ions do not take part in the formation of clusters, or if they do that the ions in the clusters are still available for conduction.

A further point of interest concerning the resistance vs. temperature curves is their non-reproducibility. Other properties showing similar behaviour have previously been discussed in the case of one-component systems. Maass [4,5] observed such effects but he later discovered that they were due to insufficient stirring [6], and this was confirmed by Atack and Schneider [7]. In the case of solutions removed from the critical point the non-reproducibility is small, as can be seen in figure 6.4 for $x_A = 0.1350$. In this case the detected variation in the specific conductivity is approximately 1.3% at 16.50°C. This compares with values of 11.0% for $x_A = 0.0698$ and 5.6% for $x_A = 0.0926$. These figures probably underestimate the possible variation as never more than six curves were obtained for each solution; but they all demonstrate that the anomalous behaviour of the solutions is much greater near the critical point than

elsewhere, as would be expected.

We will now consider the values of the specific conductivity of the various solutions as a function of mole fraction at 16.50°C. The specific conductivity vs. mole fraction curve is shown in figure 6.5 and covers the amine mole fraction range x_A=0.00-0.15. As can be seen a maximum occurs in the region x_A=0.0115 while the specific conductivity falls slowly away on the amine rich side and more quickly on the water rich side. This maximum (which has a value of 20.5×10^{-4} mhos at x_A=0.0115) illustrates the large deviations from ideality in this amine + water system. If the solution were ideal, apart from a small amount of ion formation, then maximum conductivity would be expected to occur at a much higher mole fraction.

Results were not obtained for solutions below a mole fraction of amine of 0.0001. Thus it is difficult to determine exact values of the dissociation constant (k) and equivalent conductivity at infinite dilution (Λ_∞) of triethylamine in water. Nevertheless an attempt was made to calculate these quantities, but the results are subject to a significant error as the extrapolation had to be extended over a large concentration range. If κ is the specific conductivity in mhos, k the dissociation constant

of the amine in g.ions. ml^{-1} , V the dilution of the amine in ml., Λ the equivalent conductivity and Λ_∞ the equivalent conductivity at infinite dilution in mhos ml.$(g.ion)^{-1}$, we have,

$$k = \frac{\Lambda^2}{\Lambda_\infty(\Lambda_\infty - \Lambda)V}$$

and as $\mathcal{K}V = \Lambda$,

$$k\Lambda_\infty^2 - k\Lambda_\infty\mathcal{K}V = \mathcal{K}^2V, \quad \text{whence}$$

$$\frac{k\Lambda_\infty^2}{\mathcal{K}V} - k\Lambda_\infty = \mathcal{K}$$

A plot of $\frac{1}{\mathcal{K}V}$ against $\mathcal{K}$ yielded a straight line for points in the range 0.0001 to 0.001 mole fraction of amine.

By finding the slope of the line and its intercept with the $\frac{1}{\mathcal{K}V}$ axis the values of Λ_∞ and k were found at 16.50°C to be,

$$k = 6.3 \times 10^{-7} \quad g.ions\ ml^{-1}$$

$$\Lambda_\infty = 166 \text{ mhos ml.}(g.ion)^{-1}$$

Deviations from the laws apertaining to solutions of weak electrolytes begin to appear at amine mole fractions greater than 0.001. These deviations rapidly become large, and it is only at extremely low concentrations that triethylamine can be regarded as an ideal weak electrolyte in water.

REFERENCES FOR CHAPTER SIX

1. J.E. Ablard, D.S. McKinney and J.C. Warner, J.Am.Chem.Soc. 62, 2181, (1940)

2. T. Shedlovsky, J.Am.Chem.Soc., 52, 1793, (1930)

3. A. Findlay, 'Practical Physical Chemistry', 8th Edition, Longman, Green and Company, 1954, p.209

4. R.L. McIntosh and O. Maass, Can.J.Res., B16, 289, (1938)

5. J. Marsdon and O. Maass, Can,J.Res., B13, 296, (1935)

6. S.G. Mason, S.N Naldrett, and O. Maass, Can.J. Res., B18, 103, (1940)

7. D. Atack and W.G. Schneider, J.Phys.Coll.Chem., 55, 532, (1951)

CHAPTER SEVEN

THE DENSITY OF THE SYSTEM TRIETHYLAMINE + WATER

7.1 Introduction

We decided to continue our investigation of properties of the system triethylamine + water in order to discover whether they show a maximum at $x_A = 0.13$ similar to that discovered in the viscosity vs. mole fraction curve. Consequently we decided to measure the density and coefficient of thermal expansion throughout the whole range of composition and in the temperature range 15-20°C. Tsakalotos [1] and Kohler [2] had previously made density measurements on this system and showed that the excess volume vs. mole fraction curve is approximately parabolic, but the accuracy of their measurements is not sufficient to locate the composition at the point of greatest deviation from a parabola.

7.2 The Dilatometer

Many types of dilatometer were considered, and finally the design of Owen, White and Smith [3], used for the precise determination of the density of water between 45°C and 85°C, was chosen as being most suitable for our purpose. The design of Owen, White and Smith is essentially the same as

that illustrated in figure 7.1, except that they used an ordinary glass tap instead of the special seal on the 2 mm. filling capillary. This modification had to be made for the present work as tap grease is readily soluble in triethylamine.

In the first design of greaseless seal we tried, a disc of fluon was clamped onto a flat ground flange on the end of the filling capillary. The cell was then filled with water and the side tube with mercury in order to produce a pressure which would tend to push the water past the seal. The seal was found to leak under these conditions.

The seal finally used is shown in figure 7.1. The orifice at the end of the piece of 2 mm glass capillary tube was groundto fit a 3/16th " stainless steel ball bearing, and the orifice polished with jewellers' rouge. The ball bearing was placed on top of a small piece of teflon sheet (0.005" thick) and pressed into its seating by a clip. This was then tested for leaks over several days, and none could be detected by weighing the dilatometer.

7.3 Preparation of Materials

The triethylamine and water were both prepared as described in Chapter Four. Mercury was purified by washing

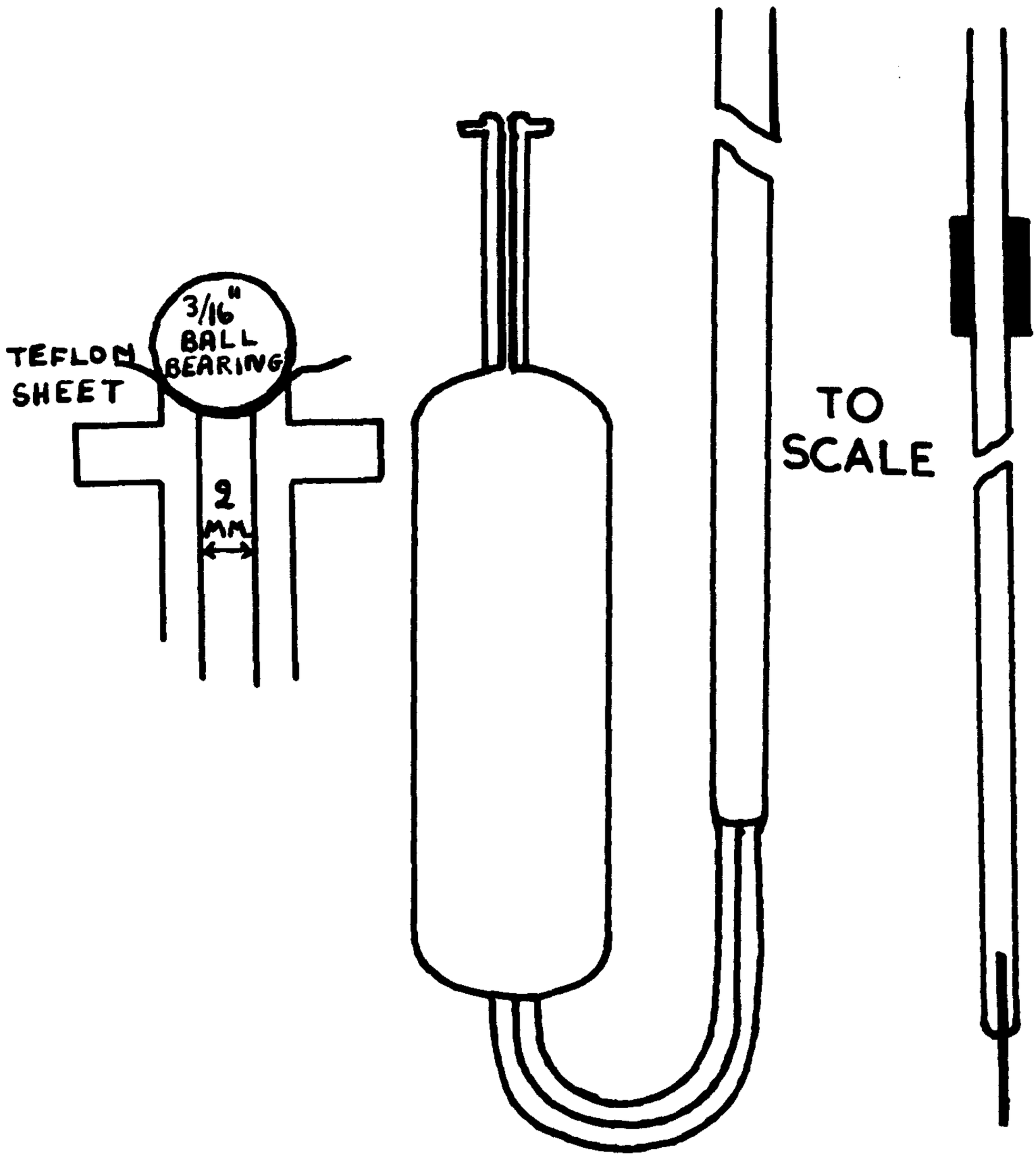

FIGURE 7·1 THE DILATOMETER

with nitric acid, and twice distilling under reduced pressure using an air leak.

7.4 Experimental

The thermostat was similar to that used in previous experiments. The dilatometer was washed with chromic acid and many times with water and finally dried and weighed. About 5 ml. of mercury were then put in, care being taken that the capillary part of the side arm was full and contained no air bubbles. The dilatometer was then reweighed and filled through the 2 mm. filling capillary with air free water for calibration purposes. Subsequently the water was replaced by solutions of known amine concentration, which had been prepared gravimetrically from triethylamine and water. When the dilatometer was being filled with amine solutions it was necessary to keep it (and the flask containing the solutions) cool in order to prevent phase separation. The weight of the amine solution could not be determined immediately, as weighing would have necessitated the dilatometer coming to room temperature with subsequent phase separation. This difficulty was overcome by weighing the dilatometer and its contents after the completion of the experiment.

The dilatometer was placed in the thermostat, making sure that the side arm was vertical by means of a spirit level, and allowed to attain thermal equilibrium. The level of mercury in the side arm was adjusted to a datum level by removing the excess with the special pipette which is also shown in figure 7.1. The pipette consists of a 0.5 mm. platinum tube sealed into one end of a piece of 5 mm. bore glass tube. A collar is fixed near the other end of the glass tube, and the position of this collar determines the datum level of the mercury in the capillary section of the side arm. Both the top of the side arm and the lower edge of the collar are ground flat. By means of this pipette the mercury above the datum level was withdrawn at different temperatures and transferred to a weighing bottle. At the completion of each series of readings the dilatometer was weighed. Then, from the original weight of the dilatometer + mercury and the total weight of mercury removed, the weight of solution was calculated.

7.5 Results

The variation of the volume of the dilatometer with temperature was determined by the initial calibration with

water and mercury. The density of mercury was obtained from the 'Handbook of Chemistry and Physics' [4], and that of water from the Tilton and Taylor equation [5]

$$1 - d = \frac{(t - 3.9863)^2}{508929.2} \times \frac{(t + 288.9414)}{t + 68.12963}$$

where d is the density in $g.ml^{-1}$ and t the temperature in ^{o}C. The calibration curve was linear in the temperature range (13-24^{o}C), and showed an increase in volume of 4×10^{-4} ml. deg^{-1} for a 45 ml.cell. The maximum deviation of any point from a straight line was less than 1×10^{-4} ml.

For each solution considered a plot was made of specific volume ($ml.g.^{-1}$) against temperature. Two of these curves are shown in figures 7.2 and 7.3. Figure 7.2 is typical for a solution near the critical composition, showing a large change of slope on passing through the phase separation temperature, and also a change in sign of the curvature from positive to negative. Figure 7.3 ($x_A = 0.2951$) does not show such a large change of slope on passing through the phase separation temperature, and neither does it show a change in the sign of the curvature, a property which disappears at approximately $x_A = 0.15$.

The excess volume of mixing was calculated for each

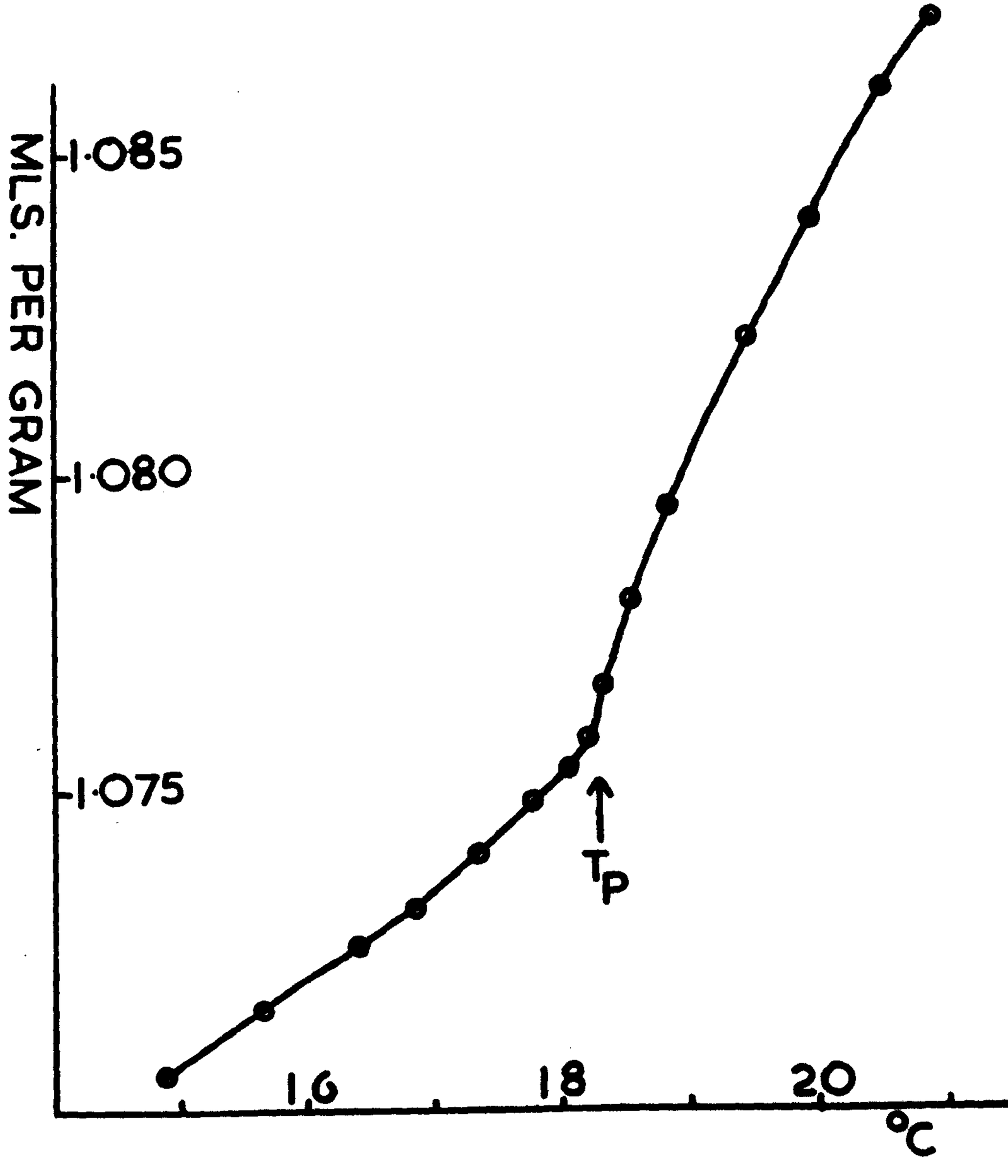

FIGURE 7·2 VOLUME PER GRAM AS A FUNCTION OF TEMPERATURE FOR MOLE FRACTION OF TRIETHYLAMINE $X_A = 0·0743$

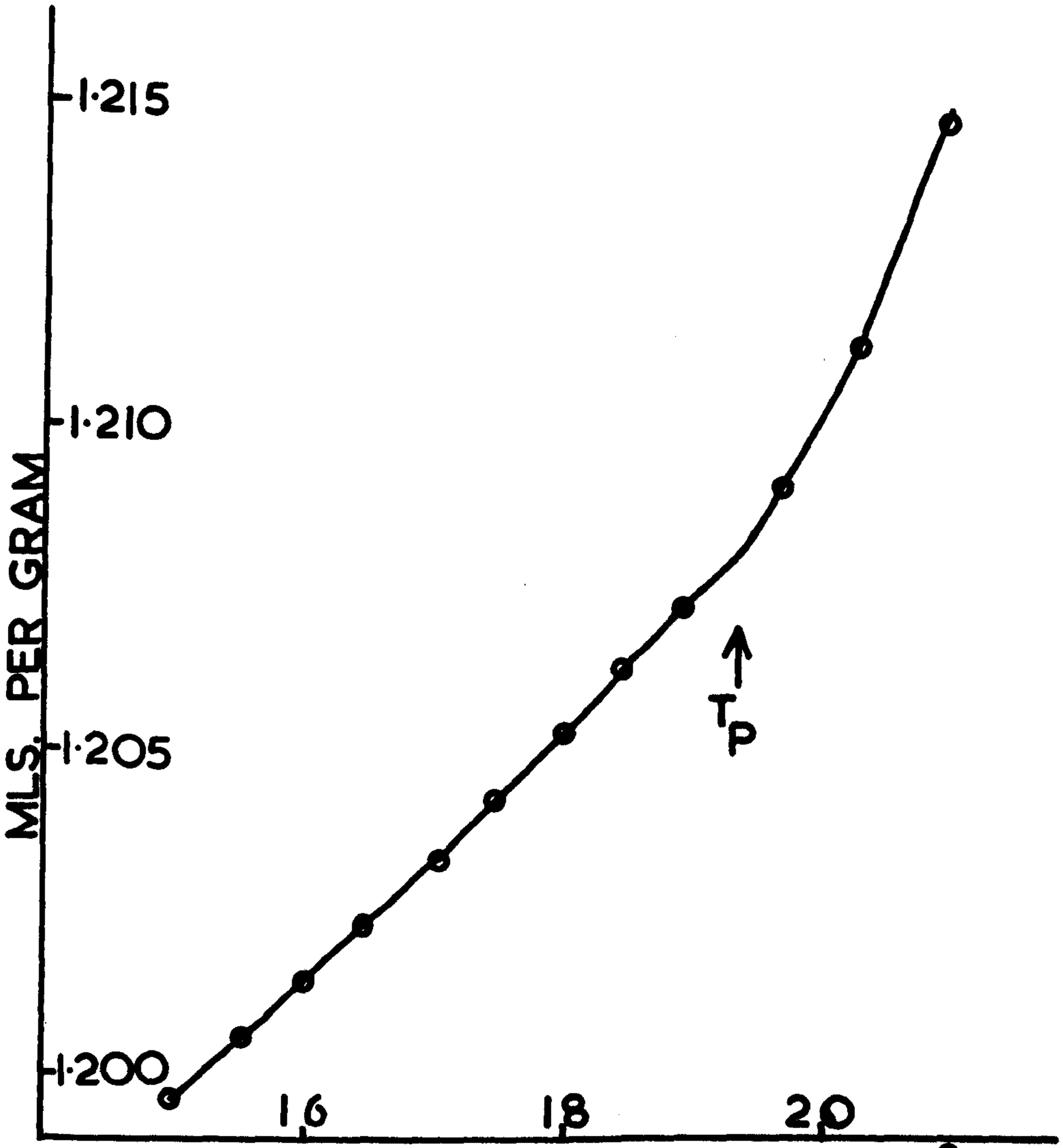

FIGURE 7·3 VOLUME PER GRAM AS A FUNCTION OF TEMPERATURE FOR MOLE FRACTION OF TRIETHYLAMINE $X_A = 0·2951$

solution at 16.50°C from the relation.

$$v^E = v - v^\circ_w x_w - v_A{}^\circ x_A, \quad x_A + x_w = 1,$$

where v is the molar volume of the solution and v°_w and $v_A{}^\circ$ represent the molar volumes of the pure water and triethylamine respectively.

$$\therefore \quad v^E = \frac{(18.016\, x_w + 101.19 x_A)}{\rho} - \frac{18.016 x_w}{\rho_w{}^\circ} - \frac{101.19 x_A}{\rho_A{}^\circ}$$

where ρ is the density of the solution and $\rho_w{}^\circ$ and $\rho_A{}^\circ$ are the densities of pure water and triethylamine respectively. The accuracy with which these excess volumes have been determined is probably better than 0.005 ml. in the low amine concentration range and 0.01 ml. at higher amine concentrations. The values of the excess volume of mixing at 16.50°C are tabulated below and plotted against mole fraction in figure 7.4.

Mole fraction of triethylamine x_A	Excess volume of mixing $-v^E$ ml.
0.0000	0.000
0.0213	0.429
0.0428	0.699
0.602	0.881
0.0743	1.019

Mole fraction of triethylamine x_A	Excess volume of mixing $-v^E$ ml.
0.1158	1.387
0.1553	1.677
0.1964	1.934
0.2951	2.361
0.3982	2.555
0.4918	2.557
0.5603	2.475
0.6659	2.213
0.7309	1.939
0.7479	1.847
0.8324	1.355
0.9034	0.865
1.0000	0.000

The excess volume of mixing vs. mole fraction curve approximates to a parabola, and figure 7.5 shows the deviation from a parabola, the parabola being fitted to the volume of mixing curve at $x_A = 0.5$. The deviation from a parabola is small compared with the magnitude of v^E, but the deep minimum in figure 7.5 probably indicates a high degree of local order in the region x_A=0.15 in

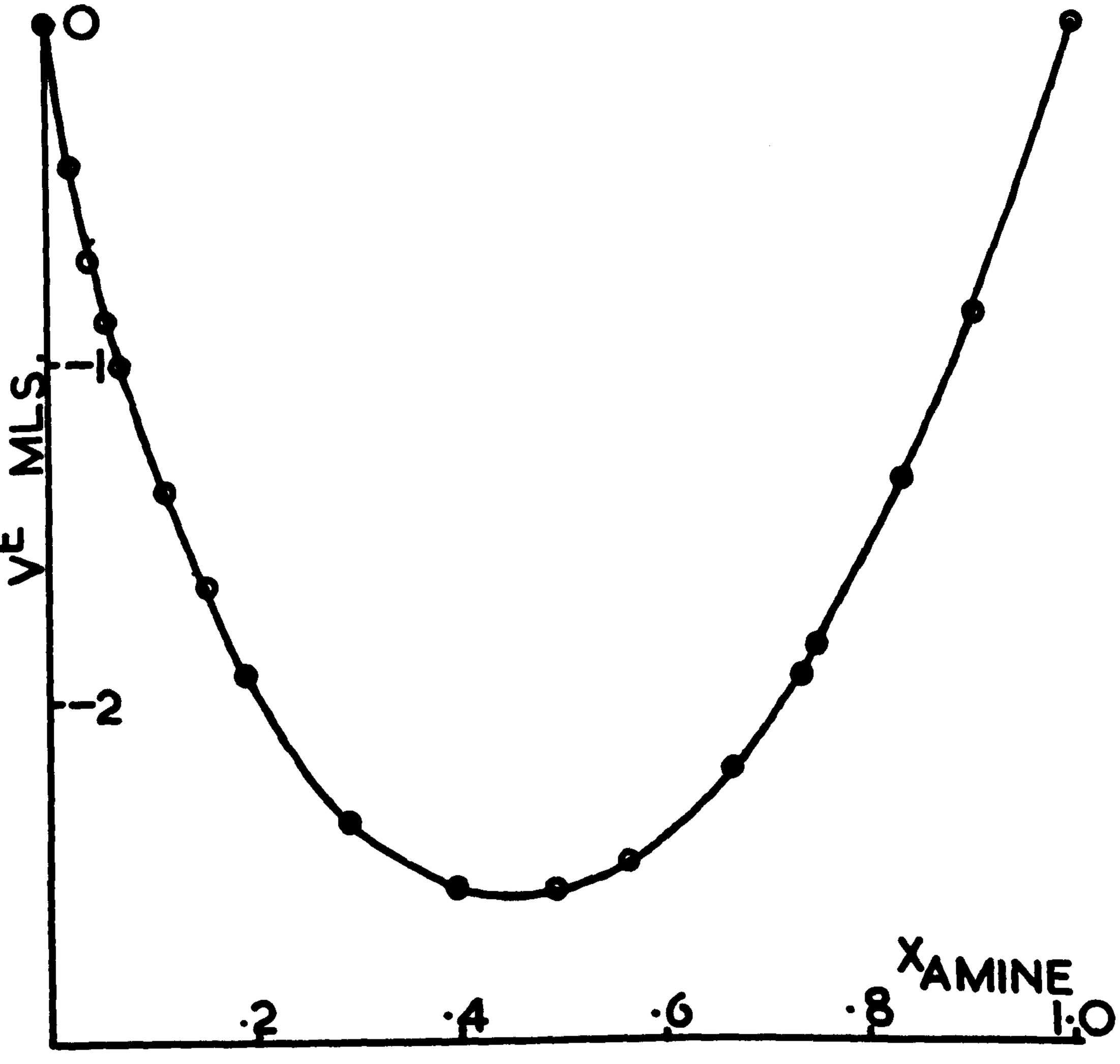

FIGURE 7·4 THE EXCESS MOLAR VOLUME OF MIXING FOR THE TRIETHYLAMINE + WATER SYSTEM AT 16·50 °C

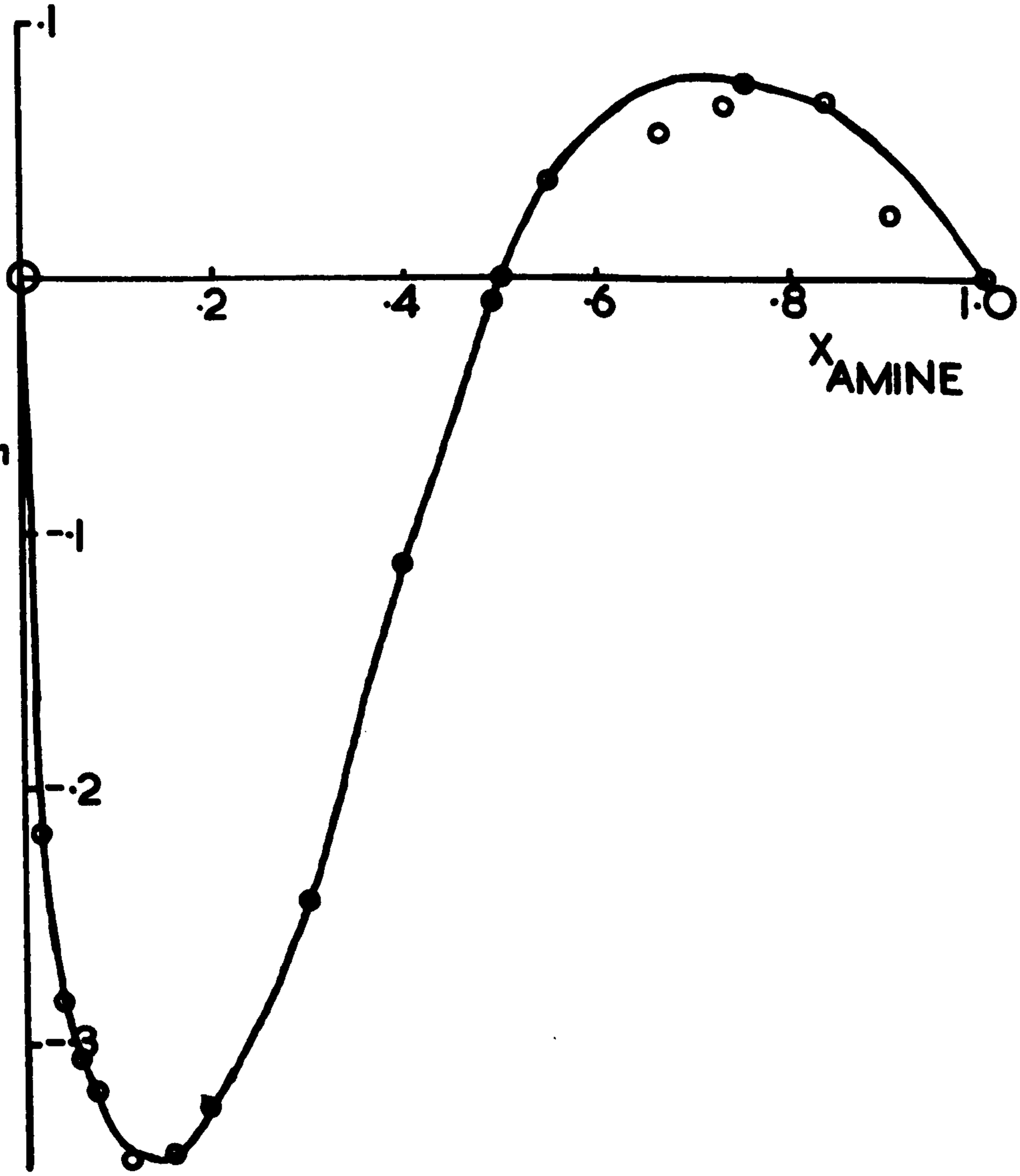

FIGURE 7·5 THE DEVIATION OF THE EXCESS MOLAR VOLUME OF MIXING FROM A PARABOLA AT 16·50°C

agreement with the deductions made from the viscosity measurements.

The thermal expansion coefficient ($\alpha = \frac{1}{V}\left(\frac{\partial V}{\partial T}\right)_P$) was also calculated from the various specific volume vs. temperature curves. This is plotted as a function of mole fraction in figure 7.6, and a maximum is found to occur at $x_A = 0.15$. Thus if this maximum persists at lower temperatures the minimum in figure 7.5 will become more significant.

In order to obtain the partial molar volumes of the two components we fitted the excess volume of mixing at 16.50°C to an equation of the form,

$$v^E = x(1-x)(A+B(1-2x) + C(1-2x)^2 + D(1-2x)^3 + \ldots)$$

The method of least squares gives the explicit equation as,

$$v^E = -x(1-x)\{10.20 + 1.48(1-2x) + 2.38(1-2x)^2 + 1.79(1-2x)^3\} ,$$

where x is the mole fraction of triethylamine.

The volume per mole at 16.50°C is therefore,

$$v = 18.036(1-x) + 138.333x - x(1-x)\{10.20 + 1.48(1-2x) + 2.38(1-2x)^2 + 1.79(1-2x)^3\} ;$$

and the partial molar volumes now can be computed according to,

$$v_A = v + (1-x)\frac{dv}{dx} , \quad v_W = v - x\frac{dv}{dx}$$

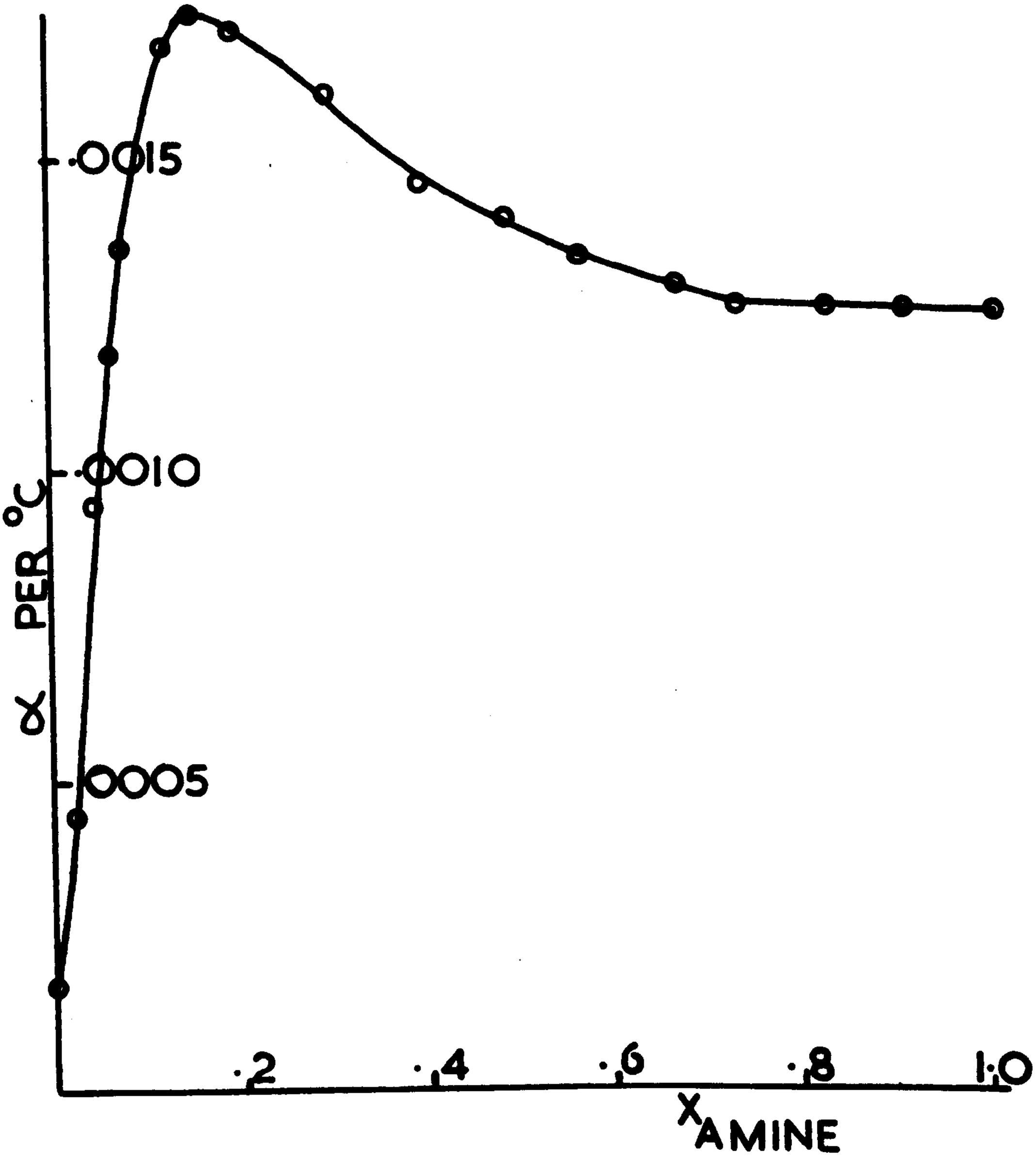

FIGURE 7·6 THE THERMAL EXPANSION COEFFICIENT (α) OF THE TRIETHYLAMINE + WATER SYSTEM

The partial molar volumes of triethylamine (v_A) and water (v_W) are given in the following table at rounded mole fractions.

Mole fraction of triethylamine	Partial molar volume of water	Partial molar volume of triethylamine
x_A	v_W ml.	v_A ml.
0.0	18.04	122.49
0.1	17.75	128.55
0.2	17.15	132.06
0.3	16.49	134.05
0.4	15.84	135.29
0.5	15.12	136.17
0.6	14.22	136.88
0.7	13.08	137.50
0.8	11.64	137.98
0.9	10.06	138.27
1.0	8.73	138.33

These values are plotted in figure 7.7. The most striking result is the value of the partial molar volume of water in pure amine. At $x_A = 1$, $v_W = 8.73$ ml. which is less than half the value for pure water. This value emphasises the large interaction which occurs between water and triethylamine by means of the hydrogen bond.

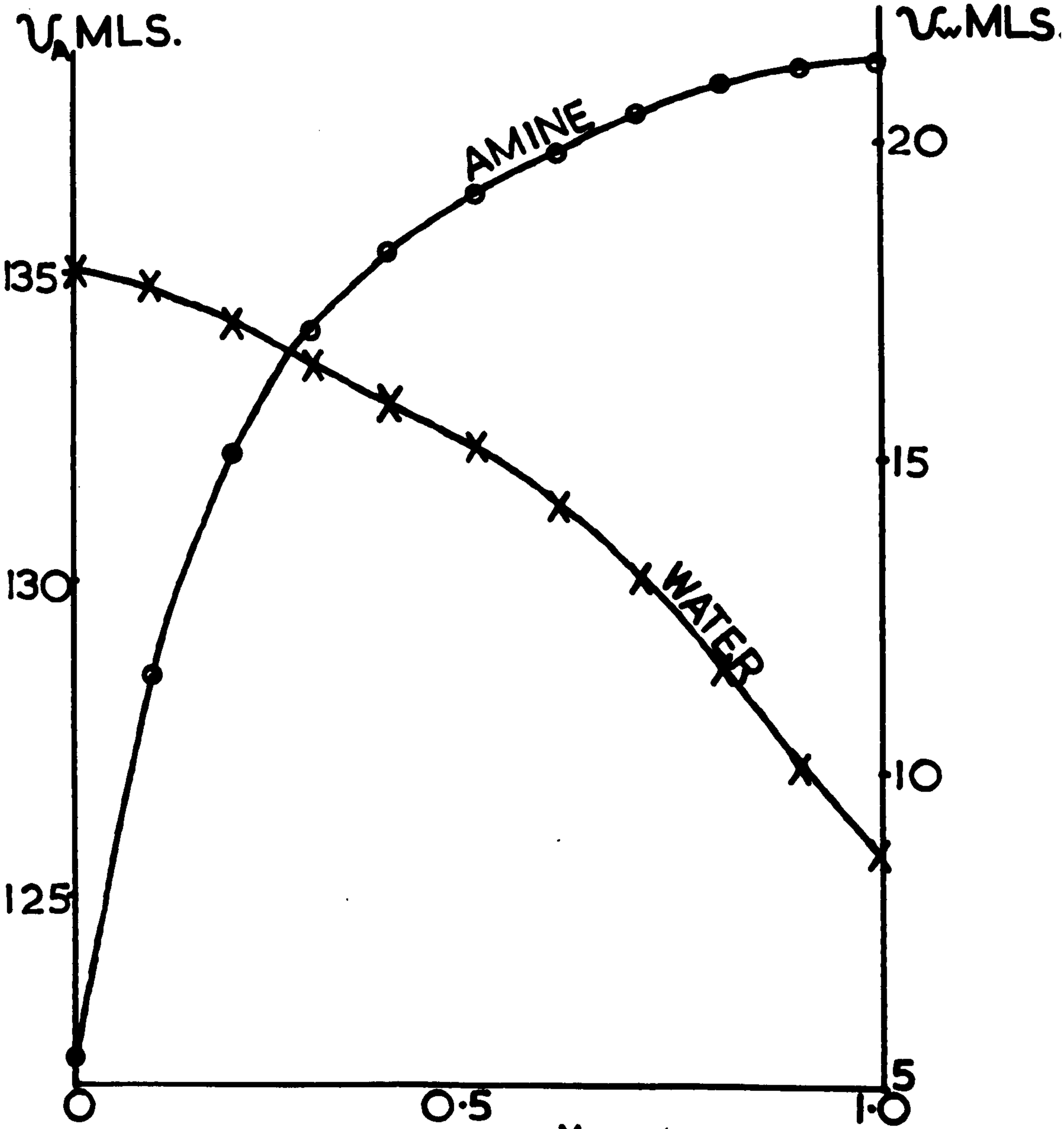

FIGURE 7·7 THE PARTIAL MOLAR VOLUMES OF TRIETHYLAMINE(V_A) AND WATER(V_w) AT 16·50°C

REFERENCES FOR CHAPTER SEVEN

1. D.E. Tsakolotos, Z.Phys.Chem., 68, 36, (1909)

2. F. Kohler, Monat.für Chemie, 82, 913, (1951)

3. B.B. Owen, J.R. White and J.S. Smith, J.Am.Chem.Soc., 78, 3561, (1956)

4. Handbook of Chemistry and Physics, 30, 1696, (1947)

5. L.W. Tilton and J.K. Taylor, J.Res.Nat.Bur.Standards, 18, 205, (1937)

CHAPTER EIGHT

FREE ENERGY OF MIXING OF THE SYSTEM TRIETHYLAMINE + WATER

8.1 Introduction

As the experimental programme described in the preceding chapters developed, it became apparent that any serious attempt at an interpretation of the behaviour of the properties discussed would require more information about the nature of the amine : water interaction. Consequently we decided to conclude this series of experiments by determining the free energy of mixing as a function of composition at three different temperatures below the critical temperature.

We had initially intended to measure the composition and virial coefficients of the vapour in equilibrium with liquid of known composition by means of a Rayleigh Interference Refractometer. These measurements, when combined with the manometrically determined vapour pressure, would enable us to calculate the free energy of mixing. The consistency of the free energy may be checked by calculating the partial pressures from the total pressure, and comparing these values with the values obtained from the vapour composition and virial coefficients.

The thermodynamic formulations, upon which this work is

based, are presented in the next section.

8.2 Theoretical

In order to measure the free energy of mixing in a binary solution it is usual to obtain information about the vapour with which the solution is in equilibrium. The required information comprises the partial pressures of the two components and the virial coefficients of the mixed vapour. It is often sufficient to obtain only the second virial coefficients, as the deviations from ideality of the vapour are usually small since the components are at relatively low concentrations. If the vapour of a binary liquid mixture is only slightly non-ideal, then its pressure is given by

$$p = \frac{n_1 + n_2}{V} RT + \frac{RT}{V^2} (B_{11} n_1^2 + 2B_{12} n_1 n_2 + B_{22} n_2^2) \quad (1)$$

where we consider n_1 moles of component 1 and n_2 moles of component 2 in a volume V; and B_{11} and B_{22} are the second virial coefficients of the pure components and B_{12} is the so-called mixed virial coefficient. The chemical potentials of the two components are then given by

$$\mu_1 = \mu_1^+ (T) + RT \ln \frac{n_1 RT}{V} + 2RT \frac{(B_{11} n_1 + B_{12} n_2)}{V} \quad (2)$$

$$\mu_2 = \mu_2^+ (T) + RT \ln \frac{n_2 RT}{V} + 2RT \frac{(B_{12}n_1 + B_{22}n_2)}{V} \qquad (3)$$

The refractive index (q) of a pure gas is given by,(1)

$$\frac{q^2-1}{q^2+2} \frac{V}{n} = P^o \left(1 + \frac{\beta n}{V} + \frac{\gamma n^2}{V^2} + ..\right) \qquad (4)$$

where P^o is the molar refractivity and is independent of temperature, while β and γ are temperature dependent coefficients. If we make the assumption that β, γ etc. can be neglected then we arrive at the Lorenz-Lorentz equation,

$$\frac{q^2-1}{q^2+2} \cdot \frac{V}{n} = P^o \qquad (5)$$

For a mixture of gases equation (5) becomes,

$$\frac{q^2-1}{q^2+2} \frac{V}{n_1+n_2} = P^o \qquad (6)$$

(Where P^o now depends upon the relative values of n_1 and n_2); and the pressure of such a mixed gas can be written,

$$pV = (n_1+n_2)RT (1 + B^1 p) \qquad (7),$$

where

$$B^1 = \frac{1}{(n_1+n_2)^2 RT} \left\{B_{11}n_1^2 + 2B_{12}n_1n_2 + B_{22}n_2^2\right\}$$

Therefore dividing (7) by (6),

$$\frac{pP^o(q^2+2)}{(q-1)(q+1)} = RT(1+B^1 p) \qquad (8).$$

For a gas at low pressure this equation now becomes

$$\frac{3pP^{o}}{2(q-1)} = RT(1+B^{1}p) \qquad (9)$$

and (9) may be written in the form

$$\frac{p}{q-1} = K(1+B^{1}p) \qquad (10)$$

A graph of $\frac{p}{q-1}$ vs. p gives a slope of KB^{1} and an intercept with the $p = 0$ axis of K. The ratio of the slope to the intercept thus gives B^{1}.

The composition of a binary vapour (of vapour pressure p and refractive index q) could then be calculated by finding the values of $(\frac{p}{q-1})_{p=0}$ for the vapour mixture $\left\{(\frac{p}{q-1})^{1,2}_{p=0}\right\}$ and for the pure components $\left\{(\frac{p}{q-1})^{1}_{p=0}, (\frac{p}{q-1})^{2}_{p=0}\right\}$. This leads to two simple equations for the partial pressures of the two components (p_1 and p_2),

$$p_1 \Big/ (\frac{p}{q-1})^{1}_{p=0} + p_2 \Big/ (\frac{p}{q-1})^{2}_{p=0} = p \Big/ (\frac{p}{q-1})^{1,2}_{p=0} \qquad (11)$$

$$p_1 + p_2 = p \qquad (12)$$

The refractive index of the vapour is related to the drum reading of the refractometer (r) by an equation of the form

$$q-1 = k(r-ar^{2}) \qquad (13)$$

where k and a are constants depending upon the instrument. We need not obtain k as it cancels out in all subsequent

calculations. a can be found if p vs. r readings are taken for a gas whose second virial coefficient is known. From equations (10) and (13) we obtain,

$$\frac{p}{r-ar^2} = K^1(1+B^1p) \qquad (14),$$

and a can be found by plotting $\frac{p}{(1+B^1p)r}$ against r.

The slope is $-K^1a$ and the intercept on the $r=0$ axis is K^1.

Another method of obtaining the refractive index of the vapour is to fill the compensating refractometer tube with nitrogen to such a pressure that the refractometer reading is zero. The pressure of nitrogen is measured and this can be related to the refractive index by the equation,

$$q-1 = k^1pN_2 \qquad (15),$$

where the β and B values of nitrogen are neglected. k^1 is a constant depending only upon the instrument and the compensating gas used, and need not be obtained as it cancels out in all calculations.

8.3 The Apparatus

I shall briefly describe the general scheme of the apparatus (figure 8.1), and then consider individually each section and explain how the final design evolved. The apparatus is capable of being reduced to low pressures

in order to carry out the measurements in the absence of atmospheric gases. Purified, gas free liquids are distilled into a cell which can be immersed in a water thermostat. The vapour from the liquid mixture is circulated through the refractometer tube and its pressure is recorded on a mercury manometer. Nitrogen gas can be placed in the compensating refractometer tube to balance the refractive index of the vapour; the pressure of this gas is recorded on a manometer. The part of the apparatus containing vapour is placed in an air thermostat.

1. The Vacuum Line

The oil pump used was an Edwards 'Speedivac' 2 S C 2 0 rotary vacuum pump. This was capable of producing a pressure lower than 10^{-3} mm. of mercury. The single stage mercury diffusion pump further reduced the pressure to lower than 10^{-5} mm. of mercury. These pressures were recorded on a Mcleod gauge which could measure pressures down to 10^{-5} mm. of mercury and detect 10^{-6} mm. The pumping section was protected from the rest of the system by a trap immersed in liquid air which condensed all vapours.

2. The Liquid Handling System

This consisted of four 250 ml. freezing flasks connected by B14 cones through mercury cut-offs to the vacuum line. The cones were joined into their sockets by means of Edwards W.E. wax, which is resistant to triethylamine. It was thus possible to distil the liquids between any selected pair of flasks and also into the cell. We decided to use mercury cut-offs instead of greased taps as triethylamine vapour attacks tap grease causing the taps to 'streak' and so leak. The disadvantage with mercury cut-offs was that, on cooling a vessel in liquid air, the mercury would distil into that vessel and contaminate the liquid in it.

3. The Cell

The cell consisted of a 250 ml. silica sphere with a flattened bottom. Two tubes led from the top of the cell and were connected to the pyrex apparatus by means of two graded seals. Thus the vapour could be circulated around the apparatus and over the surface of the liquid with which it was in equilibrium. The liquid was stirred by means of a small silica-sheafed steel rod placed in the cell. The rod was rotated by a magnet under the cell, and this magnet

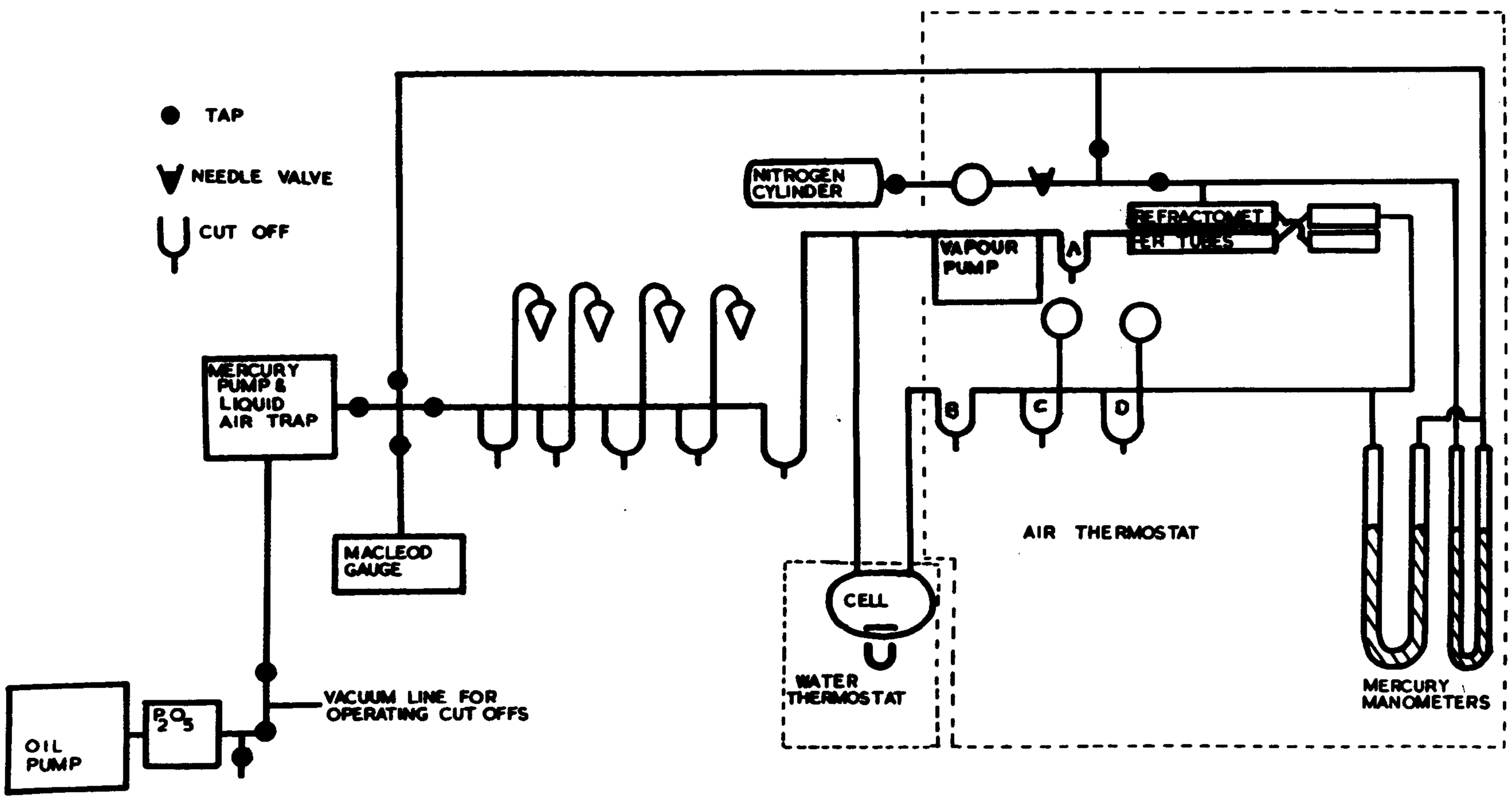

FIGURE 8·1 THE APPARATUS

was driven by means of pulleys from the thermostat stirrer. The magnet made about two revolutions per second, and this ensured adequate stirring of the liquid.

Initially a cell made of pyrex glass was used, but it was found that the vapour pressure of pure triethylamine slowly decreased with time. In a week the vapour pressure at 10°C fell from 3.149 cms. to 3.099 cms; consequently a silica cell was tried and the vapour pressure was found to be independent of time. Before the cell was attached to the apparatus it was well washed with chromic acid, then with nitric acid, and finally many times with conductivity water.

4. The Water Thermostat

The water thermostat enabled the temperature of the cell to be controlled to ± 0.01°C in the temperature range 4 - 18°C. It was necessary to provide some means of cooling, and this was carried out by passing coolant from a refrigerator through copper tubes placed in the water. The amount of coolant circulated could be regulated by means of a valve. The rate of cooling was greater than the amount actually required to maintain the thermostat at a given temperature. The small amount of heat required was supplied by electric light bulbs placed outside the glass thermostat tank. These bulbs

were controlled by a mercury-toluene regulator acting through a relay mechanism. The temperature of the thermostat could thus be controlled with an accuracy of better than 0.01°C, and was measured by means of a calibrated thermometer capable of being read to 0.005°C. The thermometer was protected from direct radiation from the bulbs by means of a small metal shield.

The thermostat was stirred by means of a small electric motor, which also rotated the magnet underneath the cell. The thermostat could be raised and lowered, so that the cell could be cooled in liquid air to enable the liquids to be distilled in and then thermostatted to measure the vapour pressure.

5. The Air Thermostat

This was a large box-like structure maintained at 30.0°C, which contained the manometers, circulating pump, and refractometer tubes. The temperature was controlled by a large mercury-toluene regulator connected through a relay to a 50 watt heating bulb. A basic quantity of heat of about 200 watts was also used, and this could be varied to allow for slight fluctuations in room temperature, by means of a series resistance. Air was circulated around

the thermostat by a fan placed behind the 200 watt heating mat and light bulb. The temperature variation at any one particular point in the thermostat was ± 0.1°C, and the variation from 30.0°C of the various regions containing the apparatus was less than ± 0.2°C.

The glass tubes, which connected the cell to the apparatus inside the air thermostat, were maintained at 30.0 (± 0.5)°C by means of heating wires wound around them. The temperature of the vapour in these tubes was measured by means of two thermistors, and the amount of heating could be adjusted by means of a variac.

6. The Circulating Pump

The pump is essentially a modification of that designed by Funnell and Hoover [2], and can be used to obtain efficient circulation of gases and vapours at low pressures. It consists of an electromagnetically operated glass piston with a soft iron core which slides to and fro, actuating valves, and causing a continuous flow of vapour. In order to achieve low pressure circulation two modifications were made to the design cited [2]. It was essential that the piston should be a tight sliding fit in the surrounding tube, and it was found possible to achieve this by fluon

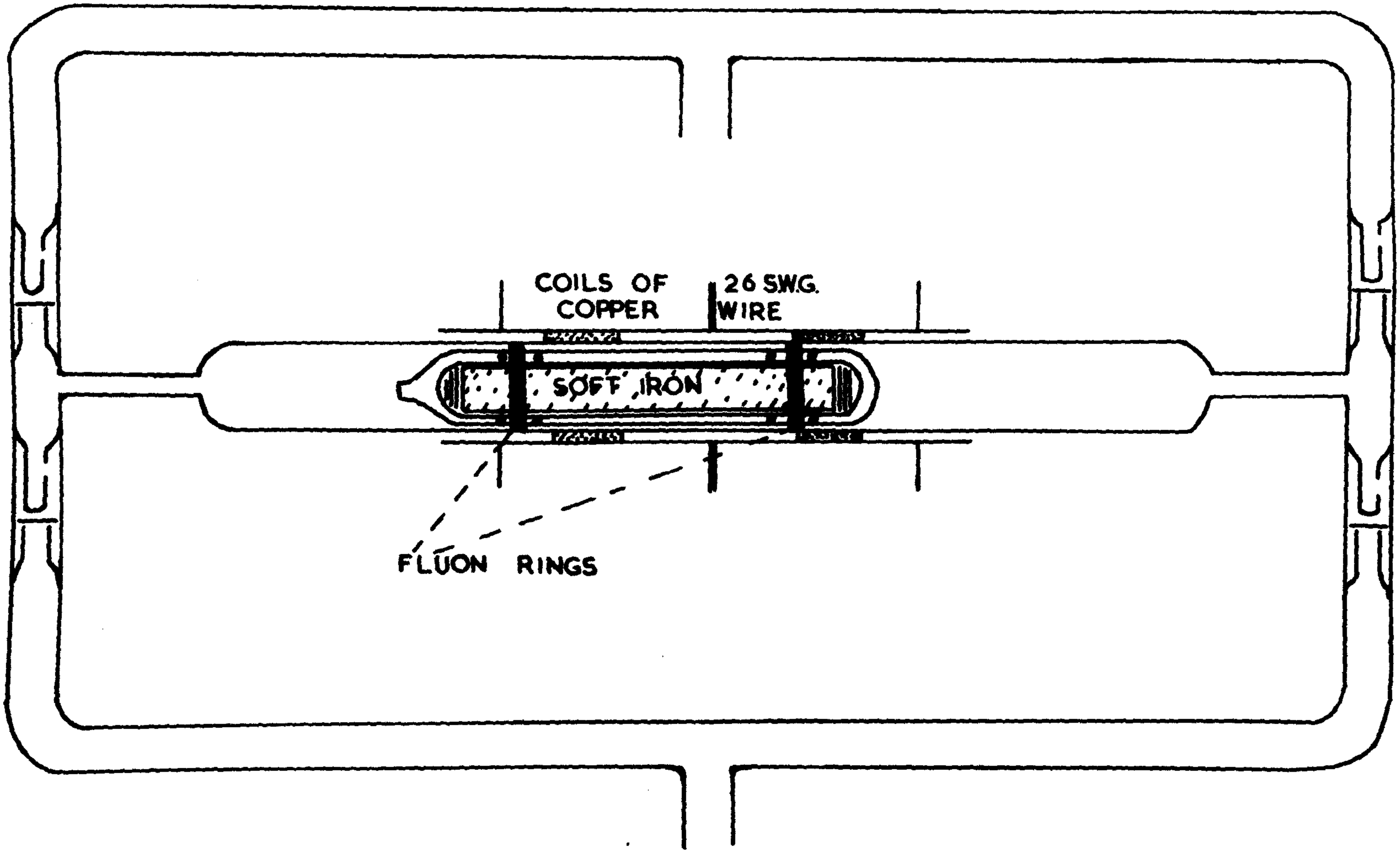

FIGURE 82 THE VAPOUR CIRCULATING PUMP

washers held on to the piston by blobs of glass. The second modification (cf. figure 8.2) consists in replacing the valve floats by microscope cover slides which seat onto the flat ground ends of tubes projecting into the valve chambers. The slides weighed about 0.05 g cm^{-2}, and altering the weight of these alters the range of pressures over which the pump is effective. Using this pump both air and water vapour could be circulated at pressures down to 1 mm. of mercury.

Figure 8.3 shows the changeover circuit for the coils which operate the pump. A voltage of from 12 - 24 v. D.C. was used to magnetise the coils, each of which consisted of approximately 300 metres of 26 s.w.g. shellaced copper wire.

7. The Manometers and Cathetometer

Originally it was hoped to obtain an accuracy of 10^{-3} cm. of Hg in the vapour pressure measurements. The proposed arrangement used an oil manometer and a spiral gauge[3,4]; the spiral gauge being used as a null reading device. It was found impossible to obtain a spiral gauge which was sufficiently sensitive and reproducible; several spirals capable of rotating more than 180°/atmosphere were tested, but they were all found to be mechanically weak and

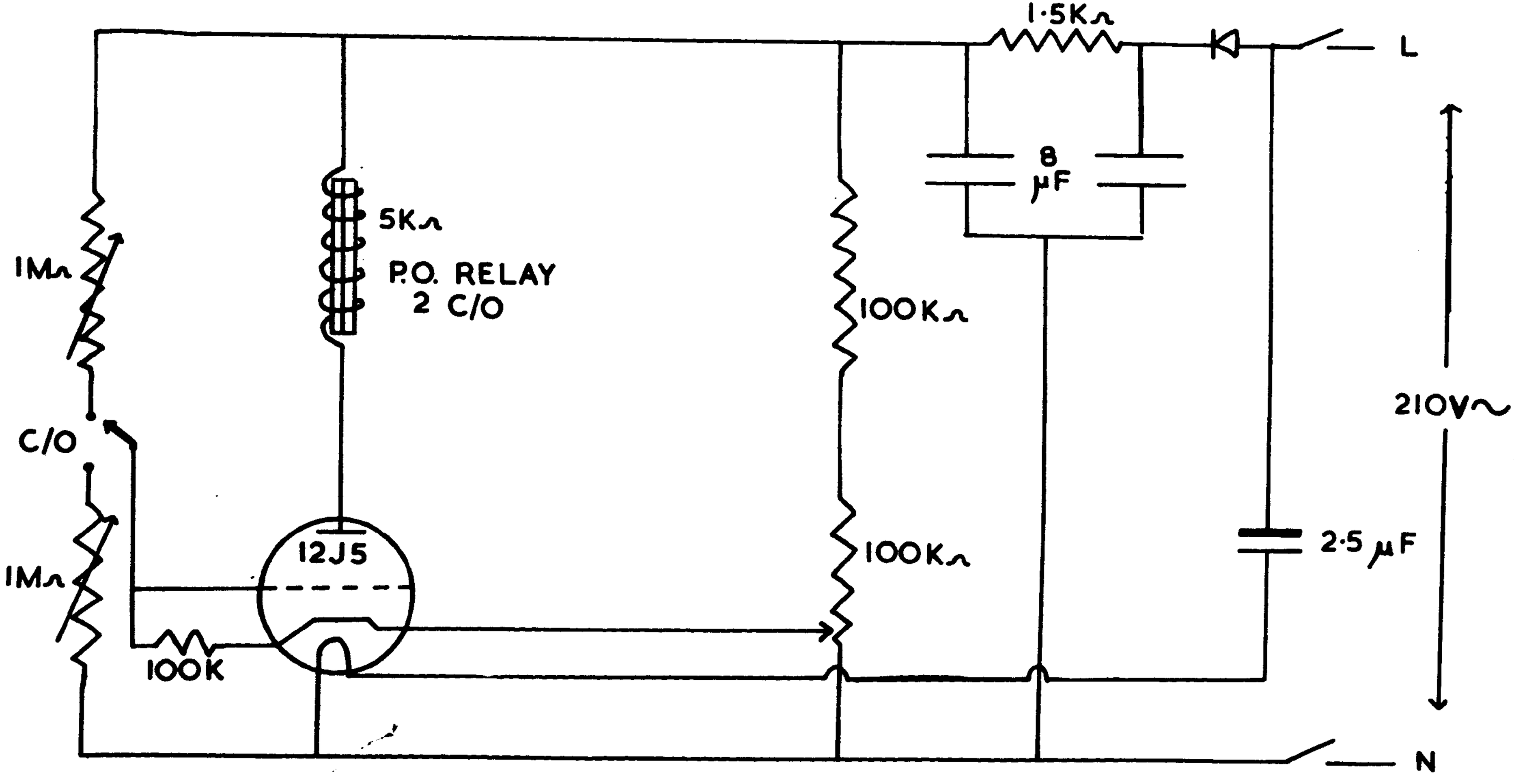

FIGURE 8·3 THE CHANGEOVER CIRCUIT

would collapse after a little use. A spiral which rotated 140°/atmosphere was tested and found to be sufficiently robust. Using a 1 metre optical path enclosed inside the air thermostat, the movement of the reflected beam corresponding to a pressure change of 10^{-3} cm. of mercury was found to be 6×10^{-3} cm. In order to measure a displacement of this order the image of a cross-wire was projected onto the mirror of the spiral gauge and viewed through a telescope. The telescope hair line could be moved by a vernier screw, and when a small pressure was applied to one side of the spiral gauge, the movement of the cross-wire image was such that one vernier division corresponded to about 1.5×10^{-3} cm. Hg pressure; this value represented the sensitivity of the method.

The reproducibility of the gauge was then tested by applying the same pressure to both sides and measuring the deflection. Figure 8.4 contains two calibration curves showing the dependence of the zero point of the spiral gauge upon pressure: at zero pressure the vernier readings show a difference of three divisions between the two curves, while at higher pressures the difference is approximately two divisions. These results, combined with the difficulty

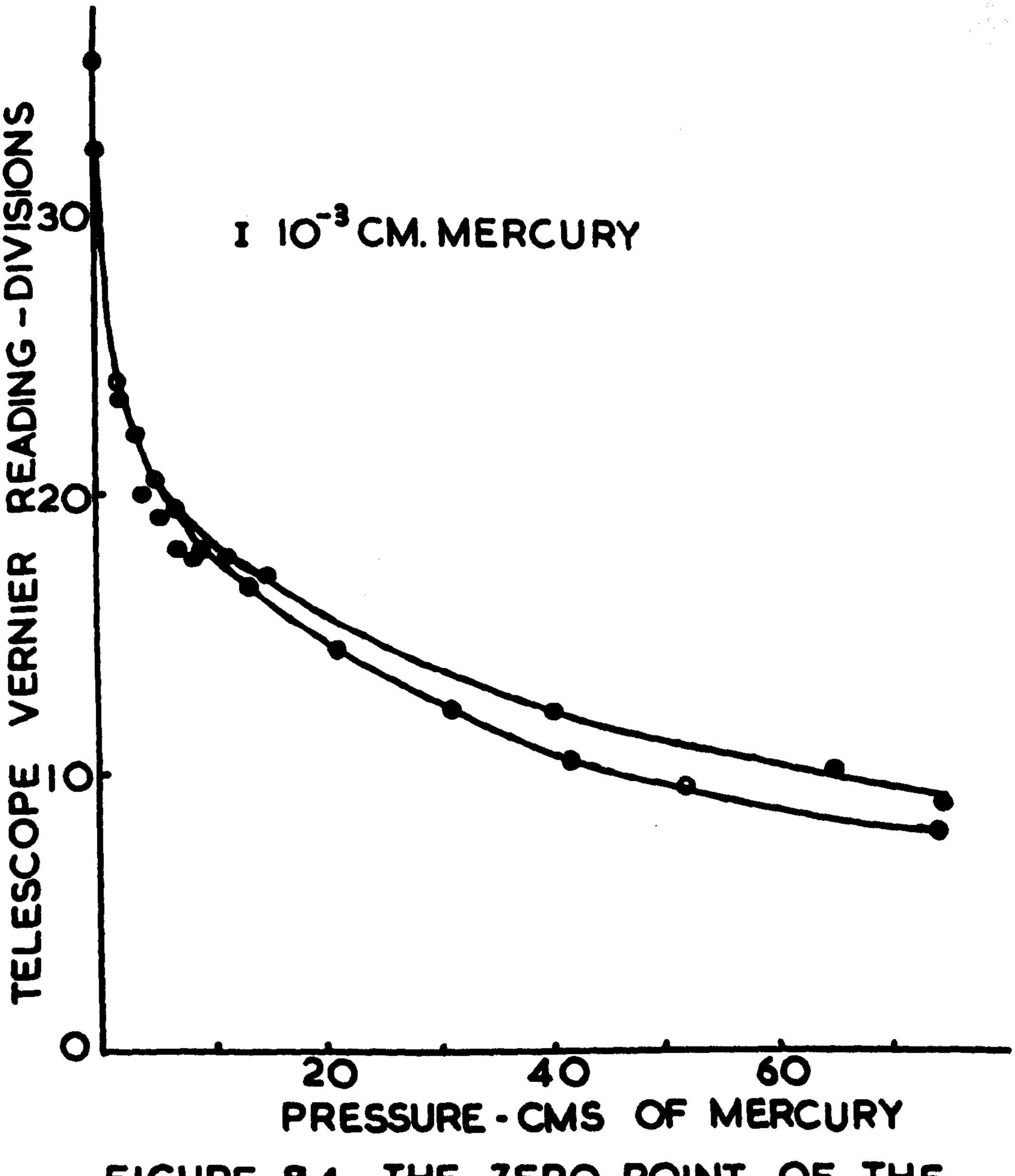

FIGURE 8·4 THE ZERO POINT OF THE SPIRAL GAUGE AS A FUNCTION OF PRESSURE

of degassing the oil in the manometer, led to the installation of a mercury manometer.

The mercury manometer was a U-tube of uniform bore (2.32 cm.) mounted behind a sheet of good quality plate glass inside the air thermostat. The manometer used for measuring the pressure of nitrogen in the refractometer tube was mounted beside the vapour pressure manometer and both were illuminated by the same moveable horizontal strip of light.

The cathetometer used to measure the manometer heights had a 100 cm. scale and could be read to 0.001 cm. It was mounted on a metal plate which was bolted to the top of a brick pillar. In order to set the scale of the cathetometer exactly vertical it was necessary to carry out a careful levelling procedure, which is given in the instruction booklet accompanying the instrument (5).

8. The Refractometer and Gas Tubes

The refractometer was a Hilger Rayleigh Interference Refractometer. It was designed to work on the refractometry of gases, of which the refractive indeces differ very little from unity. The makers suggest that it is possible to detect 0.01% of hydrogen in air at atmospheric pressure, a quantity which causes a change of refractive index of

only 0.000,000,015.

In this instrument adjacent slits are illuminated by collimated light and interference bands are formed by bringing the two beams to a focus. A movement of the interference bands will occur if the path length of one of the interfering beams is changed, and this property can be used to obtain the refractive index of a given gas. A diagram representing the working of the instrument is shown in figure 8.5. For convenience we shall suppose that the whole optical system is divided into an upper and a lower half. 8.5A is a view from above and 8.5B is a view from the side. We shall first consider the upper half of the apparatus which contains the refractometer tubes.

Light from a pointolite lamp is focussed on the narrow vertical slit A and is collimated by an achromatic object glass B, in front of which are two vertical apertures C, 4 mm. wide, 27 mm. long and 12 mm. apart. The two resulting parallel beams of light pass through the twin tubes D and E, and each fall upon a thin glass plate inclined at about 45° to the optic axis. One of these glass plates (K) is fixed, while the other (L) can be rotated about a horizontal axis perpendicular to the incident light, thus varying the

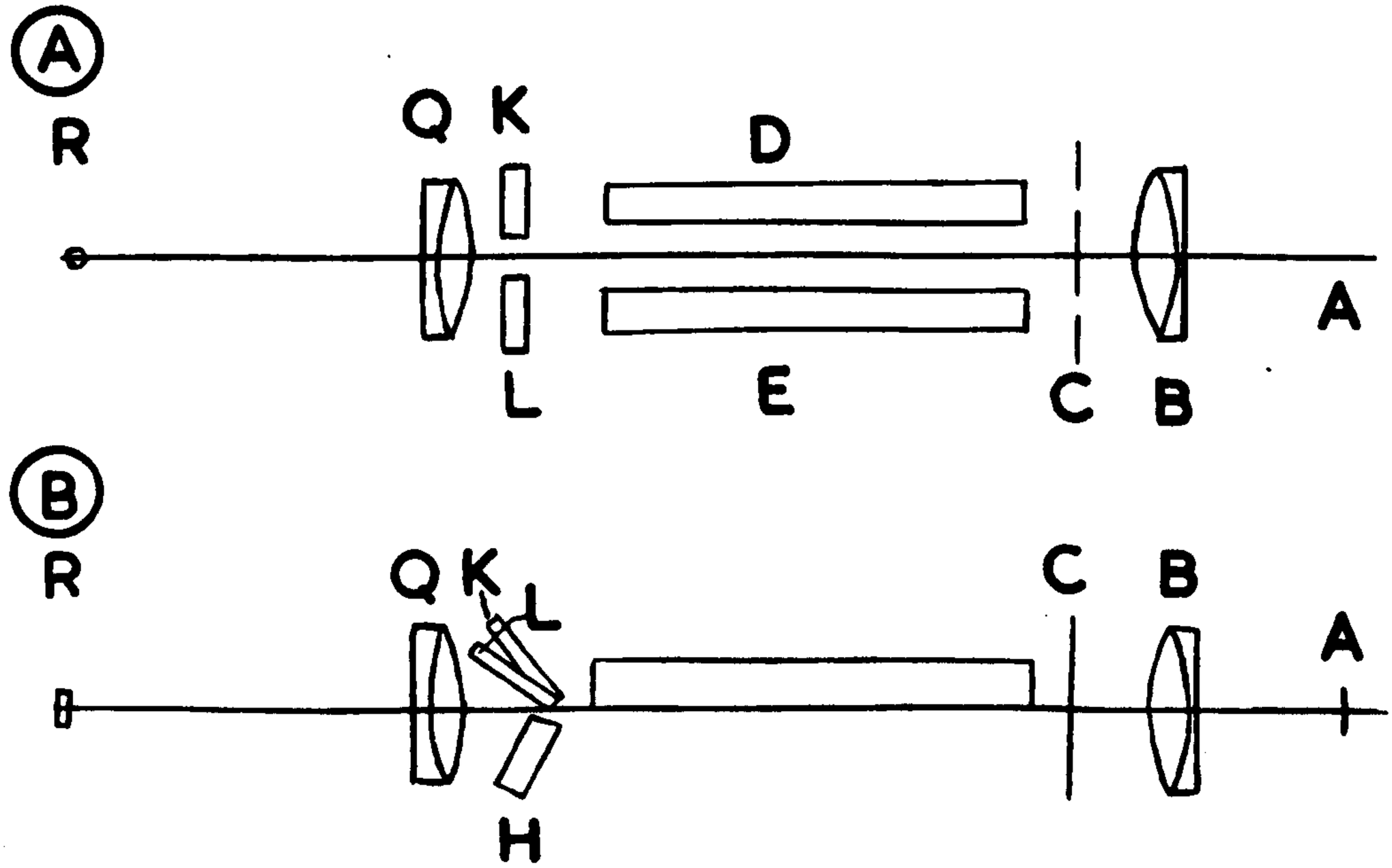

FIGURE 8·5 THE WORKING OF THE REFRACTOMETER

thickness of glass through which the light must pass. The two beams are brought to a focus by means of the achromatic telescope object glass Q, and the image is observed with a small cylindrical lens R. This lens gives a very high magnification in a horizontal direction without the loss of light which would accompany the use of a spherical lens.

The lower halves of the two beams, after leaving the two slits, travel uninteruptedly until they reach the prism H (figure 8.5C), which is simply a thick glass plate, with a bevelled edge, inclined to the axis. The object of this prism is to bring the lower beams adjacent to the upper beams with a sharp dividing line, thus cutting out obstructions which would otherwise form a gap between the band systems. The interference bands formed by the lower beams are thus observed directly below those formed by the upper beams by means of the eyepiece (R).

The eyepiece is a cylinder of glass of very small diameter with its own axis vertical. Its function is to provide a very high horizontal magnification (about 50 diameters) of the vertical band system formed by the object glass. As the lens has no magnification in the vertical

plane, horizontal lines will appear sharp at the normal distance of vision, consequently the edge of the prism H is seen clearly as the dividing line between the band systems.

The setting-up of the refractometer was commenced by placing the source of light about 6 cm. from the condenser of the collimator, and the position was adjusted so that the image of the light source fell upon the slit. The slit was opened by turning its micrometer screw through about twenty divisions. The eyepiece was now removed from the telescope, and the position of the telescope adjusted so that the image of two vertical apertures was seen, each bisected by a horizontal dividing line. The eyepiece was replaced and then rotated until two horizontal strips of light were observed, when correctly focussed by the focussing screw. The slit was then closed to about half a division and two sets of interference bands were seen divided by a fine horizontal line. If the bands were not centrally placed in the field of view, this could be adjusted by means of a small screw at the side of the eyepiece.

Initially the refractometer tubes were made of two equal length ($\sim$ 95 cm.) pieces of square glass tube with a common window at both ends. It was found impossible

to stick a common window on to two separate tubes and make a gas tight seal, so the windows were cut into two pieces and each piece stuck on separately. The adhesive used was Araldite cement, and if this was applied correctly the joint was found to be leak free. It was necessary to use only a small amount of adhesive and to have little overlap of the windows over the edge of the tube, as there was a distance of only 12 mm. between the two beams of light. These two gas tubes were placed in the paths of the beams; the righthand one (looking at the instrument from the telescope end) had an inlet and an outlet tube so that the vapour could be circulated, the lefthand one could be evacuated through a side tube.

This arrangement was found to be unsatisfactory for the measurement of the refractive indeces of vapour mixtures. On circulating the vapour from a given solution a steady refractometer reading and vapour pressure were obtained ($9.00^{o}C$, $x_A = 0.1660$, p = 3.144 cm., r = 1414 divs.). The cell was then cooled in liquid air and replaced in the thermostat, and the vapour was circulated again. The refractometer then gave a steady reading of 1296 divs. and the vapour pressure was 3.146 cms. The measurements were

again repeated, and while the pressure remained constant the refractometer gave a reading of 1324 divs.. The adsorption of the vapour onto the windows of the gas tubes probably caused these varying values; the amount and composition of the vapour adsorbed depended primarily upon the nature of the vapour which was initially circulated in the gas tubes, and not upon the nature of the final equilibrium vapour. This premise was checked by allowing equilibrium to be attained, and then blowing hot air onto one of the windows so as to desorb some of the vapour. When the tube cooled to 30°C changes in the refractometer reading of up to 20 divisions were noted.

This difficulty was overcome as shown in figure 8.1. Two tubes were inserted in the path of each beam, one being much longer than the other. In the righthand beam the long tube contained vapour and the short tube was evacuated; in the lefthand beam the short tube contained vapour and the long tube was evacuated. The adsorption effect could thus be compensated and it was hoped that the variation in r would be minimised. For a solution of amine mole fraction $x_A \simeq 0.0400$ at 10.00°C a vapour pressure of 3.187 cms. and a steady refractometer reading of 1180-1183 divisions were

obtained.

Ashton and Halberstadt [6] published a paper which suggested that, as the pressure in the gas tube was increased and the drum reading was advanced, a stage was reached where the zero order fringe was no longer achromatic, and that the achromatic fringe was next to it. This was checked by allowing gas to diffuse slowly into the righthand tube and maintaining coincidence of the upper and lower pairs of dark lines by rotating the drum. Between 200 - 300 divisions on the drum the lefthand line of the centre dark pair started to lighten, while the line to the right of the centre pair darkened. This process continued until the line to the right of the centre pair would have been taken as one of the centre pair of dark lines.

In order to overcome this difficulty we decided to use the refractometer purely as a null instrument, and to balance the refractive index of the vapour by inserting a measureable pressure of nitrogen in the other gas tube. In order to test if the zero order fringes were still the dark ones under these conditions, both tubes were filled with nitrogen at the same pressure and the dark lines did not move. The method finally used to determine the refractive

index of the vapour was to fill the compensating tube with nitrogen to a pressure which was slightly less than that needed to balance the refractive index of the vapour, and to obtain the final adjustment by means of the refractometer. The factor needed to convert a small drum reading to its equivalent nitrogen pressure (0.0164 cms. N_2/division), was obtained by finding the drum reading for small nitrogen pressures (1-2 cm.).

8.4 The Experimental Technique

1. Determination of the volume of the Apparatus

It was necessary to determine the volume of the apparatus in order to calculate the quantity of the two components in the vapour phase. All parts of the apparatus, except the cell, which contain the vapour are at 30.0°C, and the cell is at the temperature of the water thermostat (4.00, 10.00 or 18.00°C). The volume of the cell was determined before it was attached to the apparatus and was found to be 249 ml. The temperature of the water thermostat was raised to 30.0°C and the cell immersed in it: a tapped flask, whose volume (638.6 ml.) had been previously determined, was attached to the apparatus. The flask was filled with nitrogen at a given pressure and then connected with the rest of the

apparatus and the final pressure measured. The average of four determinations gave the volume of the apparatus as 2526 ml., when the height of the manometer was 18.0 cm. 2277 ml. of the apparatus are thus maintained at 30.0°C while 249 ml. are at the temperature of the water thermostat (10.00°C say). Assuming that the vapour obeys the laws for perfect gases this is equivalent to 2376 ml. at 10.0°C Thus the volume of the vapour corrected to 10.0°C equals 2376 ml. minus the volume of the liquid in the cell (V ml. say). If the partial pressures of the amine and water are p_A and p_W respectively, then the masses of the two components in the vapour are,

triethylamine, $5.75\ p_A(2376-V) \times 10^{-5}$ gm. ;

water, $1.02\ p_W(2376-V) \times 10^{-5}$ gm.

Similar calculations are performed when the temperature of the thermostat is 4.00°C or 18.00°C.

2. Preparation of Components

Both water and triethylamine were prepared as described in chapter 4. A sample of one of these liquids was placed in a 250 ml. freezing bulb and attached to the vacuum line by means of a B14 cone and socket. The bulb was frozen in liquid air and the liquid allowed to melt: this process

released dissolved gases and was repeated many times. In order to remove final traces of gaseous impurity the liquid was distilled from one flask to another, intermittingly pumping away any gas evolved. This process was repeated four times until the liquid was completely degassed.

3. Filling the Cell

In order to prepare a solution of known composition it was necessary to distil measured quantities of both the components into the cell. A quantity of water was distilled from a tapped flask, the flask being weighed before and after the distillation. As triethylamine rapidly attacks tap grease a different method had to be used in this case. A small flask was attached to one end of a 1 mm. capillary, at the other end of which was a B14 cone. The volume of the flask up to a mark on the capillary was determined at 15.00°C and was found to be 8.7177 ml.. The flask was attached to the vacuum line by W.E.wax, and filled at 15.0°C up to the mark by distilling amine into it. This quantity of triethylamine was then distilled into the cell. Making a correction for the amount of amine in the vapour phase between the mark on the cell andthe cut-off, the weight of amine distilled in one operation was 6.400 g.

For each series of experiments, 6.400 g. of amine and about 25 g. of water were initially distilled into the cell. Further quantities (6.400 g.) of amine were added until a mole fraction of about 0.23 was reached. The contents of the cell were then distilled out, and about 8 g. of water and further quantities of amine distilled in. Finally about 1.2 g. of water were used and quantities of amine again distilled in until about 64 g. had been added ($x_A \simeq 0.90$).

4. The Measurements

Calculations had shown that if the pressure could be obtained with an accuracy of 1×10^{-3} cm. of mercury, then it would be possible to calculate approximate ($\pm$ 200 ml.) values of the second virial coefficients, as these were known to be about -2000 ml. for triethylamine and -500 ml. for water at 30°C. We were chiefly interested in obtaining a value for the so-called mixed second virial coefficient as this might be numerically larger than either of those for the pure components. Unfortunately the apparatus had to be modified and it was not able to perform to this desired accuracy. On the other hand we still hoped to obtain the vapour compositions to a reasonable degree of accuracy,

provided that the effect of the adsorption of the vapour on the windows of the gas tubes had been overcome.

The cell was cooled in liquid air and quantities of triethylamine and water distilled into it. The moveable thermostat was then raised so that its water surrounded the cell. The temperature of the thermostat was recorded on an N.P.L. standard thermometer, which was calibrated in fiftieths of a degree and was capable of being read to at least 0.005°C. The thermostat, which was operated at either 4.00, 10.00 or 18.00°C, maintained a constant temperature such that all variations were less than 0.01°C. The solution was stirred and its vapour circulated through the system: after a sufficient interval of time the vapour circulating pump was switched off and the vapour pressure of the solution and the pressure of nitrogen, having an equivalent refractive index to the vapour, were measured.

In order to obtain the second virial coefficients of the vapour, a sample of the vapour was trapped by closing cut-offs A and B. Cut-off C was opened and, when equilibrium had been attained, the pressure of the vapour and of the nitrogen were recorded. Similar measurements were taken after cut-off D had been opened.

5. Calculations

The attempt to obtain the vapour virial coefficients described in the previous section led to results which appear to have no practical significance. To amplify this remark the results obtained for one particular solution ($x_A = 0.0399$, $10.00^{\circ}C$) are given. The pressure of the vapour (p) and the pressure of nitrogen (p_{N_2}), which had the same refractive index, were found to be

p cm.	3.185	1.896	1.342
p_{N_2} cm	19.00	10.96	7.59
P/p_{N_2}	0.1676	0.1730	0.1768

From equations (10) and (15) one can obtain

$$P/p_{N_2} = K^1(1 + B^1 p) \qquad (16)$$

A graph of P/p_{N_2} vs. p had a slope of $-0.0046\ (cm.Hg)^{-1}$, and the intercept with the $p = 0$ axis was 0.1822. B^1 was therefore $-0.025\ (cm.Hg)^{-1}$, and B_{12} was found to be -110,000 ml. This value is much too large for a true virial coefficient and must be caused by an error in the experiment. This error was probably due to the preferential adsorption of one of the components of the vapour onto the glass walls of the apparatus, so altering the vapour composition.

It was therefore impossible to apply equation (11) in

order to obtain the partial pressures of the components, because the $\frac{p}{p_{N_2}}$ values could not be extrapolated to zero pressure due to this preferential adsorption. Instead the $\frac{p}{p_{N_2}}$ values of the pure components, and of the vapour in equilibrium with the liquid, were determined and a modified form of equation (11) applied:

$$\frac{p_W}{\alpha} + \frac{p_A}{\beta} = p_{N_2} \quad , \quad p_W + p_A = p \qquad (16)$$

Where p_W and p_A are the partial pressures of water and triethylamine respectively, p is the vapour pressure of the solution and p_{N_2} is the pressure of nitrogen having the same refractive index as the vapour. α and β are constants which were determined for pure water vapour and pure triethylamine vapour respectively. α represents the pressure of water vapour in cm.Hg which has the same refractive index as 1 cm. of nitrogen, and β similarly represents the pressure of triethylamine vapour in cm.Hg which has the same refractive index as 1 cm. of nitrogen.

8.5 Results

For any solution the vapour pressure and the pressure of nitrogen having the same refractive index were determined. The error in the vapour pressure is solely due to the

cathetometer and is probably less than ± 0.005 cm. The error in the nitrogen pressure is chiefly due to the use of the refractometer as a null instrument. The sensitivity of the refractometer is about $1\frac{1}{2}$ divisions and this is equivalent to an error of ± 0.02 cm. in the pressure of nitrogen. The resulting error in the partial pressure of triethylamine is about ± 0.01 cm.

The values of α and β were found to be,

$$\alpha = 1.14,$$

$$\beta = 0.1256,$$

and each is the average of several values.

The following tables contain the total vapour pressures and partial pressures of triethylamine at various mole fractions, and figure 8.6 shows the vapour pressure as a function of mole fraction. In the region $x_A = 0.1$ the 18.00°C vapour pressure isotherm is very flat, and this region is reproduced on an enlarged scale in figure 8.6.

TABLE I

18.00°C

Mole Fraction of Triethylamine x_A	Vapour Pressure cm.Hg	Partial Pressure of Triethylamine from Refractive Index cm.Hg
0.0000	1.546	0.000
0.0062	3.156	1.628
0.0126	4.557	3.024
0.0428	5.538	4.027
0.0619	5.542	4.030
0.0777	5.544	4.027
0.1137	5.549	4;030
0.1470	5.553	4.035
0.1778	5.559	4.041
0.2065	5.567	4.048
0.2333	5.573	4.061
0.2768	5.589	4.073
0.3395	5.611	4.100
0.3923	5.630	4.121
0.4372	5.648	4.141
0.4759	5.661	4.155
0.5097	5.668	4.168

0.5393	5.677	4.183
0.5656	5.684	4.199
0.6325	5.697	4.230
0.7237	5.713	4.286
0.7786	5.714	4.327
0.8154	5.701	4.361
0.8415	5.687	4.394
0.8611	5.664	4.420
0.8765	5.647	4.440
0.8986	5.605	4.484
1.0000	4.780	4.780

TABLE II

10.00°C

Mole Fraction of Triethylamine	Vapour Pressure	Partial Pressure of Triethylamine from Refractive Index
x_A	cm.Hg	cm.Hg
0.0000	0.920	0.000
0.0071	1.716	0.800
0.0142	2.428	1.502
0.0399	3.185	2.288
0.0784	3.261	2.363
0.1140	3.303	2.419
0.1617	3.355	2.462
0.2053	3.398	2.507
0.2445	3.434	2.552
0.2786	3.463	2.585
0.3408	3.495	2.628
0.3931	3.525	2.660
0.4380	3.546	2.680
0.4765	3.562	2.700
0.5101	3.581	2.720
0.5397	3.589	2.735
0.5658	3.601	2.760

0.6648	3.614	2.790
0.7501	3.631	2.839
0.8009	3.635	2.866
0.8346	3.633	2.888
0.8583	3.629	2.910
0.8900	3.604	2.944
0.9175	3.570	2.980
1.0000	3.175	3.175

TABLE III

4.00°C

Mole Fraction of Triethylamine	Vapour Pressure	Partial Pressure of Triethylamine from Refractive Index
x_A	cm.Hg	cm.Hg
0.0000	0.609	0.000
0.0075	1.021	0.430
0.0149	1.429	0.834
0.0432	2.041	1.441
0.0838	2.126	1.541
0.1212	2.180	1.604
0.1557	2.232	1.658
0.1875	2.264	1.693
0.2170	2.293	1.729
0.2240	2.325	1.760
0.2797	2.361	1.794
0.3417	2.398	1.838
0.3939	2.427	1.871
0.4385	2.447	1.895
0.4770	2.464	1.915
0.5105	2.477	1.931
0.5400	2.490	1.946

0.5660	2.493	1.953
0.5840	2.496	1.960
0.6794	2.517	1.991
0.7405	2.523	2.013
0.7814	2.526	2.033
0.8112	2.528	2.047
0.8329	2.530	2.061
0.8659	2.530	2.080
0.8876	2.526	2.096
0.9032	2.519	2.108
1.0000	2.255	2.255

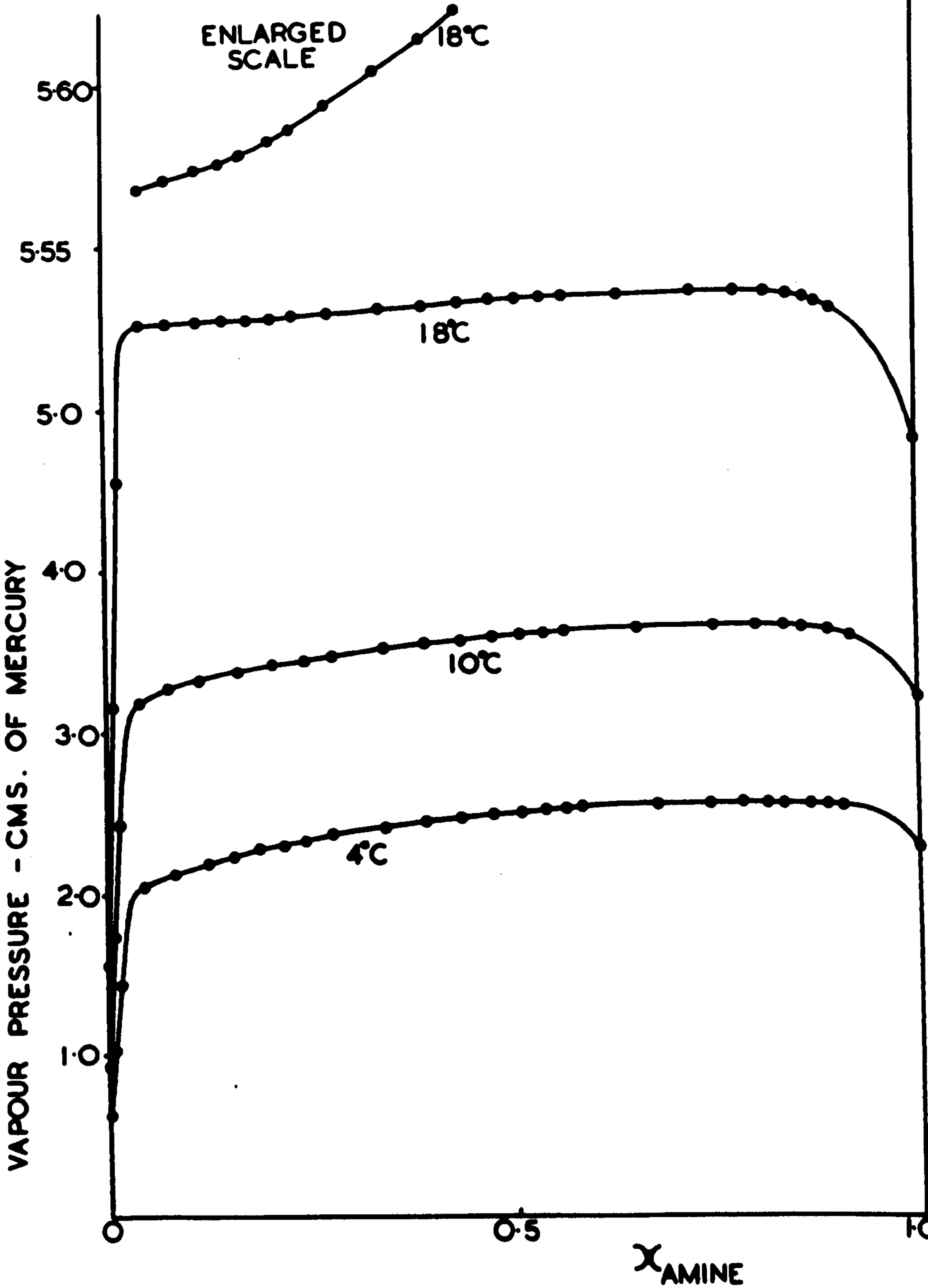

FIGURE 86 VAPOUR PRESSURE ISOTHERMS FOR THE TRIETHYLAMINE + WATER SYSTEM

8.6 Discussion

The method used to obtain the partial pressures from the total pressure was that followed by Kohler [7]. One starts with the Duhem-Margules differential equation and, assuming that the vapour behaves as a perfect gas, obtains,

$$dy = \frac{y(1-y)}{(y-x)p}\, dp \qquad (17),$$

where y is the mole fraction of one of the components in the vapour phase, x is the mole fraction of the same component in the liquid phase, and p is the total vapour pressure. p was determined as a function of x, so equation (17) can be written,

$$dy = f(y,p)\, dp \qquad (18)$$

By the method of numerical integration one can start at a point (p_o, y_o) and obtain the values of p and y at an adjacent point. One can relate the change (k) in y to the change (h) in p by means of Taylor's series,

$$k = \frac{dy}{dp} \cdot h + \frac{d^2y}{dp^2} \cdot \frac{h^2}{2!} + \frac{d^3y}{dp^3} \cdot \frac{h^3}{3!} + \cdots + \frac{d^ny}{dp^n} \cdot \frac{h^n}{n!} + R_n$$

R_n can be neglected if sufficient terms are considered in the series. Runge and Kutta [8] ignored all terms of an order higher than four and obtained k from the following scheme;

$$l_1 = f(y_o, p_o)\ dp$$

$$l_2 = f(y_o + l_{1/2}, p_o + dp/2)\ dp$$

$$l_3 = f(y_o + l_{2/2}, p_o + dp/2)\ dp$$

$$l_4 = f(y_o + l_3, p_o + dp)\ dp$$

$$k = 1/3\ (l_{1/2} + l_2 + l_3 + l_{4/2})$$

With an integration of this type it is always necessary to find an origin at which the values of y, p, and x are known. At a sufficiently small mole fraction of amine the water obeys Raoult's law and the triethylamine obeys Henry's law. In each of the three isotherms there are two points which fulfil this condition, and these two are used as starting points for the integration. At $x_A =$ 0.0071 on the 10.00°C isotherm the partial pressure of water is given by 0.9929 x 0.920 = 0.913 cm., and consequently the partial pressure of triethylamine is 0.803 cm. At $x_A = 0.0142$ the application of Raoult's law and the numerical integration give the same value of the partial pressure of triethylamine.

This integration cannot be taken past the azeotrope point ($y = x$), so it is impossible to calculate partial pressures above an amine mole fraction of 0.75. We cannot start an integration from the amine rich end of the

composition range, as solutions above a mole fraction $x_A = 0.95$ (1 g. water : 110 g. amine) cannot be made with sufficient accuracy. Consequently it is necessary to rely upon the experimentally determined partial pressures in the region $x_A = 0.75 - 1.0$.

Tables IV, V and VI contain the calculated triethylamine partial pressures, the activity coefficients of both the components, and the excess free energy of mixing. The activity coefficients and the excess free energy of mixing were calculated from the numerically integrated partial pressures up to $x_A = 0.75$, and above $x_A = 0.75$ from the experimentally determined partial pressures. The average difference between the experimental and numerically integrated partial pressures was 0.006 cm.Hg, and the maximum difference was 0.015 cm.Hg. It was not possible to check accurately the thermodynamic consistency of the activity coefficients by finding the area under the log $(\frac{\gamma_A}{\gamma_W})$ vs. mole fraction curve, as no measurements had been taken in the region $x_A = 0.90 - 1.0$.

TABLE IV

18.00°C

x_A	p_A cm.Hg	$\log_{10}\gamma_A$	$\log_{10}\gamma_W$	g^E/RT	g^E cals.
0.0062	1.620	1.732	0.0000	0.0246	14.2
0.0126	3.030	1.703	0.0000	0.0495	28.6
0.0428	4.023	1.292	0.0101	0.1497	86.6
0.0619	4.027	1.134	0.0190	0.2027	117.3
0.0777	4.029	1.036	0.0264	0.2414	139.7
0.1137	4.034	0.8710	0.0436	0.3171	183.5
0.1470	4.038	0.7592	0.0602	0.3754	217.2
0.1778	4.045	0.6775	0.0760	0.4214	243.8
0.2065	4.053	0.6134	0.0913	0.4588	265.5
0.2333	4.060	0.5612	0.1061	0.4887	282.8
0.2768	4.078	0.4884	0.1308	0.5276	305.3
0.3395	4.103	0.4028	0.1694	0.5728	331.4
0.3923	4.128	0.3428	0.2036	0.5946	344.0
0.4372	4.152	0.2982	0.2354	0.6055	350.3
0.4759	4.170	0.2632	0.2650	0.6085	352.1
0.5097	4.181	0.2345	0.2926	0.6057	350.5
0.5393	4.196	0.2117	0.3181	0.6004	347.4
0.5656	4.208	0.1920	0.3417	0.5919	342.5
0.6325	4.236	0.1464	0.4103	0.5606	324.4

0.7237	4.300	0.0931	0.5240	0.4887.	282.8
0.7786		0.0655	0.6081	0.4274	247.3
0.8154		0.0487	0.6721	0.3772	218.3
0.8415		0.0385	0.7228	0.3385	195.9
0.8611		0.0310	0.7624	0.3054	176.7
0.8765		0.0253	0.8006	0.2789	161.4
0.8986		0.0187	0.8537	0.2381	137.8

TABLE V

10.00°C

x_A	p_A cm.Hg	$\log_{10}\gamma_A$	$\log_{10}\gamma_W$	g^E/RT	g^E cals.
0.0071	0.803	1.553	0.0000	0.0253	14.2
0.0142	1.521	1.528	0.0000	0.0500	28.1
0.0399	2.288	1.257	0.0068	0.1306	73.5
0.0784	2.366	0.9778	0.0232	0.2259	127.1
0.1140	2.410	0.8233	0.0398	0.2975	167.4
0.1617	2.462	0.6812	0.0637	0.3765	211.9
0.2053	2.509	0.5852	0.0849	0.4318	243.0
0.2445	2.549	0.5165	0.1048	0.4732	266.3
0.2786	2.582	0.4651	0.1229	0.5027	282.9
0.3408	2.620	0.3840	0.1596	0.5437	306.0
0.3931	2.657	0.3282	0.1920	0.5649	317.9
0.4380	2.684	0.2856	0.2219	0.5753	323.7
0.4765	2.706	0.2524	0.2494	0.5778	325.1
0.5101	2.735	0.2271	0.2742	0.5762	324.2
0.5397	2.746	0.2047	0.2995	0.5721	321.9
0.5658	2.765	0.1875	0.3212	0.5656	318.3
0.6648	2.790	0.1212	0.4273	0.5152	289.9
0.7501	2.849	0.0778	0.5315	0.4401	247.7
0.8009		0.0519	0.6235	0.3814	214.6
0.8346		0.0374	0.6903	0.3349	188.5

0.8583	0.0285	0.7428	0.2989	168.2
0.8900	0.0178	0.8152	0.2430	136.7
0.9175	0.0099	0.8906	0.1902	107.0

TABLE VI

4.00°C

x_A	p_A cm.Hg	$\log_{10}\gamma_A$	$\log_{10}\gamma_W$	g^E/RT	g^E cals.
0.0075	0.417	1.392	0.0000	0.0240	13.2
0.0149	0.829	1.392	0.0000	0.0477	26.3
0.0432	1.451	1.173	0.0052	0.1280	70.5
0.0838	1.538	0.9107	0.0227	0.2236	123.2
0.1212	1.595	0.8350	0.0388	0.2925	161.1
0.1557	1.650	0.6721	0.0540	0.3459	190.5
0.1875	1.684	0.6000	0.0688	0.3878	213.6
0.2170	1.716	0.5452	0.0825	0.4214	232.1
0.2440	1.751	0.5030	0.0961	0.4500	247.9
0.2797	1.792	0.4533	0.1127	0.4788	263.7
0.3417	1.835	0.3766	0.1474	0.5198	286.3
0.3939	1.870	0.3234	0.1788	0.5430	299.1
0.4385	1.895	0.2824	0.2079	0.5539	305.1
0.4770	1.918	0.2511	0.2335	0.5571	306.9
0.5105	1.936	0.2258	0.2589	0.5573	307.0
0.5400	1.955	0.2055	0.2812	0.5536	304.9
0.5660	1.959	0.1861	0.3060	0.5483	302.0
0.5840	1.964	0.1735	0.3228	0.5428	298.9
0.6794	2.000	0.1147	0.4234	0.4935	271.8

0.7405	0.0811	0.5089	0.4424	243.7
0.7814	0.0621	0.5690	0.3982	219.3
0.8112	0.0487	0.6215	0.3613	199.0
0.8329	0.0404	0.6634	0.3330	183.4
0.8659	0.0273	0.7410	0.2835	156.2
0.8876	0.0200	0.7978	0.2476	136.4
0.9032	0.0149	0.8430	0.2190	120.6

The calculated excess free energy of mixing was fitted by the method of least squares to an equation of the form,

$$\frac{g^E}{RT} = x_A(1-x_A)\left\{A + B(1-2x_A) + C(1-2x_A)^2 + D(1-2x_A)^3\right\}$$

The values obtained for the isothermal constants are:

	A	B	C	D
18.00°C	2.43	0.12	0.70	0.44
10.00°C	2.31	0.09	0.66	0.35
4.00°C	2.23	0.05	0.61	0.25

The errors involved in fitting these points were less than five calories in the 18°C isotherm, and less than three calories in the other two isotherms. The deviation of the excess free energy of mixing from a parabola is shown in figure 8.7 $\left[g^E/RT - A\,x_A(1-x_A) = \varphi(x_A) \text{ vs. } x_A\right]$. This deviation becomes very large in the region $x_A = 0.15$.

The enthalpy of mixing at 10°C was determined from the dependence of the free energy upon temperature by the relationship,

$$\left(\frac{\partial\left(\frac{g^E}{T}\right)}{\partial\left(\frac{1}{T}\right)}\right)_{p,x} = h_{T,p}$$

The values of the excess free energy, the temperature - excess entropy product and the enthalpy of mixing at 10°C

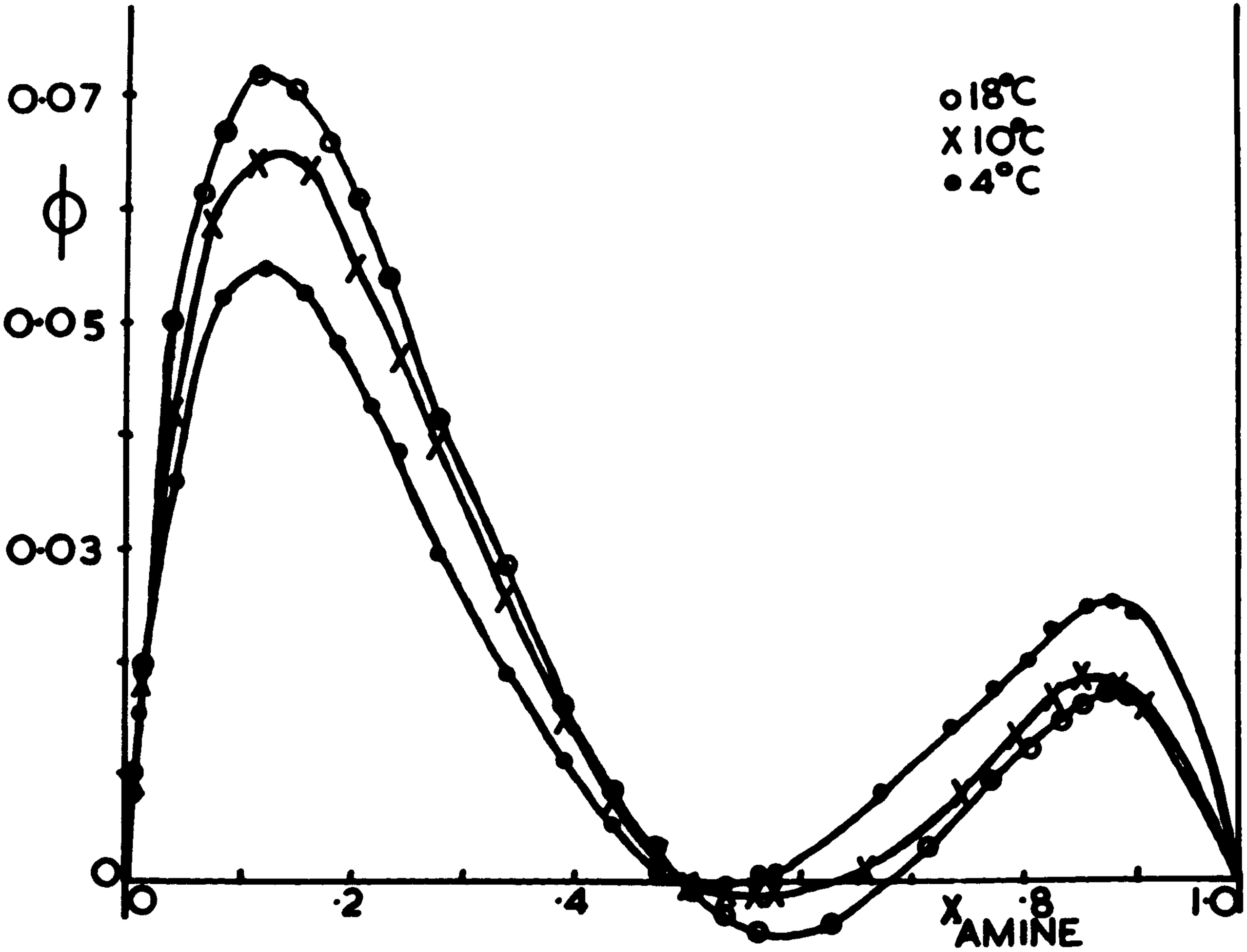

FIGURE 8·7 Φ AS A FUNCTION OF AMINE MOLE FRACTION

are given in table VII and shown in figure 8.8. The uncertainties in Ts^E and h^M appear to be less than 20 cal. for solutions of low amine concentration, and less than 50 cal. for solutions of high amine concentration.

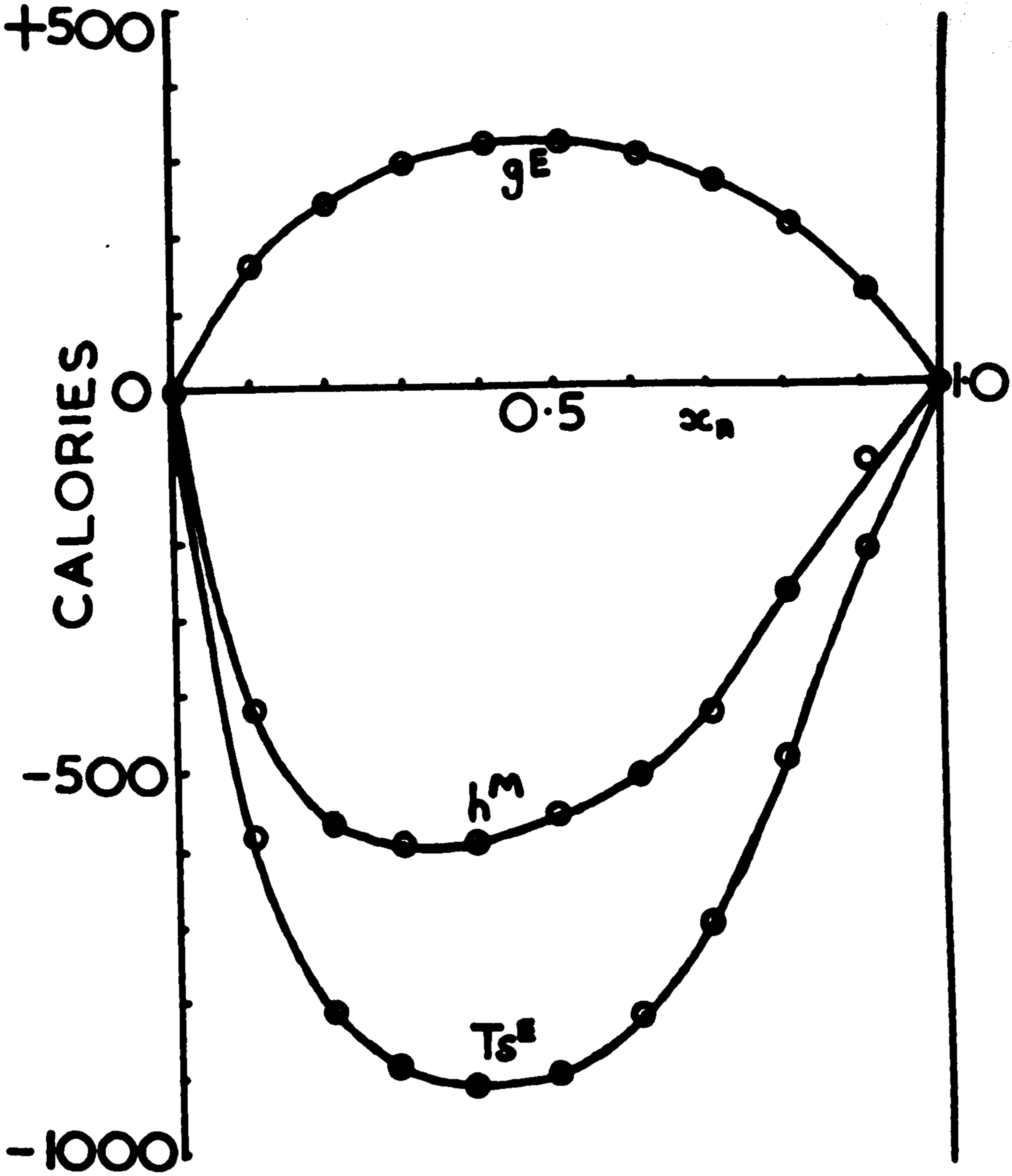

FIGURE 88 EXCESS FUNCTION CURVES AT 10°C FOR THE TRIETHYLAMINE+WATER SYSTEM.

TABLE VII

10.00°C

x_A	g^E	TS^E	h^M
	cal.	cal.	cal.
0.1	155	-570	-410
0.2	240	-800	-560
0.3	291	-880	-590
0.4	320	-900	-580
0.5	325	-880	-550
0.6	311	-810	-500
0.7	273	-690	-420
0.8	215	-500	-280
0.9	124	-220	-100

REFERENCES FOR CHAPTER EIGHT

1. H.M. Ashton and E.A. Guggenheim, Proc.Roy.Soc., B69, 693, (1956)
2. W.S. Funnell and G.I. Hoover, J.Phys.Chem., 31, 1099 (1927)
3. S.G. Yorke, J.Sci.Ins. 22, 196, (1945)
4. idem, ibid, 25, 16, (1948)
5. 'The Use of Cathetometers', The Precision Tool and Instrument Co.Ltd. (1958)
6. H.M. Ashton and E.S. Halberstadt, Proc.Roy.Soc., A245, 373, (1958)
7. F. Kohler, Monat für Chemie, 82, 913, (1951)
8. C. Runge and H. Kutta, Vorlesungen über numerisches Rechnen, S.286, Berlin, (1924)

CONCLUSION

By analysis of the experimental results discussed in the previous chapters it should be possible to obtain some information as to the type of molecular interactions which occur in the system triethylamine + water. The large negative excess entropy of mixing, associated with solutions near a lower critical point, implies that the interactions must depend upon the relative orientations of the molecules. In the case of the system triethylamine + water the interactions which occur are probably due to hydrogen bonding.

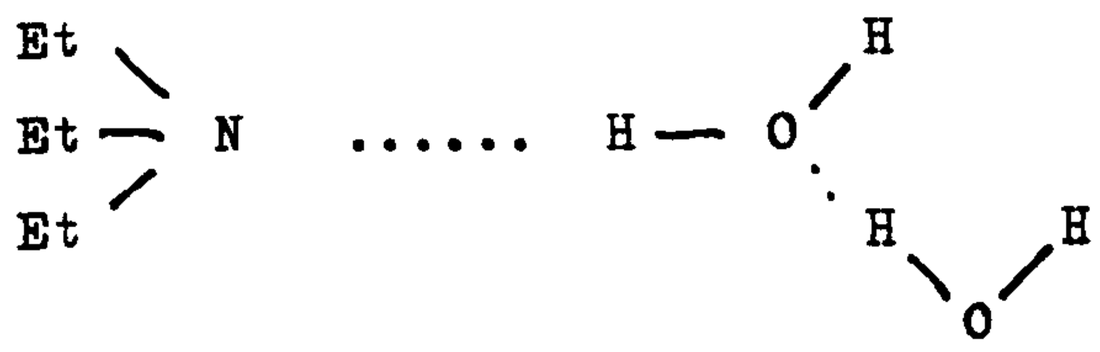

When one considers the viscosities of the triethylamine + water solutions, the interactions between the molecules appear to be extremely large. The maximum viscosity occurs at a mole fraction of amine $x_A \simeq 0.13$, and is approximately six times the value one would expect if water and triethylamine formed an ideal solution. This viscosity can probably be accounted for by assuming that the molecules form clusters

of various sizes held together by hydrogen bonds: these clusters contain molecules in a localised lattice and the extent and number of these clusters is a maximum at $x_A = 0.13$. It is probable that in the region of $x_A = 0.13$ the whole solution exists as a 'loose localised lattice'- a structure in which lattice type order can be observed up to a certain number of molecular diameters away from a given centre molecule. This hypothesis is partially supported by the conductivity measurements. Different values of the specific conductivity could be obtained depending upon the previous history of the solution. This 'hysteresis' effect did not only occur in the critical region (as determined from the shape of the viscosity curves) but also at temperatures below this. Thus at a certain temperature the number of ions in solution depends upon the history of the solution; and if we assume that the clusters contain ions, then one would have to break down these clusters in order to obtain another conductivity value. The break-down of these clusters can occur by phase separation in solution, and on cooling the solution would reform and have a new conductivity value.

At $x_A = 0.13$ the solution probably exists as a large

'localised lattice structure' containing few free molecules. Mole fractions different from this contain small clusters with the same structure and larger quantities of free molecules. At $x_A = 0.14$ there is a maximum in the coefficient of expansion, and this might be explained by assuming that the clusters form with a contraction in volume and that they tend to break up with increase of temperature. This breakup of clusters with increase of temperature is in agreement with the decrease of viscosity with temperature which occurs outside the critical region. In the critical region there is an increase of viscosity with temperature, a property which is observed in all binary liquid systems showing consolute behaviour and which is probably due to the formation of two phases on a microscopic scale. If clustering is a maximum at $x_A = 0.13$ then one might expect that the volume of mixing would contain a minimum at this point; this is not found to be the case as v^E is approximately symmetrical about $x_A = 0.5$. If the deviation of v^E from a parabola is calculated then a maximum negative deviation occurs at $x_A = 0.14$ as shown in figure 7.5. This deviation is practically eliminated at 18^oC so it cannot be explained solely on the basis of cluster formation, as clusters would

still exist at this temperature.

If there is a large degree of cluster formation in the region $x_A = 0.13$, then it is to be expected that there will be a large negative contribution to the excess entropy of mixing. It is difficult to discover a suitable method of examining the excess entropy of mixing, as no theoretical calculations have been performed for a mixture of two polar molecules of different sizes. The temperature-excess entropy product at $10^{\circ}C$ is approximately parabolic, and if we proceed as in the previous paragraph and calculate the deviation from a parabola we find the negative deviation is greatest at $x_A = 0.14$. Thus while the clustering effect has not been rigorously established, it seems probable that if clusters do exist they have an average formula of the form $(Et_3N.6H_2O)_n$.

If an attempt is made to explain the existence of the critical mole fraction at $x_A = 0.073$, one immediately notices that this is half-way on the amine mole fraction scale to $x_A = 0.14$. In most simple solution models the critical mole fraction is often in the region of $x = 0.5$: at $x_A = 0.077$ there are six water molecules to every lattice unit

$Et_3N.6H_2O$, and thus the existence of the critical mole fraction at $x_A = 0.073$ may be considered to be in agreement with this picture. At $x_A = 0.25$ there is one molecule of Et_3N to every lattice unit $Et_3N.6H_2O$, and equally this point could be the critical mole fraction. The critical mole fraction may occur at $x_A = 0.073$ rather than at $x_A = 0.25$ because $\gamma_A(x_A \rightarrow 0, 18^\circ C) \simeq 50$, while $\gamma_W(x_W \rightarrow 0, 18^\circ C) \simeq 12$. As can be seen in figures 4.1 and 4.4, small amounts of impurity show a large effect in the region $x_A = 0.25 - 0.30$, and it may be that there is a slight tendency to produce an L.C.T. in this region which is shown up by the presence of a third component.

It is difficult to decide without microscopic evidence upon the arrangement of the molecules in the 'loose lattice'. One possibility would be a large globular structure held together by hydrogen bonds and having a surface composed mainly of C-H groups. Such a globule would have less tendency to dissolve in water than in amine and this might explain the values of the activity coefficients discussed in the previous section.

All the evidence available seems to point to a cluster like association of molecules with the average formula of

each cluster $(Et_3N.6H_2O)_n$, and the resulting solution showing large positive deviations from ideality. In order to interpret the free energy results in terms of a solution model, it would be necessary to obtain an estimate of the number and size of the cluster particles. If, for example, one made the assumption that only the basic lattice unit $Et_3N.6H_2O$ existed in solution one could obtain an equilibrium constant on the basis of the equation

$$\underset{1-x-6\alpha}{6H_2O} + \underset{x-\alpha}{Et_3N} \rightleftharpoons \underset{\alpha}{Et_3N.6H_2O} ,$$

then the excess free energy of mixing would be

$$\frac{g^E}{RT} = x \ln \frac{x-\alpha}{x}\gamma_A + (1-x) \ln \frac{1-x-6\alpha}{1-x}\gamma_W - \ln(1-6\alpha) ,$$

where α is related to k by the equation

$$k = \frac{\alpha \gamma_c (1-6\alpha)^6}{(x-\alpha)\gamma_A (1-x-6\alpha)^6 \gamma_W^6} ,$$

and γ_c is the activity coefficient of $Et_3N.6H_2O$. The use of this equation would be an interesting first step to the interpretation of the free energy results if a value for k could be obtained. If the degree of clustering of molecules is quite large then it would also be necessary to determine the vapour virial coefficients, in order to obtain accurate free energy values and also an idea of

the nature of the cluster particle in the vapour.